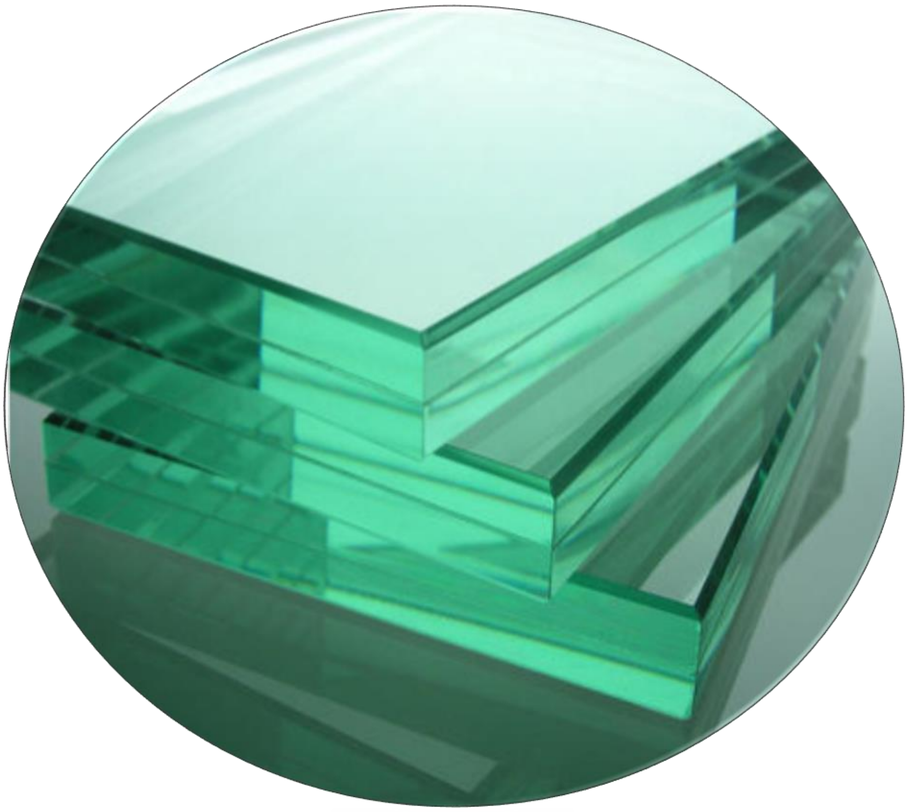

The Interplay between the Structural and Sustainable Performance of Laminated Glass

Z.B. (Dannia) Yang

TU Delft

The Interplay between the Structural and Sustainable Performance of Laminated Glass

by

Z.B. (Dannia) Yang

To obtain the degree of Master of Science

at the Delft University of Technology,

to be defended publicly on July 19th, 2021

Student number: 4895584

Project Duration: July 1st, 2020 – July 19th, 2021

Supervisors: Ir. Chris Noteboom

Dr. Henk Jonkers

Prof. Dr. Ir. Jan Rots

Table of Contents

List of Figures

Contact Information

Student's Information:

Zhibo (Dannia) Yang
Msc. Civil Engineering
Specialization: Building Engineering (Structural Design)
Student number: 4895584

Committee's Information:

Ir. Chris Noteboom
Email: C.Noteboom@tudelft.nl
Faculty: Civil Engineering and Geoscience
Section: Applied Mechanics

Dr. Henk Jonkers
Email: H.M.Jonkers@tudelft.nl
Faculty: Civil Engineering and Geoscience
Section: Materials and Environment

Prof. Dr. Ir. Jan Rots
Email: J.G.Rots@tudelft.nl
Faculty: Civil Engineering and Geoscience
Section: Applied Mechanics

Part I Introduction	Chapter 1 Introduction				
Part II Theoretical Framework	Chapter 2 Glass	Chapter 3 Interlayers	Chapter 4 Laminated Glass	Chapter 5 Experimental Results from Literature	Chapter 6 Connections
Part III Structural Analysis	Chapter 7 Analytical Method				
Part IV Sustainability Analysis	Chapter 8 EPD and Shadow Cost	Chapter 9 End-of-Life Options			
Part V Case Study: Glass Floor	Chapter 10 Structural Analysis	Chapter 11 Sustainability Analysis			
Part VI Conclusion	Chapter 12 Conclusion				

General Summary

There are many different types of interlayer, such as PVB (polyvinyl butyral), SentryGlas (ionomer), and EVA (ethylene-vinyl acetate). Each type of interlayer has its unique chemical composition, and these different chemical compositions will lead to different structural properties and sustainability performances. This master's thesis will answer the question: *which type of interlayer, in combination with laminated glass, is the most optimal when considering both its structural and sustainability performances*.

In order to answer this research question, a literature review is first done on the current existing information on this subject matter. The literature review includes information on the production process of float glass, and the different types of interlayers, the facture patterns of laminated glass, the post-breakage behaviour of laminated glass, the manufacturing process of laminated glass, and experimental results of tensile tests and four-point bending tests.

The literature review of the experimental results include tensile tests and four-point bending tests. The tensile tests are for different interlayers, and the results are shown in stress versus strain graphs. The four-point bending tests are for laminated glass with different interlayers, and the results are shown in load versus displacement graphs. Additionally, the effect of temperature, UV radiation, and relative humidity on laminated glass with different interlayers are analysed, and the results are show in midspan deflection versus time graphs.

Here are some conclusion from the literature review. Tensile tests from literature on PVB, SGP, and EVA interlayers show that SGP interlayer has the highest maximum stress and initial stiffness, and EVA interlayer has the highest ductility. Four-point bending tests from literature on laminated glass with PVB, SGP, and EVA interlayer show that laminated glass with SGP will break at a largest force and displacement. The mid-span deflection of laminated glass with SGP interlayer is affected the least by temperature, and the mid-span deflection of laminated glass with EVA interlayer is affected the least by radiation.

After the literature review, a sustainability analysis is conducted with Environmental Product Declarations and end-of-life options. Environmental Product Declarations from different glass production companies and design firms are used to calculate the shadow costs of laminated glass. Specifically, the shadow costs are calculated for 7 impact categories for the production stage (A1 and A3), the waste processing stage (C3), the disposal stage (C4), and the benefits and loads beyond system boundaries section (D). In addition, the end-of-life recycling options of float glass, interlayer, and laminated glass are explored, and this is done through analysing current practices in the industry and current research in this field.

From the shadow cost component of the sustainability analysis, it was concluded that the amount of shadow cost of the interlayer component is significantly lower than that of the glass component. By comparing the shadow cost of the 7 impact categories, it can be seen that the shadow cost of the global warming impact is always the highest by far, and the shadow costs of the acidification impact and the eutrophication impact are lower but still substantial. Within the production stage (A), the shadow cost from manufacturing stage (A3) is higher than that of the raw material stage (A1). Within the end-of-life stage (C), it can be seen that the shadow cost is reduced in almost all of the 7 impact categories even with 5% recycling and 95% disposal in comparison with 100% disposal.

Here are some conclusion from the end-of-life recycling component of the sustainability analysis. The problem with recycling float glass is that glass can only go back into the float glass industry if it do not have any contamination like aluminium or nickel. So instead, the vast majority of recycled float glass are downcycled to produce bottles, insulation materials, or embankments. One company that downcycle glass is Maltha. Saint Gobain breaks down float glass into cullet to make new float glass, but this is only for pre-consumer glass.

The problem with recycling interlayer is that it is difficult to ensure the quality of the product, because it is difficult to identify the manufacturer and the formulation after a number of years. Shark Solutions is a company that downcycle interlayer into carpet backing, paint and coatings, and sound dampening. Kuraray recycles PVB trimmings to make new PVB interlayer.

The problem with recycling laminated glass that it is difficult to fully separate the interlayer and the glass component to produce new laminated glass, because it is difficult to completely remove all the glass shards from the interlayer. Covanord is a company that downcycle laminated glass to make glass bottles and carpet tile. Delaminating Resources (Delam) is a company that can delaminate laminated glass with heat, time, and steam, and this company can fully recycle both components.

After the literature review and the sustainability analysis, a case study is conducted on the glass floor at the train station in Delft, because this case study will be able to incorporate both the structural and the sustainability aspect. The structural aspect of the case study contains analytical calculations and finite element simulations in DIANA, and the sustainability aspect of the case study contains shadow cost calculations. For the sustainability aspects of the case study, the shadow costs are calculated for the laminated glass configuration that satisfy the structural requirements.

From the structural aspect of the case study, it was concluded from the hand calculation that laminated glass with PVB, SGP, and EVA interlayer requires a configuration of 12.12.12.12, 12.12.10, and 12.12.10.10 respectively. The percent difference in between the stress values from the hand calculations, the 2D linear static analysis, the 2D geometrically nonlinear analysis, and the 3D linear static analysis are within 10% for ultimate limit state and the post-breakage scenarios.

For the structural aspects of the case study, the serviceability limit state, the ultimate limit state, and the post-breakage behaviour are considered for laminated glass with PVB, SGP, and EVA interlayer. Specially, hand-calculations, 2D linear static analysis, 2D structurally nonlinear analysis, and 3D linear static analysis are conducted in DIANA. The loading conditions are based on the Eurocode, and the glass calculations are based on the Dutch code NEN2608. The 2D analysis are done with the equivalent thicknesses based on

NEN2608, and the 3D analysis is conducted with stacked glass elements and interface elements in between.

For the sustainability aspects of the case study, it was concluded that, during the production stage (A), the shadow costs of PVB, SGP, and EVA are €31.6, €22.3, and €29.1 respectively. During the disposal stage (C), the shadow costs of PVB, SGP, and EVA are €0.5, €0.3, and €0.4 respectively.

The information from the previous sections of the conclusion are organized into a multi-criteria analysis for the interlayers. SGP interlayer shows better performance in its maximum stress, its stiffness, its durability against temperature, and its durability against relative humidity. SGP have proven to show less delamination over time, so it should have better durability against relative humidity. The cost of PVB interlayer is more than twice as high as that of EVA interlayer.

	Tensile strength of Interlayer	Stiffness	Strain before Breakage	Durability against temperature	Durability against solar radiation	Durability against relative humidity	Cost
PVB Interlayer	+	0	0	0	0	0	-
SGP Interlayer	+	+	-	+	0	+	N/A
EVA Interlayer	-	-	+	0	+	0	+

Here is a multi-criteria analysis for laminated glass with different interlayers. Laminated glass with SGP interlayer led to a lower shadow and economic cost in the case study, and laminated glass with SGP interlayer could be better for reuse due to the fact that it is more durable and has better resistance against delamination.

	Shadow cost	Reuse	Recycling	Cost
PVB (12.12.12.12 HS)	-	0	+	-
SGP (12.12.10 HS)	+	+	0	+
EVA (12.12.10.10 HS)	0	0	0	N/A

Part I: Introduction

Chapter 1: Introduction

In part 1, the generation information related to this research will be provided. The general information includes the context of the research, the problem that led to this research, the scope and limitations of this study, the research objective, the research questions, and the methodologies for solving those research questions.

1.1. Context

With the ever increasing speed and scale of global warming, sustainability has never been as important as it is nowadays. This increasing speed and scale of global warming can be seen in the average global temperature and atmospheric CO2 concentration over time in figure 1. Examples like the increasing number of forest wild fires, heat waves, and flooding has clearly demonstrate the increasing effect of climate change. Under the Paris Agreement, nations are making pledges to reduce their greenhouse gas emissions. The European Union is aiming to reduce its greenhouse gas emission by at least 40% by 2030 in contribution to the Paris Agreement goals (Ministerie van Algemene Zaken, 2020).

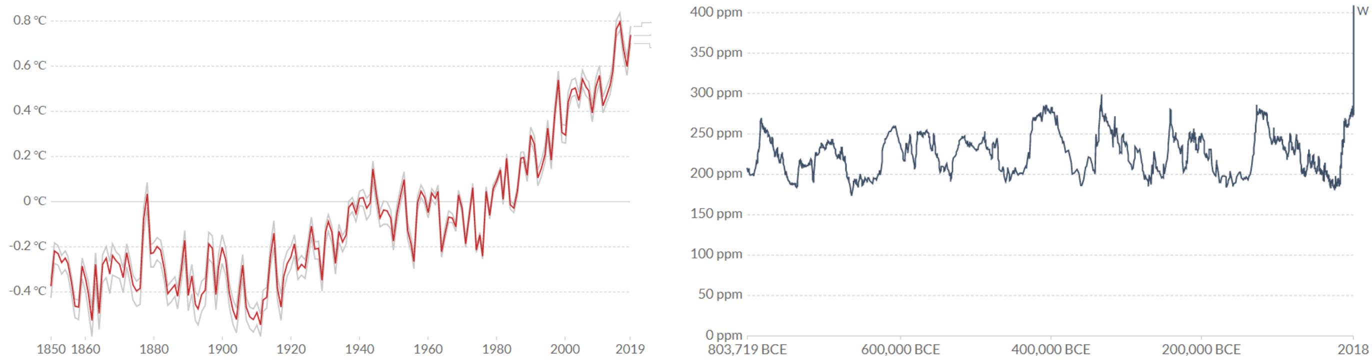

Figure 1. Average Global Temperature and Atmospheric CO2 Concentration (Ritchie & Roser, 2017)

It is important to consider the buildings and the construction industry when thinking about reducing carbon dioxide emissions, because the buildings and the construction industry account for around 39% of the total carbon emission (WorldGBC, 2019). Within the building and the construction industry, glass is one of the more commonly used materials, and it is 100% and infinitely recyclable. However, in the Netherlands, only 5-10% of waste float glass ends up back in the float glass sector, while the rest of them are downgraded to container glass or glass fibres (Stichting Vlakglas Recycling Nederland, 2018) (Hestin, Veron, & Burgos, 2018).

Laminated glass is a type of structural glass that is widely used in the buidling industry, and this is because of its advantages properties, like safety and security, UV protection, sound control, heat control, and design versatility. Laminated glass is constructed with interlayers in between two or more layers of float glass panels in order to hold the glass pieces together after the glass panels have already cracked. In addition, for laminated glass with more than two layers, even if both outer panels had already lost their strength, the inner panels are still unharmed and can still provide structural support to the building.

1.2. Problem Statement

There are many different types of interlayer, including PVB (polyvinyl butyral), SentryGlas (ionomer), EVA (ethylene-vinyl acetate), TPU (thermoplastic polyurethane), and PC (polycarbonates), PET (polyethylene terephthalate), PMMA (polymethylmethacrylates), and epoxies. Each type of interlayer has its unique chemical composition, and these different chemical compositions will lead to different structural properties and sustainability performances. For example, the different structural properties may include different strengths, stiffnesses, and bending deflections. In addition, the different interlayers have different chemical compositions and production processes, which will lead to different amount of carbon emission during its life cycle.

The problem is that there is no way to holistically compare the many types of interlayer in the market while taking into consideration the structural capability and the sustainability performance. Only by fully understanding both the structural and sustainability aspect of the different interlayers, can the designer make an informed decision in between the numerous products available in the market.

1.3. Scope and limitations

The scope of this research will include the different types of interlayers, including PVB (polyvinyl butyral), SentryGlas (ionomer), EVA (ethylene-vinyl acetate), TPU (thermoplastic polyurethane), and PC (polycarbonates), PET (polyethylene terephthalate), PMMA (polymethylmethacrylates), and epoxies. This research will focus on laminated glass made with IGU units instead of laminated glass made with other types of glass, like cast glass.

Sustainability can be a very general term, and this research will not include everything related to sustainability. This research will focus on the embodied energy, the shadow cost during its life time, current sustainable technologies, and end-of-life options. In addition, any future possibilities will also be included.

1.4. Research Objective

The objective of this thesis is to compare both the structural and the sustainability performance of the different types of interlayers for laminated structural glass. The goal is to find a way to take both the structural performance and sustainability aspect into account when choosing the best type of interlayer for laminated glass.

It should be noted the research will not compare the different types of interlayer by itself, instead this research will focus on the different types of interlayer in combination with glass panels. This is because the type of interlayer will have an effect on the amount of glass panels required, which will also have an effect on the sustainability performance of the structural member.

Specifically, the functional unit of this research will be a glass floor plate at the train station in Delft, and the functional unit is shown in figure 2. A glass plate are chosen as the functional unit, because it is one of the mostly commonly used structural elements.

Figure 2. Laminated Glass Floor Plate at the Delft Station

1.5. Research Questions

1.5.1. Main Research Question

Which type of interlayer, in combination with laminated glass, is the most optimal when considering its structural and sustainability performances?

1.5.2. Sub Research questions

a) What is the structural performance of the different types of interlayers considering the construction condition like the moisture, the solar radiation, and the temperature?
b) What is the durability situation and the expected lifetime of the different types of interlayers?
c) Taking the embodied energy and the shadow cost of the interlayers' entire lifetimes into considerations, what are the sustainability performance of the different types of interlayers?
d) What are the end-of-life possibilities (eg. reduce, reuse, and recycle) for the different types of interlayers in laminated glass?
e) How much do the different types of interlayers cost in laminated glass?

1.6. Methodology

1.6.1. What is the durability situation and the expected lifetime of the different types of interlayers?

Information on the expected lifetime of the different types of interlayer will be obtained from different suppliers. Specifically, the expected lifetime of the different types of interlayers from sample projects from the will be compared. The different environmental conditions of the projects and the project types will be taken into consideration.

1.6.2. Taking the embodied energy and the shadow cost of the interlayers' entire lifetimes into considerations, what are the sustainability performance of the different types of interlayers?

The sustainability information will be assessed by performing LCA (Life Cycle Analysis) on the different types of interlayers with their EPD (Environmental Product Declaration). The Environment Product Declaration will be obtained from interlayer manufacturers. Some examples of interlayer manufacturers include Kuraray, Dupont, Eastman, and Huntsman. The Life Cycle Analysis will be performance according to the SBK (Stichting Bouwkwaliteit) method. The different types of interlayer will be analysed based on the 11 impact categories, which include its effect on human toxicity, ecotoxicity, and depletion of abiotic resources.

1.6.3. What are the end-of-life possibilities (eg. reduce, reuse, and recycle) for the different types of interlayers in laminated glass?

Both the most current technologies related to sustainability and the end-of-life options (eg. reduce, reuse, and recycle) can be investigated through literature review of the existing technologies and techniques. This information can also be explored by asking design firms and interlayer manufacturers about their current practices related to sustainability and end-of-life options. Specifically, for each type of interlayer, the different end-of-life options will be compared; for example, it is possible to compare whether it is more sustainable to reuse the entire laminated glass or to down-cycle it to a different product.

1.6.4. What is the structural performance of the different types of interlayers considering conditions like the moisture, the solar radiation, and the temperature?

The structural performances can be analysed through a literature review of the existing experimental information; for example, there are experimental results of tensile strength of the different interlayers, as well as 4-point bending test of laminated glass with different types of interlayers. Experimental information related to the environmental condition is also available; for example, there are experimental information on the structural performance of the different interlayers at different temperature, relative humidity, and UV conditions. In addition, the experimental information can also be confirmed with a finite element analysis with the software DIANA.

1.6.5. How much do the different types of interlayers cost in laminated glass?

The unit costs of these interlayers are not shown on the website of the manufacturers, so the different costs of the different type of interlayers will be obtained through interviews with the interlayer manufacturers. Then, the cost of the glass panels will be added onto the cost of the interlayers for the total cost of the laminated glass, and the total cost of the laminated glass will be compared.

1.6.6. Which type of interlayer, in combination with laminated glass, is the most optimal when considering its structural and sustainability performances?

A scoring system like a MCA (Multi Criteria Analysis) will be completed to provide a holistic comparison in between the different interlayers in laminated glass. This MCA will take into account the information from all the sub-questions, like the sustainability potentials, structural performance, cost, service life, and end-of-life options. This way, a well-informed decision can be made when deciding on the most optimal type of interlayer to be used for laminated glass.

First, the type and thickness of the interlayer and the glass panels are calculated with an analytical analysis. Then these results will be used to calculate the cost, the shadow cost, and design life using the parametric software Grasshopper. These numerical results will also be displayed on a bar graph in Grasshopper as well. Also, a rating of either negative, neutral, or positive will be given to each interlayer's sustainability potential, structural performance, cost, service life, and end-of-life options.

Part II: Theoretical Framework

Information, which found in existing literature, are summarized in this section. Specifically, there are information on glass in general, the production process of glass, laminated glass in general, the different types of interlayers, results of experimental tensile tests, results of four-point bending tests, Environmental Product Declarations in general, possible recycling options, and possible reuse options.

Chapter 2: Glass

Glass is an isotropic and non-crystalline solid, and it is commonly used in construction, tableware, and optics due to its ability to allow light to pass through. Glass cannot deform plastically before fracture, and it is sensitive to cracks, flaws, and stress concentrations. Although class is brittle, it is also durable and has resistance against chemicals.

2.1. Material Properties

The main ingredients used in history are sand, ash from sea plants, and chalk. Sand contains silica in the form of quartz. Ash from sea plants contain sodium carbonate, and chalk is a form of limestone. Nowadays, the main ingredients are determined by the price, durability, and viscosity. Soda-lime glass is the most common type of glass, and it is made with 73% silica, 13% soda oxide, and 10% lime. Figure 4 shows the chemical reaction that take place during glass formation. Additive like colouring agents can be used for some special characteristics. Fining agents can be used to create homogeneity and remove bubbles, and melting flux can be used to melt at lower temperature. Figure 3 shows the basic mechanical properties of glass.

$$Na_2CO_3 \longrightarrow Na_2O + CO_2$$

$$Na_2O + SiO_2 \longrightarrow Na_2SiO_3$$

Figure 3. Chemical Reaction for Glass Formation

Compressive Strength	880-930 MPa
Tensile Strength**	30-90 MPa
Flexural Strength	30-100 MPa
Young’s Modulus	70-75 MPa
Poisson's Ratio	0.23
Density	2,500 kg/m^3
**Tensile strength is related to flaws	

Figure 4. Properties of Glass (Haldimann, Luible, & Overend, 2008)

2.2. Production Process of Float Glass

Float glass is a type of soda-lime-silica, and it is very commonly used in the construction industry. Figure 5 shows the production process of float glass. Stage 1 of the float glass production process is melting and refining, and it is when fine-grained ingredients are melted and refined at 1100 degrees in the furnace (Pilkington, 2020).

Stage 2 is the flat bath step, and it is when glass from the furnace is poured from the furnace onto a shallow bath of molten tin. The glass floats on the tin and spreads out to form a flat surface. The thickness of the glass is controlled by the speed the solidifying glass is drawn off from the bath. In this step, the glass starts at 1100 degrees, and leaves the flat bath as a solid ribbon at 600 degrees (Pilkington, 2020).

It is optional to add the coating step in between the flat bath step and the annealing step. During this step, coatings that change the optical properties is applied to the glass at high temperature. Coatings that are used to reflect visible and infrared wavelength and be added in this step, and Chemical Vapour Deposition (CVD) can be used to lay down the coating (Pilkington, 2020).

Step 3 is the annealing step, and temperature is closely controlled in a lehr, or a long furnace. This step is used to relieve the stress in the glass to prevent poor glass quality. Step 5 is the inspection step, and glass with any flaws will need to be disposed. Step 6 is the cutting step, and diamond wheels are used to cut the ribbon into the desired dimensions.

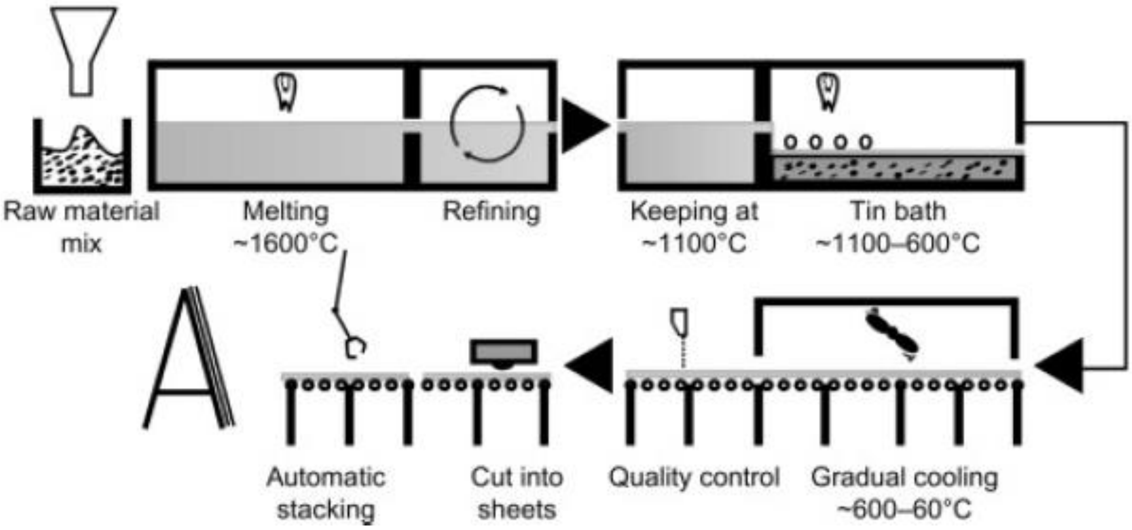

Figure 5. Float Glass Production Process (Achintha, 2016)

2.3. Annealed, Heat-strengthened, and Fully-Tempered Glass

Annealed float glass fails at relatively low stresses and in large shards. Heat-strengthened glass or fully tempered glass differ based on the level of pre-stress, and fully tempered glass experiences more pre-stressing than heat-strengthened glass. This difference in between fracture pattern can be seen in figure 6. Compared with that of annealed float glass, the pre-stressed glass experiences more energy release during failure, so the pre-stressed glass also show more extensive crack branching.

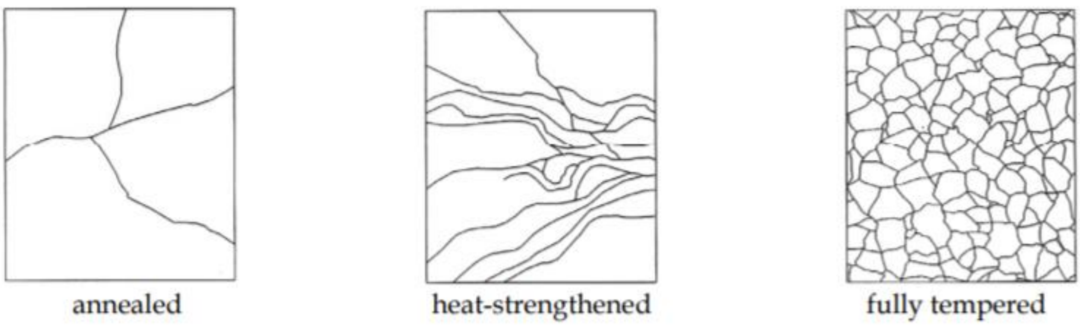

Figure 6. Fracture pattern of annealed, heat-strengthened, and fully tempered float glass (Schittich, 1999

Chapter 3: Interlayers

There are many different types of interlayer for laminated glass, and they include PVB (polyvinyl butyral), SentryGlas (ionomer), EVA (ethylene-vinyl acetate), TPU (thermoplastic polyurethane), PC (polycarbonates), PET (polyethylene terephthalate), and PMMA (polymethylmehacrylates). PVB is the most commonly used, but SentryGlas is five times stronger and one hundred times stiffer than PVB. EVA can be used in combination with solar cells.

3.1. PVB (polyvinyl butyral)

PVB was first introduced in the 1930s, and it is widely used due to its properties, which include high mechanical strength, high deformation before breakage, good adhesion to glass, and high light transmission. Specifically, PVB is composed of 76-80wt% vinyl butyral, 18-22wt% vinyl alcohol, and 1-2wt% vinyl acetate (Martín et al., 2020). Figure 7 shows the chain structure of PVB. Its elasticity can be improved through the addition of plasticizers (Martín et al., 2020). Kuraray carries Butacite, which are recycled PVB interlayers that are produced from the cutoffs wastes of its normal PVB interlayers.

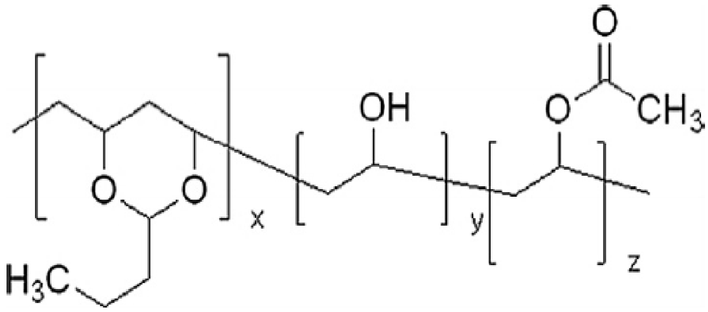

Figure 7. PVB Chain Structure (Martín et al., 2020)

3.1.1. Plasticized PVB (Polyvinyl Butyral)

Plasticized PVB, also known as structural PVB, is PVB interlayer with lower level of plasticiser. Plasticizers need to be added to the PVB chains in order to improve elasticity of the interlayer. When the concentration of plasticiser decrease, the mobility between chains will starts at a higher temperature, which means that the glass transition temperature increases. The lower level of plasticiser will lead to an increase in its glass transition temperature, and will therefore lead to an increase in its strength, stiffness, and viscosity. A common product of plasticized PVB interlayer is the Saflex DG-41 interlayer by Eastman Chemical Company or the PVB ES by Kuraray.

3.2. SentryGlas (ionomer)

SentryGlas, a type of ionomer was introduced in 1964 by the company DuPont, and SentryGlas is the only ionomer interlayer on the market. SentryGlas is much stiffer, because it can achieve high stiffness through crosslinking (Martín et al., 2020). Figure 8 shows the chain structure of SGP interlayer. It is also less sensitive to load duration and working temperature than other interlayers; PVB started to decrease its stiffness at 20 degrees, but SentryGlas can do so until 55 degrees (Martín et al., 2020). In addition, laminated glass with SentryGlas can withstand storms, impacts and powerful blasts (Achintha, 2016).

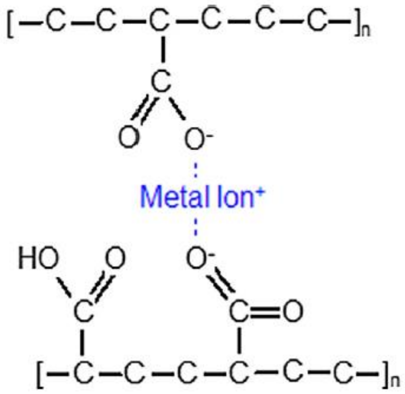

Figure 8. SGP Chain Structure (Martín et al., 2020)

3.3. EVA (ethylene-vinyl acetate)

EVA is the copolymer of ethylene and vinyl acetate, and there are 3 different types of EVA copolymer depending on its VA (vinyl acetate) content: EVA (ethylene-vinyl acetate), PEVA (polyethylene-vinyl acetate), and VAE (vinyl acetate-ethylene copolymer) (Martín et al., 2020). Figure 9 shows the chain structure of EVA interlayer. In comparison with other types of interlayers, EVA provides some unique properties like high electrical resistivity, optical transmission, low fusion and polymerization temperature, and solar radiation and moisture resistance (Martín et al., 2020). When combining EVA interlayer with glass panels, EVA interlayer does not require an autoclave. Solar cells cannot be heated, and this is why EVA can be used in combination with solar cells.

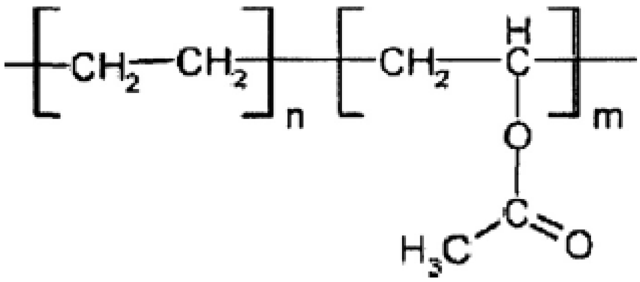

Figure 9. EVA Chain Structure (Martín et al., 2020)

	PVB	SGP	EVA
Price	4.02 – 4.82 €/m2	n.a.	1.74 – 1.91 €/m2
Density	915 – 1070 kg/m3	950 kg/m3	945 – 955 kg/m3
Water absorption (ASTM D-570)	3.6 wt.%	n.a.	0.15 – 0.5 wt.%
Coefficient of thermal expansion	22-40 $k^{-1}*10^{-15}$	10-15*10^{-5} cm/cm°C	160 – 190 *10^{-5} cm/cm°C
Transmittance	88 – 89 %	n.a.	90 – 92 %
Yellowness index	12.5	2.5	1.9
Ultimate tensile strength	20.8 MPa	34.5 MPa	9.5 – 10 MPa
Elongation at failure	190 – 350 %	400 %	880 – 930 %
Young modulus	2.36 MPa	300-480 MPa	7 – 9 MPa
Poisson’s ratio	0.5	0.442 – 0.5	0.47 – 0.49
Glass transition temperature	8 – 42 °C	55 °C	-77 to -69 °C
Joining technique	Lamination	Lamination	Vacuum lamination, autoclave, or vacuum bags (CNCGlass, 2013)
Ultimate tensile strength	33 MPa	n.a.	20.8 MPa
Elongation failure	190%	n.a.	450%

Figure 10. PVB, SGP, and EVA Properties (Foil Thickness 0.76 mm) (Martín et al., 2020)

3.4. TPU (thermoplastic polyurethane)

TPU provides some great properties like high tensile strength, toughness, resistance to UV, abrasion and chemical degradation (Martín et al., 2020). Figure 11 shows the chain structure of TPU interlayer. TPU are often used for security and ballistic resistance glass applications because of its high bonding strength (Martín et al., 2020). However, TPU is not widely used due to its high price.

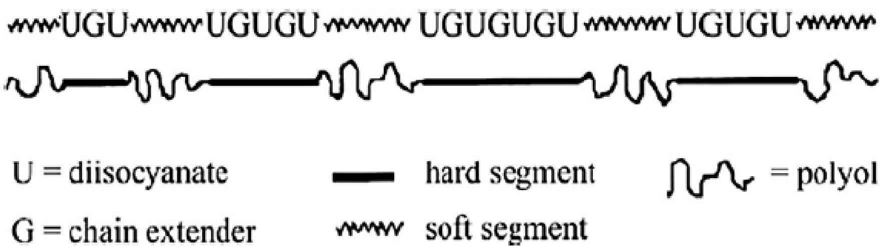

Figure 11. TPU Chain Structure (Martín et al., 2020)

3.5. PC (polycarbonates)

Weller et al. developed a hybrid beam with TPU and PC, and figure 12 shows the TPU and PC hybrid beam (Martín et al., 2020). Compared to TPU without PC, this new hybrid type has better post-breakage performance, higher ductility, and lower density (Martín et al., 2020). Toughened glass with polycarbonate interlayers are used in bulletproof glass (Achintha, 2016).

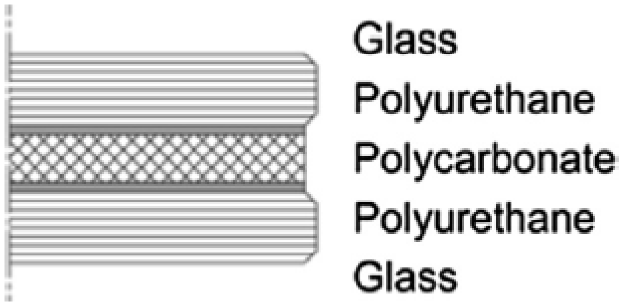

Figure 12. TPU and PC Hybrid Beam Devloped by Weller et al (Martín et al., 2020)

3.6. Poured Resin

Poured resin lamination is currently commonly used to laminate cast glass, patterned glass, or curved glass that are difficult to laminate with sheet interlayers. Poured resin interlayers are not as durable as sheet interlayers, so they are only used in locations where safety is not critical. The poured resin lamination process involves creating a cavity between 2 glass panels. Liquid resin is then poured into the cavity and cured with UV lights, heat or a catalytic reaction.

3.7. PET (polyethylene terephthalate)

Polyethylene terephthalate (PET) interlayer allow for the installation of light-emitting diodes (LED) within the glass. This feature is used by lighting engineers.

3.8. PMMA (polymethylmehacrylates)

PMMA (polymethylmehacrylates) is an economical alternative to polycarbonate (PC) tensile strength, flexural strength, transparency, and UV tolerance are more important than impact strength, chemical resistance, and heat resistance (Hydrosight, 2004).

Chapter 4: Laminated Glass

Laminated glass is produced by combining 2 or more sheets of glass with interlayers in between. The glass panels and the interlayer are combined by autoclaving at 1400 degrees and pressure up to 14 bar (Achintha, 2016). Laminated glass is commonly used for windows and windshields of automobiles. It is also possible to use heat-treated glass instead of float glass in laminated glass.

One benefit of laminated glass is its safe failure mode. Once the glass panel breaks, the interlayer can lock together the broken glass pieces and interacts with the remaining unbroken glass sheets. The interlayer also has some tensile strength when the broken pieces are locked in compression from arching action (Achintha, 2016). Laminated glass can also reduce the risk of injury from glass shards since the glass shards are held together by the interlayer.

Most structural elements like glass columns, glass beams, and glass stairs are made with more than 2 layers of laminated glass. This way, the inner panels are not exposed and are not prone to damage. The increased number of layers can also increase the strength of the laminated member, and the equivalent thickness and post-breakage structural capacity can be calculated according to NEN 2608:2014.

4.1. Post-Breakage Behaviour

The post breakage behaviour of laminated glass can be categorized into 3 stages, and figure 13 shows the post-breakage stress distribution of the 3 stages. Stage 1 is when the glass sheets are fully intact. Stage 2 is when the bottom panel has been fractured, and the top panel is taking all the load. Stage 3 is when the top panel has also been fractured. The interlayer is in tension, and the glass pieces are locked together in compression (Haldimann, Luible, & Overend, 2008). In this stage, the remaining load bearing capacity is dependent on the type of interlayer, so it is important to pick the right type of interlayer (Haldimann, Luible, & Overend, 2008).

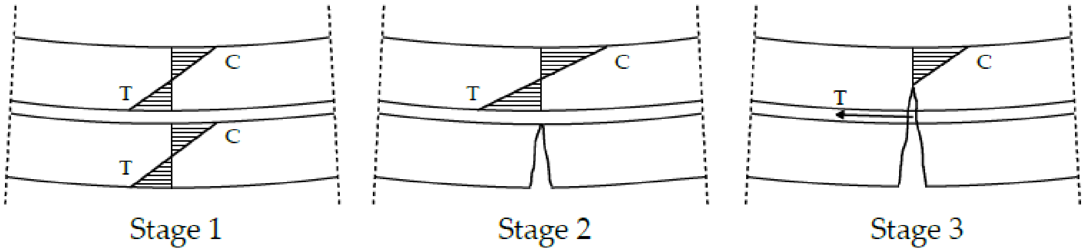

Figure 13. Post-Breakage Stress Distribution (Haldimann, Luible, & Overend, 2008)

4.2. The Manufacturing Process

The conventional lamination process with an autoclave can be used to produce laminated glass with PVB, SGP, and EVA interlayer (Martín et al., 2020). The conventional lamination process will require an autoclave, which is used to apply heat and pressure to the glass and interlayer assembly. In comparison with that of laminated glass with PVB interlayer, an autoclave with lower pressure and temperature can be used for laminated glass with EVA interlayer.

EVA interlayers can also be combined with glass through the vaccum lamination process or the lamination process with an infrared furnace, convection furnace (Martín et al., 2020). Vacuum lamination is when the glass and interlayer are placed in a silicon vacuum bag, and use the vacuum pump. Heating to 60 degrees celsius for 15 minutes, and then 130 degrees celsius for 40 minutes (CNCGlass, 2013).

Chapter 5: Experimental Results

This chapter includes the experimental results from literature, and these experimental results include tensile tests and four-point bending tests. The results of the tensile tests are shown in the stress-strain relationship. The results of the four-point bending tests are shown in load-displacement relationship. Additionally, the effect of temperature, UV radiation, and relative humidity are show in deflection-time curves.

5.1. Tensile Tests

The results of the tensile tests are shown in the stress-strain relationship, and the tensile behaviour of PVB, SGP, EVA, and TPU interlayers can be compared from the results. The stress-strain curves of PVB and SGP interlayer from three different sources are used for confirmation, and the stress- strain curves of EVA interlayer from two different sources are used for confirmation. The stress-strain behaviour for plasticized PVB and TPU are also included in this section.

5.1.1. PVB Interlayers

Figure 14 shows the results of 3 different tensile tests of PVB, and all 3 experiments were conducted at similar testing speeds. The testing speed of 10mm/min, 50mm/min, 100mm/min, and 200mm/min are equivalent to 0.004/s, 0.02/s, 0.04/s, and 0.08/s respectively. The results from 3 tensile show similar stress-strain relationships.

The graphs show viscoelastic behaviour, which is in line with the properties of PVB interlayers. The stress-strain behaviour of the viscoelastic material begins with a linear-elastic stage, exponental growth stage, and failure stage.

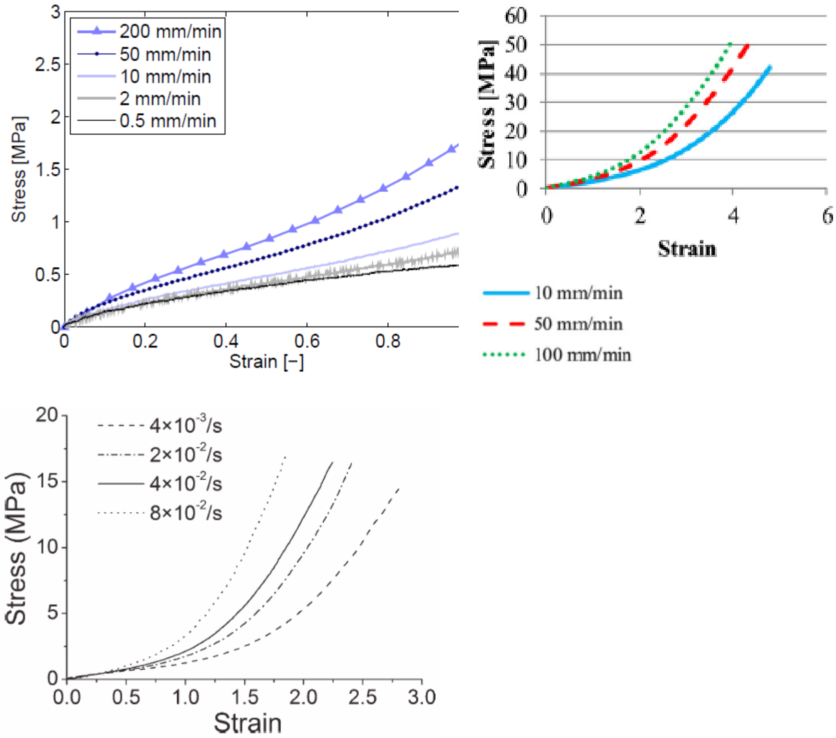

Figure 14. Stress-strain curve of SGP interlayer (Fors, 2014) (Centelles, Martín, Solé, Castro, & Cabeza, 2020), (Liu et al., 2012)

5.1.2. SentryGlas Interlayers

Figure 15 shows the results of 3 different tensile tests of SentryGlas, and all 3 experiments were conducted at similar testing speeds. The testing speed of 10mm/min, 50mm/min, 100mm/min, and 200mm/min are equivalent to 0.004/s, 0.02/s, 0.04/s, and 0.08/s respectively. The results from 3 tensile show similar stress-strain relationships.

The graphs show elasto-plastic behaviour, which is in line with the properties of SGP interlayers. The stress-strain behaviour of the elasto-plastic material has 5 phases: viscoelastic response, strain softening, stress stabilization, strain hardening, and facture.

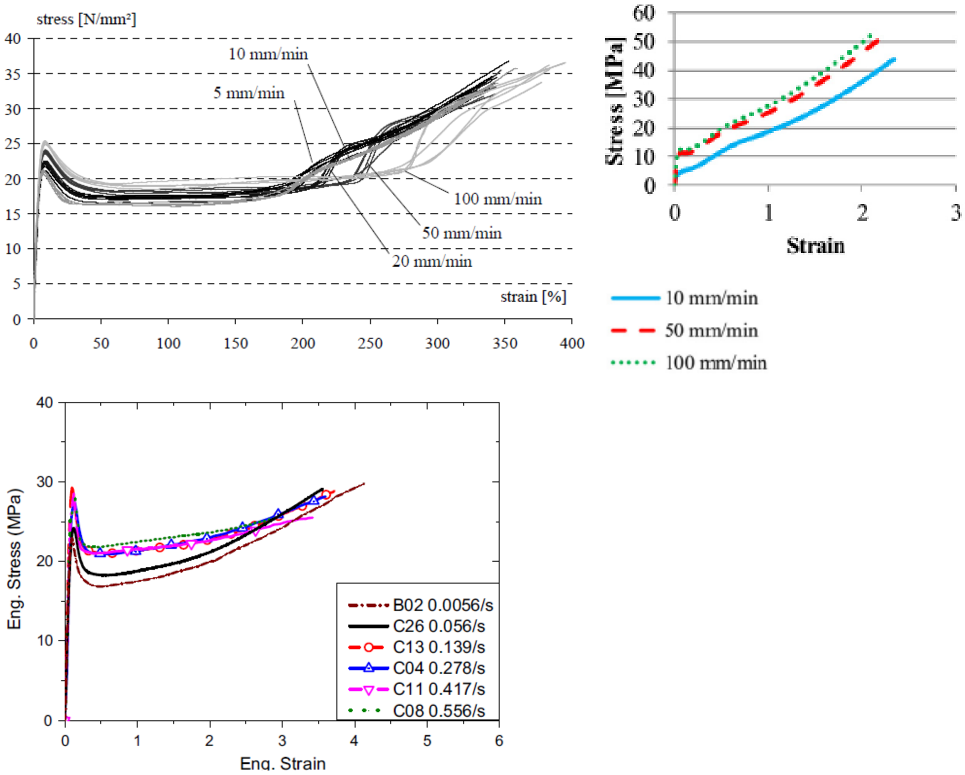

Figure 15. Stress-strain curve of SGP interlayer (Belis, Depauw, Callewaert, Delincé, & Impe, 2009) (Centelles, Martín, Solé, Castro, & Cabeza, 2020) (Zhang, Shi, Hao, & Cui, 2015)

5.1.3. EVA Interlayers

Figure 16 shows the results of 2 different tensile tests of EVA interlayer, and the 2 graphs from tensile tests show similar stress and strain relationship for the tested EVA interlayers. The graphs show viscoelastic behaviour, which is in line with the properties of EVA interlayers. The stress-strain behaviour of the viscoelastic material begins with a linear-elastic stage, exponental growth stage, and failure stage.

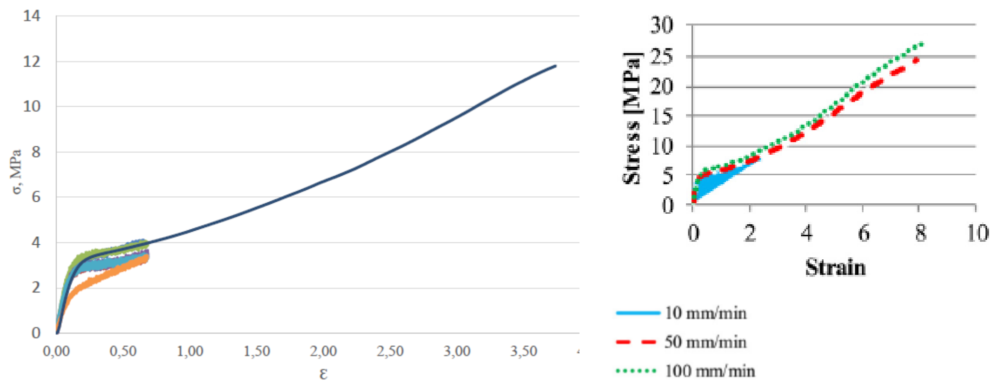

Figure 16. Stress-strain curve of EVA interlayer (Sable, Skukis, Japins, & Kalnins, 2017) (Centelles, Martín, Solé, Castro, & Cabeza, 2020)

Figure 17 shows the stress-strain curves of PVB, SGP, EVA, and TPU interlayers. The tensile tests show that the SentryGlas interlayer has the highest initial stiffness and the highest maximum stress at 45 MPa. In comparison with PVB and SGP interlayers, EVA interlayer has the highest ductility at the strain of 7. PVB interlayer without plasticizer has a lower initial stiffness as well as lower ductility. PVB interlayer with plasticizer, however, has similar stress-strain performance as that of SentryGlas interlayer.

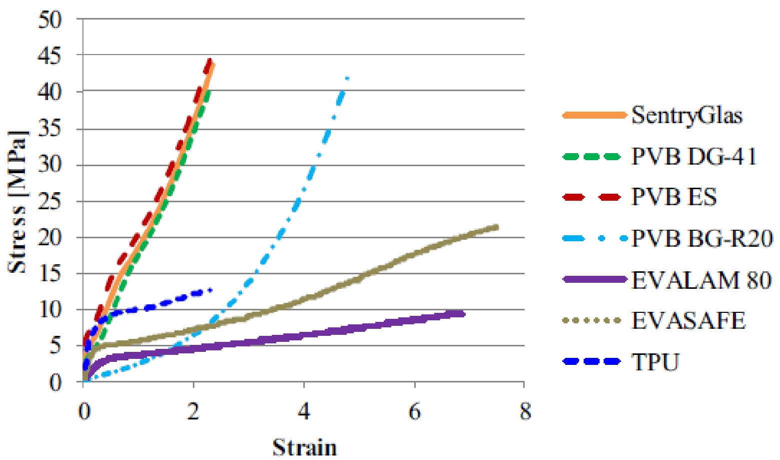

Figure 17. Stress-strain curve of PVB, SGP, EVA, and TPU (Centelles, Martín, Solé, Castro, & Cabeza, 2020)

5.2. Four-Point Bending Tests

The results of the four-point bending tests are shown in load-displacement relationship, and the four-point bending behaviour of laminated glass with PVB, SGP, and EVA interlayers can be compared from the results. The load-displacement curves of laminated glass with PVB, SGP, and EVA interlayer from three different sources are used for confirmation.

Figure 18 shows the load and displacement curve of 1.52mm PVB, SGP, and EVA in combination with 4mm thick 1100mm by 360mm glass panels. Figure 19 shows the load and displacement curve of 0.76mm PVB, 0.89mm SGP, and 0.38mm EVA in combination with 5mm thick 500mm by 100mm glass panels. Figure 20 shows the load and displacement curve of 1.5mm PVB, 1.52mm SGP, and 0.89mm EVA in combination with 6mm thick 1100mm by 360mm glass panels.

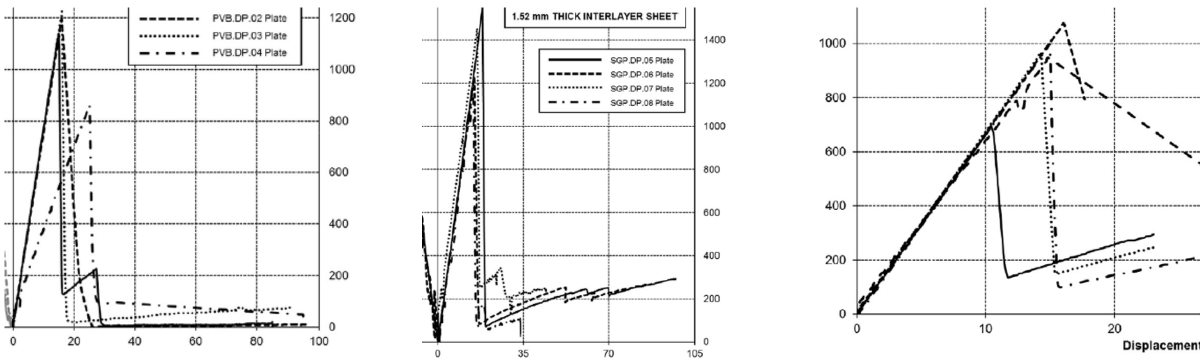

Figure 18. Load-displacement curve PVB, SGP, and EVA (Castori & Speranzini, 2017)

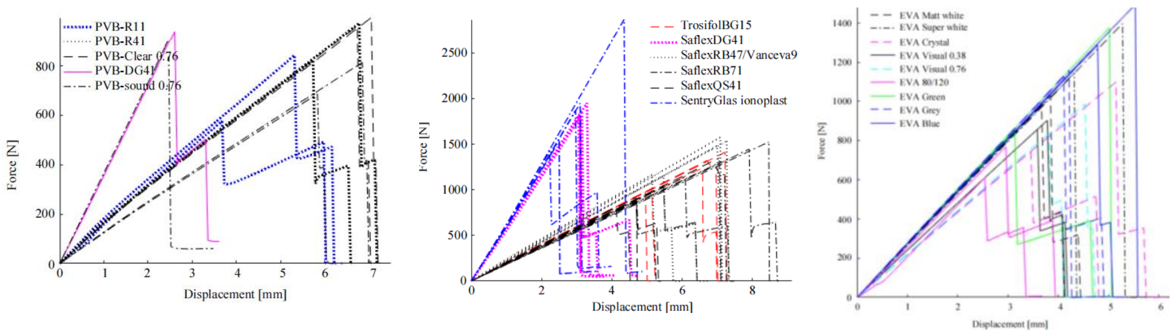

Figure 19. Load-displacement curve PVB, SGP, and EVA (Sable, Kinsella, & Kozłowski, 2019)

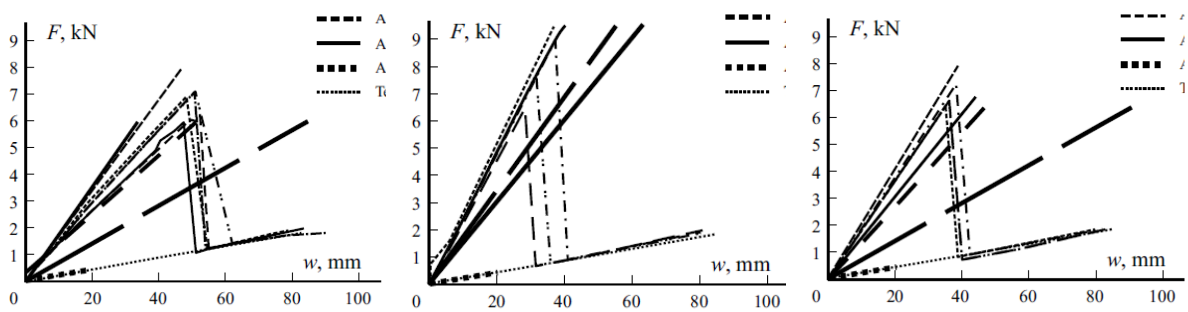

Figure 20. Load-displacement curve of PVB, SGP, and EVA (Serafinavicius, Kvedaras, & Sauciuvenas, 2013)

For the four-point bending tests, the first peak of the force-displacement is the point where the bottom glass panel breaks, and the interlayer is bonding the broken glass pieces together. The second peak is the point where the top glass panel breaks. All the graphs above show this failure mechanism with the bottom panel breaking first, and the top panel breaking afterwards at a much lower force.

It is not possible to compare the force-displacement graph of each individual interlayer in between different experiments, because each experiment uses different types of glass panels, and the results of the four-point bending test is heavily dependent on the dimension and thickness of the float glass panels used. Therefore, only the force-displacement graph of the same experiment will be compared for the properties of the different types of interlayers.

The force-displacement graphs show that SentryGlas interlayers can withstand a much larger amount of forces and a larger displacement. PVB and EVA interlayers seem to have similar performances, with EVA having slightly better properties.

5.3. Temperature, Solar Radiation, and Relative Humidity

The effect of temperature, UV radiation, and relative humidity on laminated glass with PVB, SGP, and EVA interlayers are also explored, and the results are show in deflection-time curves. The effect of temperature, humidity, and UV radiation can be observed by imposing heat, moisture, and solar radiation onto laminated glass with PVB, SGP, and EVA interlayer, and comparing its mid-span deflection with a sample without any external influence. Additionally, the deflection with only the effect of temperature, with only the effect of humidity, and with only the effect of UV radiation is also shown in this section, and this information is shown for laminated glass with PVB, SGP, and EVA interlayers.

5.3.1. Temperature

Figure 21 shows the results of four-point bending tests with and without the effect of temperature for laminated glass with PVB, SGP, and EVA interlayers. The experiments were performed in oven controlled temperature at 100 °C for 2 hours, and the mid-span deflection were measured with a LVDT. This experiment shows that temperature affects the mid-span deflection of laminated glass with SGP interlayer the least, and temperature affects the mid-span deflection of laminated glass with PVB and EVA interlayers by the same amount.

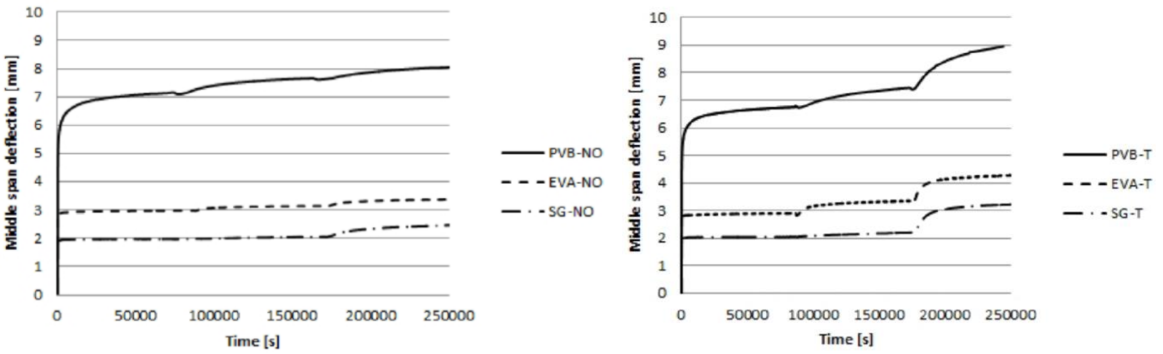

Figure 21. Middle Span Deflection over Time under Normal Conditions and under the Effect of Temperature (Serafinavicius, Lebet, Louter, Kuranovas, & Lenkimas, 2014)

5.3.2. Solar Radiation

Figure 22 shows the results of four-point bending tests with and without the effect of UV radiation for laminated glass with PVB, SGP, and EVA interlayers. Radiation source that emit spectrum similar to solar radiation were used in this experiment. This experiment was performed for 2000 hours (83 days) at a temperature of 45 °C and relative humidity level of 50%. This experiment shows that solar radiation affects the mid-span deflection of laminated glass with EVA interlayer the least, and solar radiation affects the mid-span deflection of laminated glass with PVB and SGP interlayers by the same amount.

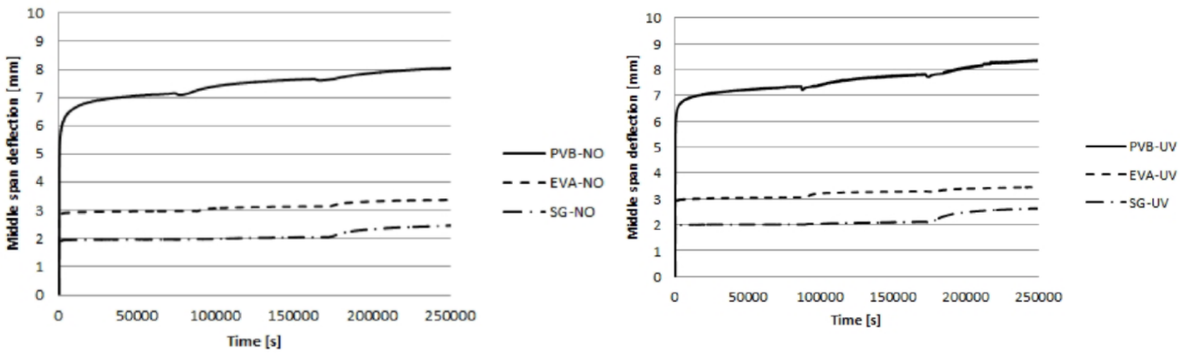

Figure 22. Middle Span Deflection over Time under Normal Conditions and under the Effect of UV Radiation (Serafinavicius, Lebet, Louter, Kuranovas, & Lenkimas, 2014)

5.3.3. Relative Humidity

Figure 23 shows the results of four-point bending tests with and without the effect of relative humidity for laminated glass with PVB, SGP, and EVA interlayers. The specimens were placed in a special humidity box with condensation effect, or 100% relative humidity level. The special humidity box is set to a controlled temperature of 50 °C, and the specimen was kept there for 336 hour (14 days). This experiment shows that relative humidity does not affect the deflection of laminated glass with PVB, SGP, and EVA interlayers.

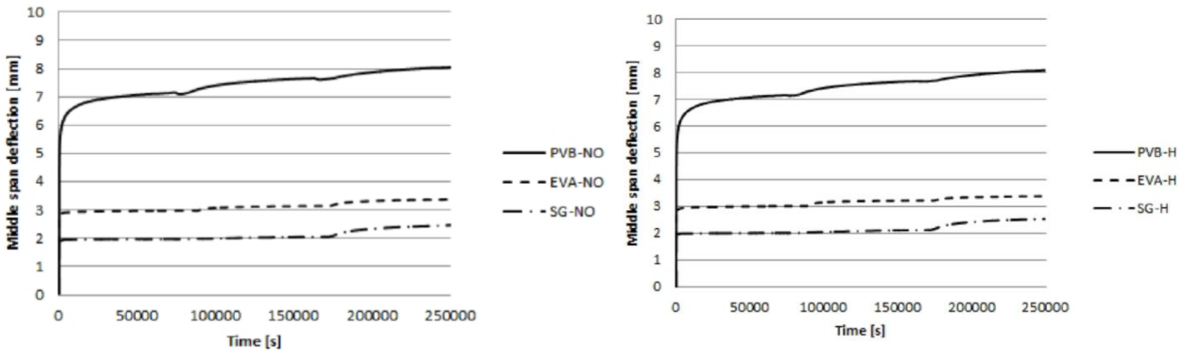

Figure 23. Middle Span Deflection over Time under Normal Conditions and under the Effect of Humidity (Serafinavicius, Lebet, Louter, Kuranovas, & Lenkimas, 2014)

5.3.4. Temperature, Solar Radiation, and Relative Humidity

Figure 24 shows the results of four-point bending tests with and without the effect of temperature, humidity, and UV radiation for laminated glass with PVB, SGP, and EVA interlayers. The specimens were first placed in oven controlled temperature at 100 °C for 2 hours. Then, these specimens are placed in a humidity box with 100% relative humidity level and a controlled temperature of 50 °C for 336 hour (14 days). After that, these specimens are placed under a radiation source that emit spectrum similar to solar radiation for 2000 hours (83 days) at a temperature of 45 °C and relative humidity level of 50%.

This experiment shows that temperature, humidity, and UV radiation affects the mid-span deflection of laminated glass with PVB interlayer the most, and temperature, humidity, and UV radiation affects the mid-span deflection of laminated glass with SGP and EVA interlayers by the same amount.

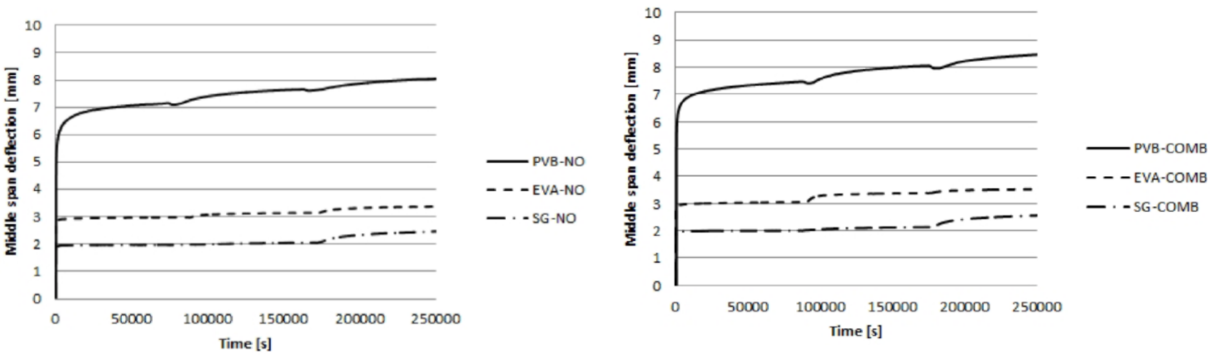

Figure 24. Middle Span Deflection over Time under Normal Conditions and over Time under the Effect of Temperature, Humidity, and UV Radiation (Serafinavicius, Lebet, Louter, Kuranovas, & Lenkimas, 2014)

Figure 25 shows the results of four-point bending tests with and without the effect of temperature, humidity, UV radiation, and combination for laminated glass with PVB, SGP, and EVA interlayers. For laminated glass with all 3 types of interlayer, temperature has the greatest impact on the mid-span deflection, and humidity barely has any impact on the mid-span deflection. UV radiation has considerable impact on the mid-span deflection for laminated glass with PVB interlayer, and UV radiation has very little impact on the mid-span deflection of laminated glass with SGP and EVA interlayer.

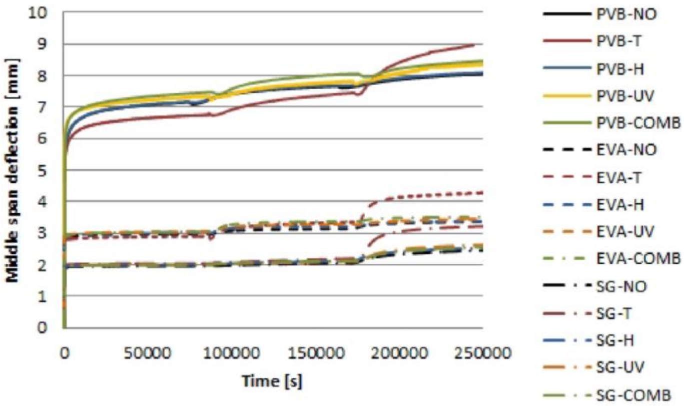

Figure 25. Effect of Temperature, Humidity, and UV Radiation (PVB, SGP, EVA Interlayer) (Serafinavicius, Lebet, Louter, Kuranovas, & Lenkimas, 2014)

Chapter 6: Connections

This chapter analyses the effect of connections on the type of interlayer to be used for laminated glass, and the conclusions of Hoogerwaard's master's thesis is used for this section. Specifically, the type of interlayer suitable for 6 different types of moment resisting portal frame connections and 6 different types of façade connections are concluded.

6.1. Connections

In Hoogerwaard's thesis, he analysed the sustainability aspects of the different types connections, and he took the types of interlayers into account in his study. Figure 26 shows the results of the multi-criteria analysis for the different types of connection for a moment resisting portal frame.

For moment resisting portal frame connections, SentryGlas interlayer would be necessary for the embedded connections, and PVB interlayer would be sufficient for adhesive connections and bolted connections (Hoogerwaard, 2020). For façade connections, SentryGlas would also be more suitable for the embedded connections, and PVB would be sufficient for all the ot her types of façade connections (Hoogerwaard, 2020).

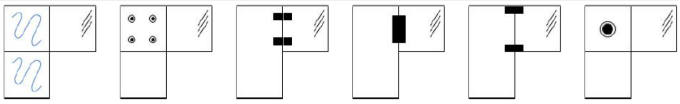

Type	Adhesive*	Bolted, rigid	Embedded	Embedded	Embedded	Bolted, hinged
Extra and /or treated glass[1]:	Heat-strength-ened is recomm ended, but not necessary	Heat-strength-ened is possible	Heat-strength-ened is possible	Heat-strength-ened is possible	Heat-strength-ened is done in literature	Heat-strength-ened is possible
Type of lamination [2]:	PVB	PVB	SentryGlas	SentryGlas	SentryGlas	PVB
Total indirect impact score	+	0	-	-	-	0

Figure 26. Effect of Connection on Interlayer Type in Moment Resisting Portal Frame Connections (Hoogerwaard, 2020)

The environmental impact of the different types of connections are concluded in the total indirect environmental impact score, which takes into account the extra and/or treated glass and the type of lamination. The extra and/or treated glass results is takes into account whether extra glass and/or heat treated glass is required to meet the structural requirements. For the type of lamination, Geert assumed Sentryglas to have a higher environmental impact than PVB; therefore, in this study, sentryglass is alloted a score of "-", and PVB is alloted a score of "0". However, it is also important to consider that SGP will require less glass thickness to meet the structural requirements and will allow for potential reuse.

When comparing the indirect impact score of moment resisting portal frame connections, it becomes apparent that adhesive connections are prefferred. This is because the glass usage of adhesive connection can be minimized, and PVB interlayer is sufficient for this type of connection. The choice of a bolted connection will lead to a higher environmental impact than that of ahesive connections, because heat-strengthened glass will be required. The choice of an embedded connection will lead to the highest environmental impact, because it will lead to the need to use head-strengthened glass panels and SGP interlayer. In addition, embedded connections are the least preferred with the need to use extra glass, heat-treated glass, and SentryGlas interlayers.

Part III: Structural Analysis

This section is on the structural analysis of laminated glass, and it is made up of a chapter on the analytical method and a chapter on the computer simulation. The chapter on the analytical method contains the methods to ensure that a laminated glass design is structurally safe under its ultimate limit state, its serviceability limit state, and its post-breakage state. The chapter on the computer simulation includes information for creating a finite element model in DIANA.

Chapter 7: Glass Design

This chapter contains information on how to analyse the structural performance of laminated glass with different types of interlayer using an analytical method. Specifically, this chapter includes information on the design life, the consequence class, the value of permanent and imposed loads, load combination calculations, deflection requirements, shear stiffness calculations, value of design thickness, tensile strength calculations, equivalent thickness calculations, and post-breakage calculations.

7.1. Design Life and Consequence Class

The design life is 50 years for typical buildings and structures. Consequence class 2 (CC2) is used for residential and office building, which is associated with reliability class 2 (RC2). Figure 27 shows the consequence classes as defined in the Eurocode EN 1990 Table B1.

Consequences Class	**Description**	**Examples of buildings and civil engineering works**
CC3	**High** consequence for loss of human life, *or* economic, social or environmental consequences **very great**	Grandstands, public buildings where consequences of failure are high (e.g. a concert hall)
CC2	**Medium** consequence for loss of human life, economic, social or environmental consequences **considerable**	Residential and office buildings, public buildings where consequences of failure are medium (e.g. an office building)
CC1	**Low** consequence for loss of human life, *and* economic, social or environmental consequences **small or negligible**	Agricultural buildings where people do not normally enter (e.g. storage buildings), greenhouses

Figure 27. Consequence classes (EN 1990 Table B1)

7.2. Values of Permanent and Imposed Loads

Permanent vertical loading is equal to the weight of the structure and its finishes, and figure 28 shows the values of distributed and point loads and their corresponding ψ factors. The point load of the imposed vertical loading is applied on the surface area of 100 x 100mm at the most unfavourable position. The point load of the imposed horizontal loading is applied on a surface area of 200 x 200mm at the most unfavourable position. The height of zone a is equal to 0.1m.

Building type category	Load [kN/m^2]	Point Load [kN]	ψ0	ψ1	ψ2
Residential	1.75	3.0	0.4	0.5	0.3
Office	2.5	3.0	0.5	0.5	0.3
Public	5.0	7.0	0.6	0.7	0.6

Figure 28. Value of loads (NEN-EN 1991-1) and ψ factors (NEN-EN 1990 NB)

7.3. Load Combination Calculations

Figure 29 shows the design value of actions for ULS combinations Ψ accounts for statistical nature of the load. KFI account for the consequence and reliability class, and KFI is equal to 1 for RC2.

Permanent actions		Leading variable action	Accompanying variable actions	
Unfavourable	Favourable		Main (if any)	Others
$1{,}35G_{kj;sup}$[a]	$0{,}9G_{kj;inf}$	--	$1{,}5\psi_{0;1}Q_{k;1}$	$1{,}5\psi_{0;i}Q_{k;i}$ ($i > 1$)
$1{,}2G_{kj;sup}$[b]	$0{,}9G_{kj;inf}$	**$1{,}5Q_{k,1}$**	--	$1{,}5\psi_{0;i}Q_{k;i}$ ($i > 1$)

Figure 29. Load Combination for the Design Actions in ULS (NEN-EN 1990+NB.4–1.2(B))

Persistent and transient design situations	Permanent actions		Accompanying variable actions	
	Unfavourable	Favourable	Main (if any)	Others
characteristic	**$G_{kj;sup}$**	**$G_{kj;inf}$**	**$Q_{k,1}$**	**$\psi_{0;i}Q_{k;i}$**
frequent	$G_{kj;sup}$	$G_{kj;inf}$	$\psi_{1;1}Q_{k;1}$	$\psi_{2;i}Q_{k;i}$
quasi-permanent	$G_{kj;sup}$	$G_{kj;inf}$	$\psi_{2;1}Q_{k;1}$	$\psi_{2;i}Q_{k;i}$

Figure 30. Load Combination for the Design Actions in SLS (BS EN 1990 NA.2.2.6)

7.4. Deflection Requirements

Maximum deflection of an edge of a laminated glass pane: $u_{max} = \frac{l_z}{100}$

l_z is the length of the edge (NEN2608 9.2(1))

Floor/roof used by people: w2 + w3 ≤ 3/1000 * ℓrep

in frequent load combination (Dutch Annex of Eurocode EN1990)

Roof: w2 + w3 ≤ 1/250 * ℓrep

characteristic load combination with imposed, wind, or snow load (Dutch Annex of Eurocode EN1990)

Figure 31 shows the visual representations of the vertical deflections w1, w2, and w3. w2 is the long-term part of the deflection under permanent loads, and w3 is the additional part of the deflection due to the variable actions.

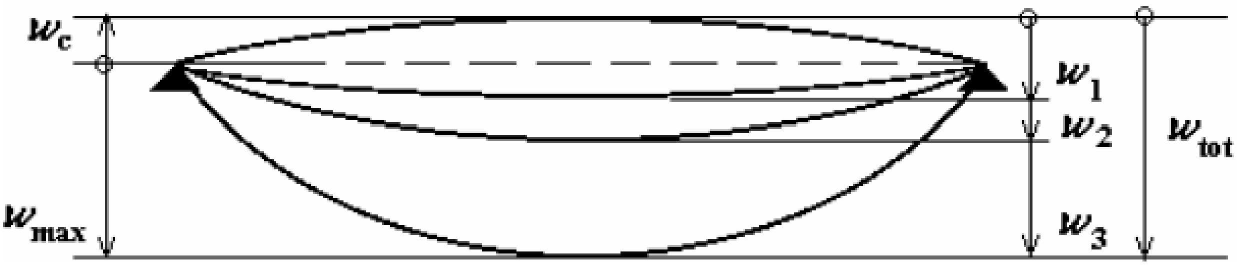

Figure 31. Vertical deflections as defined in (EN 1990)

In practice, maximum horizontal or vertical displacement: $l/250$

characteristic load combination

Balustrade total deformation: 20mm

characteristic load combination (NEN-EN1990)

7.5. Shear Stiffness Calculations

Shear Stiffness is dependent on the temperature and load duration, and the shear stiffness of interlayer at different load duration in standard temperature Tg=17°C from NEN2608 are shown in figure 32. The shear stiffness of interlayer at different load from NEN2608, prEN16613, and NS3510 are compared in figure 33.

Period	Load case	Load duration [s]	PVB G [N/mm2]	SGP G [N/mm2]
5 sec	Wind	5	13.77	181.28
10 sec		10	10.32	174.76
1 min		60	3.62	144.45
5 min		300	1.65	132.27
1 h		3600	0.95	96.3
24 h		86400	0.6	49.01
7 x 24 h		604800	0.5	32.96
1 month	Snow	2592000	0.42	22.22
50 years	Permanent	1.58E+09	0.05	6.42

Figure 32. Shear stiffness of interlayers (NEN2608 Table C.1)

Load duration [s]	PVB G NEN260 [N/mm2]	PVB G prEN 16613 [N/mm2]	PVB G NS 3510 [N/mm2]
5	13.77	3.3	3.3
10	10.32		
60	3.62		
300	1.65		
3600	0.95		
86400	0.6		
604800	0.5		
2592000	0.42	0.33	0.4
1.58E+09	0.05	0.33	0.4

Figure 33. Shear Modulus of PVB Interlayer

7.5.1. Maxwell Model of Shear Stiffness Calculations

Generalized Maxwell Model can be used to calculated the shear modulus of the interlayer at a given time instant t. The generalized Maxwell Model is a parallel chain of a single spring and several spring-dashpot Maxwell units, and a scheme of the generalized Maxwell chain is shown in figure 34. G_∞ is the long-term response of the chain, and Gp is the shear stiffness of the spring. ηp is the viscosity of the purely viscous damper. The shear stiffness modulus are horizontally shifted for the value of the shift factor, and the time-temperature superposition principle curve is shown in figure 35.

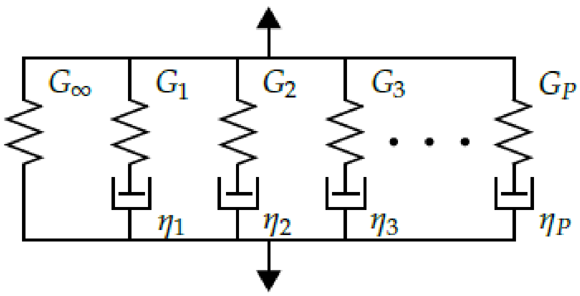

Figure 34. Scheme of the generalized Maxwell chain (Hána et al., 2019)

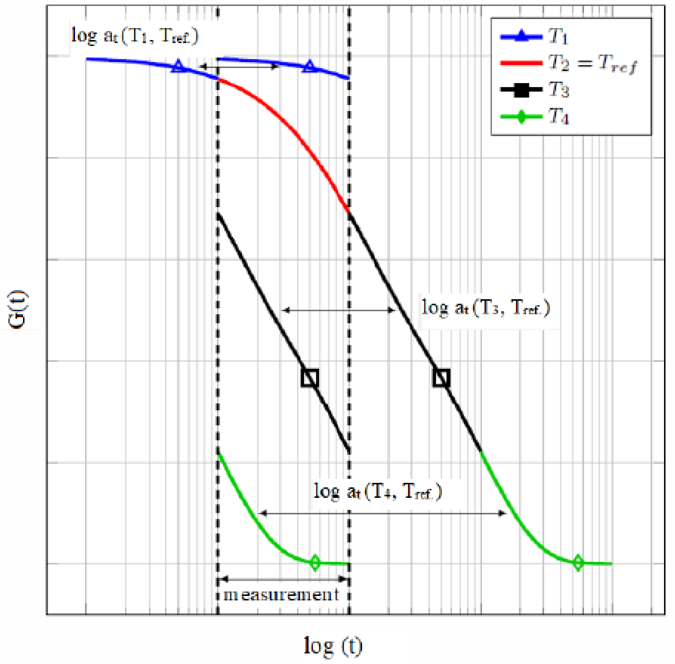

Figure 35. Time-temperature superposition principle master curve (Hána et al., 2019)

7.5.2. Inputs for Shear Modulus Calculations: EVA Interlayer

The input parameters for the generalized Maxwell model for EVA interlayer from 2 different sources are used to calculated the shear modulus of EVA interlayer at 17°C of different load durations, and the input parameters from the 2 sources are shown in figure 36 and figure 37. Source 1 is a paper Experimental and Numerical Study of Viscoelastic Properties of Polymeric Interlayers Used for Laminated Glass: Determination of Material Parameters by Hána et al. Source 2 are obtained from the textbook Dynamic Systems in Applications by Awrejcewicz, J. Since the 2 different sources yield similar results, the first source, which had a slightly lower result, will be used for the future calculations.

		Hána et el's Journal	Awrejcewicz's Textbook	Units
Long-term shear modulus	G∞	682.18	1009	kPa
Reference temperature	T0	20	20	°C
Parameters	C1	339.102	113	
	C2	1185.816	404	°C

Figure 36. Parameters for the generalized Maxwell model for EVA interlayer (EVALAM 80-120) (Hána et al., 2019) (Awrejcewicz, 2018)

p	Ɵp [s]	Gp [kPa] (Hána et el's Journal)	Gp [kPa] (Awrejcewicz's Textbook)	p	Ɵp [s]	Gp [kPa] (Hána et el's Journal)	Gp [kPa] (Awrejcewicz's Textbook)
1	10^{-9}	6933.9		**12**	10^{2}	445.1	350
2	10^{-8}	3898.6		**13**	10^{3}	300.1	411
3	10^{-7}	2289.2		**14**	10^{4}	401.6	126
4	10^{-6}	1672.7		**15**	10^{5}	348.1	425
5	10^{-5}	761.6		**16**	10^{6}	111.6	203
6	10^{-4}	2401.0		**17**	10^{7}	127.2	224
7	10^{-3}	65.2	1177	**18**	10^{8}	137.8	206
8	10^{-2}	248.0	447	**19**	10^{9}	50.5	133
9	10^{-1}	575.6	265	**20**	10^{10}	322.9	278
10	10^{0}	56.3	323	**21**	10^{11}	100.0	
11	10^{1}	188.6	267	**22**	10^{12}	199.9	

Figure 37. Parameters for the generalized Maxwell model for EVA interlayer (EVALAM 80-120) (Hána et al., 2019) (Awrejcewicz, 2018)

7.5.2.1. Shear Modulus Calculations: Hána et el's Journal

In this section, the input parameters from the 2 sources are entered into the generalized Maxwell model to calculate the shear modulus of EVA interlayer at different load durations. The results of the calculations are shown in figure 38 and figure 39.

Shift factor: $log_{10}\alpha_T = -\frac{C1\ (T-T0)}{C2+T-T0}$

$= -\frac{339.102*(17-20)}{1185.816+17-20}$

= 0.860

Shift relaxation time for p=1: Ɵp,0 = αT* Ɵp = $10^{0.860}*10^{-9}$ = 7.246*10^{-9}

Shift relaxation time for p=2: Ɵp,0 = αT* Ɵp = $10^{0.860}*10^{-8}$ = 7.246*10^{-8}

Shift relaxation time for p=22: Ɵp,0 = αT* Ɵp = $10^{0.860}*10^{12}$ = 7.246*10^{12}

Relaxation shear modulus for t= 50 years:

G(t) = G∞ + $\sum_{p=1}^{p} Gp * e^{-\frac{t}{\theta p,0}}$

= 0.68218 + (6.9339$* e^{-\frac{1576800000}{7.246*10^{-9}}}$ + 3.8986$* e^{-\frac{1576800000}{7.246*10^{-8}}}$ + ... + 0.1999$* e^{-\frac{1576800000}{7.246*10^{12}}}$)

= 1.35N/mm2

7.5.2.2. Shear Modulus Calculations: Awrejcewicz's Textbook

Shift factor: $log_{10}\alpha_T$ = - $\frac{C1\ (T-T0)}{C2+T-T0}$ = - $\frac{113*(17-20)}{404+17-20}$ = 0.845

Shift relaxation time for p=1: $\Theta_{p,0} = \alpha_{T*}\ \Theta_p$ = $10^{0.845}*10^{-3}$ = 7.005$*10^{-3}$

Shift relaxation time for p=2: $\Theta_{p,0} = \alpha_{T*}\ \Theta_p$ = $10^{0.845}*10^{-2}$ = 7.005$*10^{-2}$

Shift relaxation time for p=14: $\Theta_{p,0} = \alpha_{T*}\ \Theta_p$ = $10^{0.845}*10^{10}$ = 7.005$*10^{10}$

Relaxation shear modulus for t= 50 years:

G(t)= G∞ + $\sum_{p=1}^{p} Gp * e^{-\frac{t}{\theta p,0}}$

=1.009 + (1.177$* e^{-\frac{1576800000}{7.005*10^{-3}}}$ + 0.447$* e^{-\frac{1576800000}{7.005*10^{-2}}}$ + ... + 0.278$* e^{-\frac{1576800000}{7.005*10^{3}}}$)

= 1.41N/mm^2

Tijdsduur [s]	EVA G(t) Hána et el's Journal	EVA G(t) Awrejcewicz's Textbook
5	3.43	3.77
10	3.40	3.67
60	3.27	3.45
300	3.07	3.23
3600	2.65	2.84
86400	2.16	2.46
604800	1.87	2.21
2592000	1.70	1.99
1576800000	1.35	1.41

Figure 38. Calculated Shear Modulus of EVA Interlayer

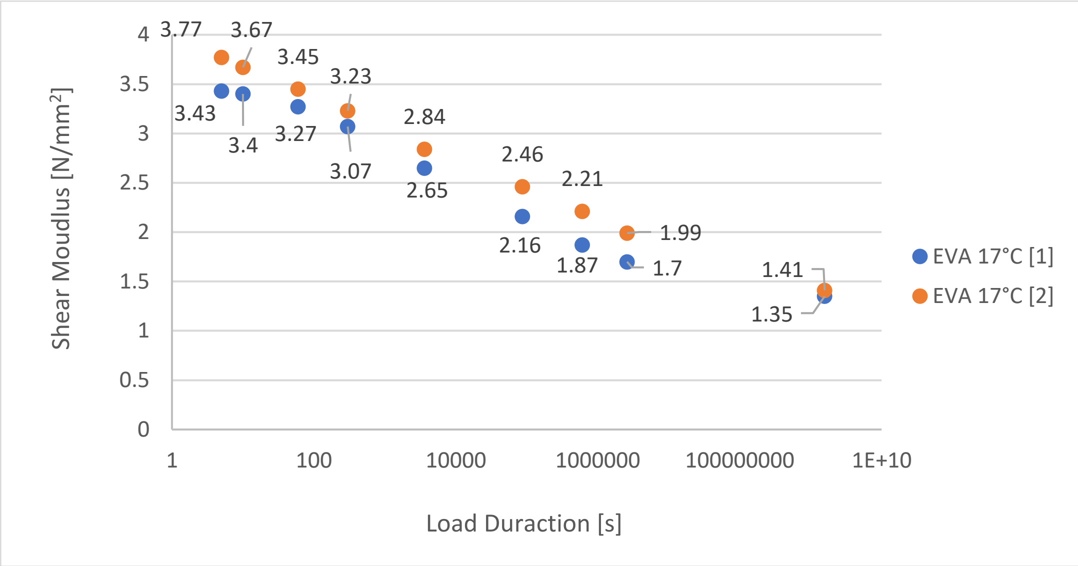

Figure 39. Shear Modulus of EVA Interlayer

7.6. Values of Design Thickness

The Thickness of the float glass is less due to manufacturing tolerance and cost, and the value of the design thickness are shown in figure 40.

Glass thickness specified [mm]	3	4	5	6	8	10	12	15	19
Design thickness t_{pl} [mm]	2.8	3.8	4.8	5.8	7.7	9.7	11.7	14.5	18

Figure 40. Specified and Design Glass Thickness (EN572)

7.7. Tensile Strength Calculations

Tensile strength:

$$f_{mt;u;d} = \frac{k_a \times k_e \times k_{mod} \times k_{sp} \times f_{g;k}}{\gamma_{m;A}} + \frac{k_e \times k_z \times (f_{b;k} - k_{sp} \times f_{g;k})}{\gamma_{m;V}}$$

Size effect factor k_a:

$k_a = 1$ normally

$k_a = 1.644 \times A^{-\left(\frac{1}{25}\right)}$ uniformly distributed surface pressure and nonlinear stress calculation OR point load

A is the area of the load (mm2)

Edge quality factor k_e:

k_e=1 loaded out of pane, heat-strengthened glass

k_e=0.8 loaded in pane, heat-strengthened glass

Surface quality factor k_{sp}: k_{sp}= 1 loaded out of pane, float glass

Characteristic tensile (bending) strength: $f_{g;k}$ = 45 N/mm^2

Glass material factor $\gamma_{m;A}$: $\gamma_{m;A}$=1.8

$\gamma_{m;A}$=1.6 if wind load is normative

Prestress tensile strength $fb_{;k}$: $fb_{;k}$ = 70 N/mm^2 heat-strengthened float glass

Prestress factor $\gamma_{m;V}$: $\gamma_{m;V}$ = 1.2

Zone factor k_z: k_z = 1 (heat-strengthened; zone 1, zone 1, zone 4)

consider without prestress (heat-strengthened; zone 3)

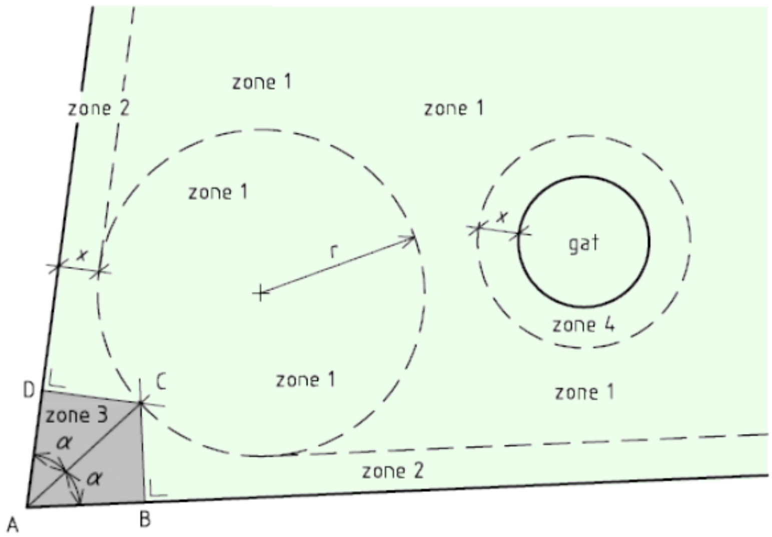

Figure 41. Glass zones (NEN 2608 figure 2)

Load Duration factor k_{mod}: Load duration factor takes into account stress corrosion

$$k_{mod} = \left(\frac{5}{t}\right)^{\frac{1}{c}}$$

c is the corrosion factor, usually 16 (NEN2608 Table 5)

t is the load duration in seconds

7.8. Equivalent Thickness Calculations

Equivalent Glass Thickness ULS (mm): $t_{gg;u} = MIN\left(t_{gg;i;u}\right)$

Design value ULS (mm):

$$t_{gg;i;u} = \sqrt{\frac{(1-\omega_\sigma) \times \sum_{j=1}^{n}\left(t_{pl;j}^3\right) + \omega_\sigma \times \left(\sum_{j=1}^{n}\left(t_{pl;j}\right)\right)^3}{t_{pl;i} + 2 \times \omega_\sigma \times t_{m;i}}}$$

Equivalent glass thickness SLS (mm):

$$t_{gg;ser} = \sqrt[3]{(1-\omega_w) \times \sum_{i=1}^{n}\left(t_{pl;i}^3\right) + \omega_w \times \left(\sum_{i=1}^{n}\left(t_{pl;i}\right)\right)^3}$$

$t_{pl;i}$	Glass plate thickness in mm
$t_{pl;j}$	Glass plate thickness in mm
n	Number of glass plates
$t_{m;j}$	Distance center glass plate and laminated glass unit

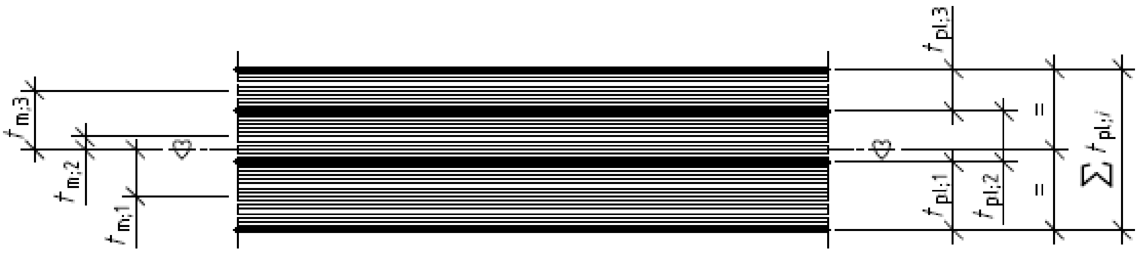

Figure 42. Laminated glass unit with indicated distances for calculation of the equivalent thickness (NEN2608 Annex F)

Shear Coupling factor ω: Shear coupling factor describes the shear interaction

Shear coupling factor of interlayer ULS:

$$\omega_w = \frac{1}{1 + \frac{\beta}{L_w}}$$

Shear coupling factor of interlayer SLS:

$$\omega_\sigma = \frac{1}{1 + \frac{\beta}{L_\sigma}}$$

$$\beta = \frac{1}{2} \times \frac{\pi^2}{L_A^2} \times \frac{E_g}{1 - v_g^2} \times \frac{X}{G_{tl}}$$

Factor in N/mm² X:

$$X = \max\left(\begin{array}{c}\sum_{i=1}^{n-1}\left(t_{pl;i} \times t_{v;i}\right) \\ \sum_{i=2}^{n-1}\left(t_{pl;i} \times t_{v;i-1}\right)\end{array}\right)$$

E_G	Young's modulus glass in N/mm2
v_g	Poisson ratio glass
G_{tl}	Shear modulus interlayer in N/mm2
n	Number of glass layers
$t_{pl;i}$	Glass plate thickness
$t_{v;i}$	Interlayer thickness

Shape factor determined by geometry:

$$L_A^2 = \frac{1}{\frac{1}{B^2} + \frac{1}{H^2}}$$

Shape factor SLS:

$$L_w = k_w \times \left(\frac{2 \times a}{z}\right)^{-0.04354}$$

Shape factor ULS:

$$L_\sigma = k_\sigma \times \left(\frac{2 \times a}{z}\right)^{-0.60906}$$

$$z = \frac{B_1 + H_1}{2}$$

B	Width of element in mm
H	Height of element in mm
k_w	factor according to NEN2608 Table C.3
a	Shortest length of element in mm
k_σ	factor according to NEN2608 Table C.3
B_1	Width of point load in mm (parallel to B), equal to B in case of uniform pressure
H_1	Height of point load in mm (parallel to H). equal to H in case of uniform pressure

$\frac{B}{H}$	k_w	k_σ
≤ 0,3	0,893	1,697
0,4	0,895	1,697
0,5	0,925	1,726
0,6	0,944	1,747
0,7	0,965	1,773
0,8	0,982	1,800
0,9	0,994	1,815
1,0	1,002	1,832
1,1	0,998	1,832
1,2	0,993	1,832
1,3	0,986	1,829
1,4	0,978	1,822
1,5	0,970	1,808
1,6	0,961	1,793
1,7	0,952	1,776
1,8	0,943	1,759
1,9	0,934	1,742
2,0	0,925	1,726
2,1	0,917	1,713
2,2	0,910	1,703
2,3	0,903	1,698
2,4	0,898	1,697
2,5	0,895	1,697
≥ 2,6	0,893	1,697

Figure 43. kw and k factors (NEN 2608 Table C.3)

7.9. Post-breakage Calculations

According to NEN 2608 Annex D, the Method of Fine and Kinney can be used to calculate the post-breakage situation. The values for the Method of Fine and Kinney can be found in figure 44 and figure 45.

The risk of the damage: RS=WS x BS x ES

Damage to structural element	**Risk**
Lateral breakage on one side	$RS < 70$
Lateral breakage on two sides	$70 < RS < 400$
Complete breakage of the structural element	$RS > 400$

Figure 44. Determination of the Degree of Damage (NEN 2608 Annex D)

Probability of damage with or without intent	*WS*	Exposure of structural element	*BS*	Consequence of complete break	*ES*
Virtually impossible	0.1	Very seldom	0.5	First aid	1
Practically impossible	0.2	A few times per year	1	Minor injury	3
Conceivable, but very improbable	0.5	Monthly	2	Serious injury	7
Only possible in the long term	1	Weekly	3	One death	15
Unusual, but possible	3	Daily	6	More than one death	40
Very possible	6	Constant	10	Catastrophe, many deaths	100
Can be expected	10				

Figure 45. Determination of Risk of Breakage of the Structural Elements (NEN 2608 Annex D)

Part IV: Sustainability Analysis

This section includes a chapter on the EPDs and shadow costs and a chapter on the end-of-life recycling options. The chapter on the EPDs and shadow costs describe the methods and the final results of the shadow costs of different stages of the life-time and the different impact categories. The chapter on the end-of-life recycling options describe the different options for recycling float glass, interlayer, and laminated glass.

Chapter 8: EPDs and Shadow Costs

In this chapter, Environmental Product Declarations from different glass production companies and design firms are used to calculate the shadow costs of laminated glass, and these shadow costs are displayed in bar graphs. Specifically, the shadow costs are calculated for 7 impact categories for the production section (A1 to A3), the waste processing section (C3), the disposal section (C4), and the benefits and loads beyond system boundaries section (D). Additionally, the shadow cost of the contribution by the PVB interlayer, the float glass, and the fixed process and the shadow costs of different configurations of laminated glass are analysed.

8.1. Life Cycle Analysis

Life Cycle Analysis (LCA) is a methodology that take into account all of the environmental impacts associated with all the stages of the life-cycle of a product, process, or service. A Life Cycle Analysis can either be cradle-to-grave, cradle-to-gate, or cradle-to-cradle. The cradle-to-grave analysis takes into account the environmental impact from raw material extraction to the disposal of the product. The cradle-to-gate analysis takes into account the environmental impact from manufacturing of the product until it leaves the factory gate. The cradle-to-cradle analysis is conducted when the waste is used for a new cycle. Instead of performaing a Life Cycle Analysis on all of the environment impacts, it is also possible to focus on 1 specific issue: there are methodologies that focus on a product's carbon footprint or embodied energy.

Embodied energy is the total amount of energy required to produce any product or service, and the energy is considered to be embodied or incorporated in the product. Specifically, embodied energy would include the amount of energy used during the mining and processing the natural resources, manufacturing, transportation, and product delivery (Achintha, 2016). Float glass has an embodied energy of 15MJ/kg (Achintha, 2016).

The carbon footprint of a building is the carbon dioxide equivalent of all the greenhouse gases associated with the construction and the operation of the building in its lifetime (Achintha, 2016). The carbon footprint can be divided into capital carbon and operational carbon. Capital carbon, or embodied carbon, is the carbon associated with the materials and construction process, and operational carbon is carbon associated with the operation and maintenance (Achintha, 2016).

8.2. Environmental Product Declaration

An Environmental Product Declaration is a declaration of the environment impact of the life-cycle of a product. According to the standard EN 15804, the entire life cycle in the EPD is divided into 4 stages: its product stage, construction process stage, use stage, and the end of life stage. The 4 stages are futher categorized, and figure 46 shows the specific categories in detail. The environmental impact of each category are added together for the total impact of the product.

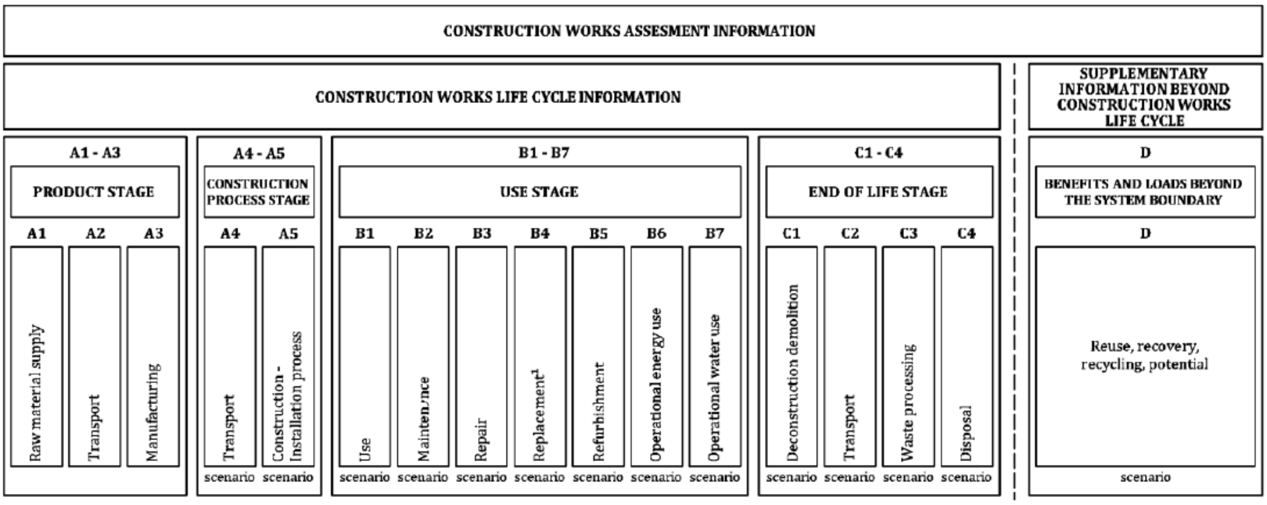

Figure 46. Different Modules within an EPD according to Standard EN 15804

The environmental impact of the EPD include human toxicity, ecotoxicity, and depletion of abiotic resources, and these 3 sections can be further categorized into 11 specific categories. The 11 impact categories and their shadow cost are shown in figure 47. This categorization is determined by SBK (Stichting Bouwkwaliteit or institution for the quality of buildings) in the Netherlands. The environmental impact is quantified in the shadow cost of the environmental impact, and the units used are equivalent euros. Information on the shadow costs can be found in the NMD (nationale milieu database or dutch national environmental database).

	Impact category	**Equivalent unit**	**Shadowcosts, €/equivalent**
Human toxicity	Human toxicity	1,4 DCB-eq	0.09
	Climate change	kg CO_2-eq	0.05
	Ozone layer depletion	kg CFC-11-eq	30
	Photochemical oxidants (smog)	kg C_2H_4	2
Ecotoxicity	Acidification	kg SO_2-eq	4
	Eutrophication	kg $(PO_4)_3$–eq	9
	Ecotoxicity, fresh water	1,4 DCB-eq	0.03
	Ecotoxicity, salt water	1,4 DCB-eq	0.0001
	Ecotoxicity, terrestical	1,4 DCB-eq	0.06
Depletion of abiotic resources	Non energy containing resources, as for example minerals	kg SB-eq	0.16
	Energy containing resources, fossil fuels	kg Sb-eq	0.16

DCB = Dichlorobenzene
CFC = Chlorofluorocarbons
Sb = Measured compared to antimony, or stibium (Sb)

Figure 47. Eleven Impact Categoried to assess the Environmental Impact

8.3. Shadow Costs

8.3.1. Sample Calculations

Figure 48 shows an sample calculation of how the shadow cost of the 7 impact categories is calculated. The first column in the table below shows the environmental impact in kilogram for 1m2 of laminated glass; for example, the global warming impact for 1m2 of laminated glass is 32.100 kg of CO2, and this information is found in the Environmental Product Declaration of laminated glass. The second column shows the global warming impact per kilogram of laminated glass, and this is calculated by dividing the first column by the weight of 1m2 of laminated glass.

The third column shows the environmental cost in euro per kilogram of impact. The last column shows the shadow cost in euro per kilogram laminated glass, which is calculated by multiplying the third column by the fourth column. After the shadow cost of the each of the 7 impact categories are found, the total shadow cost of the laminated glass is found by adding the shadow cost of the 7 impact categories.

Impact Category	Env. Impact [kg X]	Env. Impact per kg laminated glass [kg X/kg glass]	Environmental cost [euro/X]	Shadow Cost [euro/kg]
Global warming (GWP100) [kg CO2]	32.100	1.546	0.05	0.077
Ozone layer depletion (ODP) [kg CFC-11]	0.000	0.000	30	0.000
Acidification [kg SO2]	0.131	0.006	4	0.025
Eutrophication [kg (PO4)3-]	0.039	0.002	9	0.017
Photochemical oxidation [kg Ethene]	0.008	0.000	2	0.001
Abiotic depletion, non fuel [kg Antimone]	0.000	0.000	0.16	0.000
Abiotic depletion, fuel [MJ]	416.000	0.010	0.16	0.002
Total Shadow Cost				0.122

Figure 48. Production Stage (A1 to A3) 44.2 SGG STADIP from Saint Gobain

Global Warming Impact per 1m² glass = 32.100 $kgCO_2/1m^2$ glass

Global Warming Impact per kg glass = $\frac{\text{global warming impact in kg CO2}}{weight\ of\ 1m2\ laminated\ glass}$

$= \frac{32.100 \text{ kg CO2}}{1m2} * \frac{1\ m2}{20.76kg}$

= 1.546 $kgCO_2$/kg laminated glass

Environmental cost of global warming = 0.05 euro/$kgCO_2$

Shadow cost of global warming = global warming Impact per kg glass * env. cost

= 1.546 $kgCO_2$/kg laminated glass * $\frac{0.05\ euro}{kgco2}$

= 0.077 euro/kg laminated glass

Total shadow cost = shadow cost of global warming + acidification + eutrophication + photoch. oxidation + abiotic depl.

= 0.077 euro/kg + 0.025 euro/kg + 0.017 euro/kg + 0.001 euro/kg + 0.002 euro/kg

= 0.122 euro/kg laminated glass

8.3.2. Production Stage, End-of-Life Stage, and Benefit and Load Beyond System Boundaries

In this section, the shadow costs of the 7 impact categories from section A1 to A3, section C3, section C4, and section D are displayed in bar graphs. Specifically, the shadow cost information from AGC, Saint Gobain, and Okalum GmbH are compared in this section. Section A1 to A3 is the production process stage; section C3 and C4 are waste processing stage and disposal stage respectively. Section D shows the benefit and load beyond the system boundaries. The stages that are related to transportation and maintenance, which include section A4, section B2, and section C2, are not taken into account in this analysis. This is because they are heavily dependent on its assumptions and are too subjective.

Figure 49 shows the shadow cost of 44.2 laminated glass from AGC. For the 44.2 laminated glass from AGC, when comparing the shadow cost of the different stages, it can be seen that the production process stage (A1 to A3) has a much higher shadow cost than that of the waste processing stage (C3), the disposal stage (C4), and the benefits and load beyond system boundaries (D).

For the 44.2 laminated glass from AGC, when comparing the shadow cost of the 7 impact categories, it can be seen that the shadow cost of the global warming impact is always the highest for all stages. The shadow costs of the acidification impact and the eutrophication impact are the second and third highest respectively; the shadow cost of these 2 impact categories are significantly lower than that of global warming impact, but they still have a substantially amount of shadow cost.

For 44.2 laminated glass from AGC, the amount of benefit and load beyond the system boundaries, from section D, are due to the recycling of PVB and glass trimming and the recycling of packing waste like wood and cardboard.

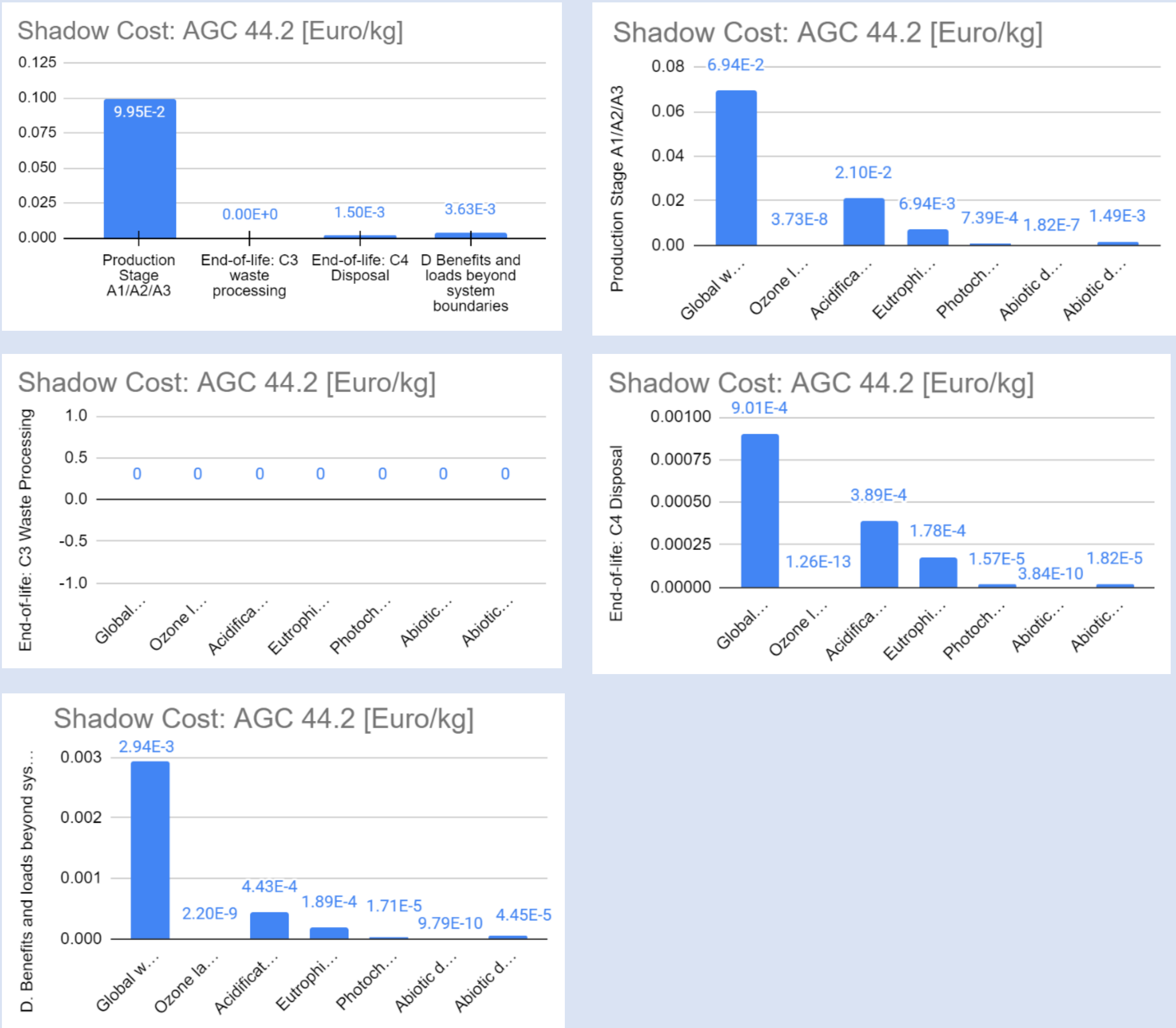

Figure 49. Shadow cost of AGC 44.2

Figure 50 shows the shadow cost of 44.2 laminated glass from Saint Gobain. The shadow cost of the 44.2 laminated glass from Saint Gobain shows the same trend as that of the 44.2 laminated glass from AGC. For the 44.2 laminated glass from Saint Gobain, the production process stage (A1 to A3) has a much higher shadow cost than that of the other stage; in addition, the shadow cost of the Global Warming (GWP100) impact is always the highest, followed by the shadow cost of the Acidification impact and the Eutrophication impact respectively.

At the end-of-life stage, Saint Gobain assumed 5% recycling and 95% waste disposal while AGC assumed 100% waste disposal. This is why EPD of Saint Gobain includes both the waste processing stage (C3) and the disposal stage (C4) while the EPD of AGC only includes disposal (C4). The sum of the shadow cost of the waste processing stage (C3) and the disposal stage (C4) of Saint Gobain is lower than the shadow cost of the disposal stage (C4) of AGC, and this shows that the shadow cost can be slightly reduced in almost all the impact categories even with a 5% recycling rate.

This EPD from Saint Gobain did not include section D, but cullent are considered input material without environmental burden in section A3.

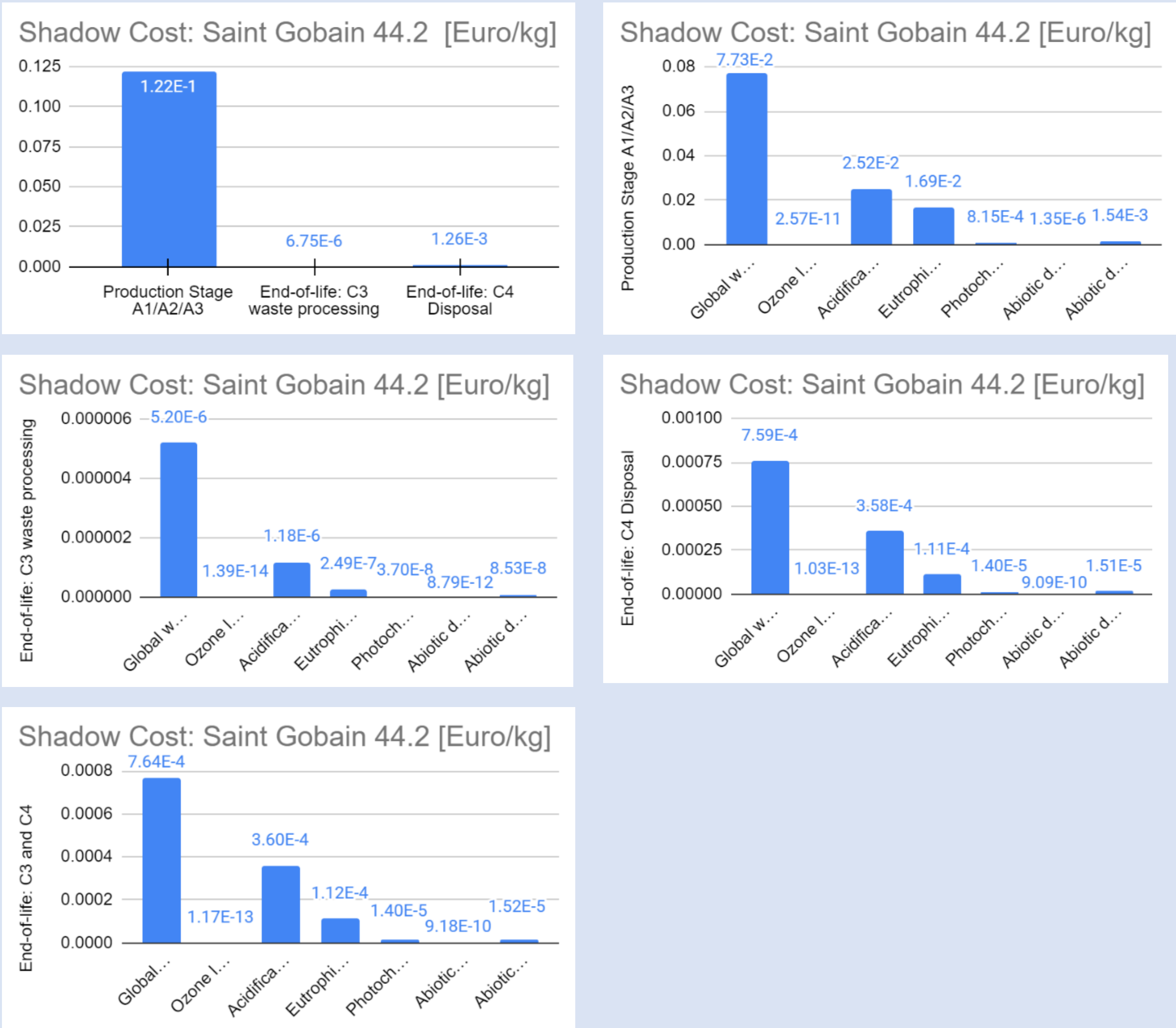

Figure 50. Shadow Cost of Saint Gobain 44.2

Figure 51 shows the shadow cost of 44.2 laminated glass from Okalum GmbH. The shadow cost of the 44.2 laminated glass from Okalum GmbH further confirmed the trend from that of Saint Gobain and AGC. For the 44.2 laminated glass from Okalum, the production process stage (A1 to A3) has a much higher shadow cost than that of the other stage; in addition, the shadow cost of the global warming impact is always the highest, followed by the shadow cost of the acidification impact and the eutrophication impact respectively.

Just like Saint Gobain, Okalum also assumed both recycling and waste disposal at the end-of-life stage. The shadow cost of Okalum at the disposal stage (C4) is lower than that of Saint Gobain, and the shadow cost of Okalum at the waste disposal stage (C3) is higher than that of Saint Gobain. Perhaps Okalum assumed a much higher recycling rate than the 5% assumed by Saint Gobain.

The sum of the shadow cost of Okalum for the waste processing stage (C3) and the disposal stage (C4) is lower than that of Saint Gobain in almost every impact category. This shows that perhaps the shadow cost can be reduced in almost all the impact categories with an increasing recycling rate.

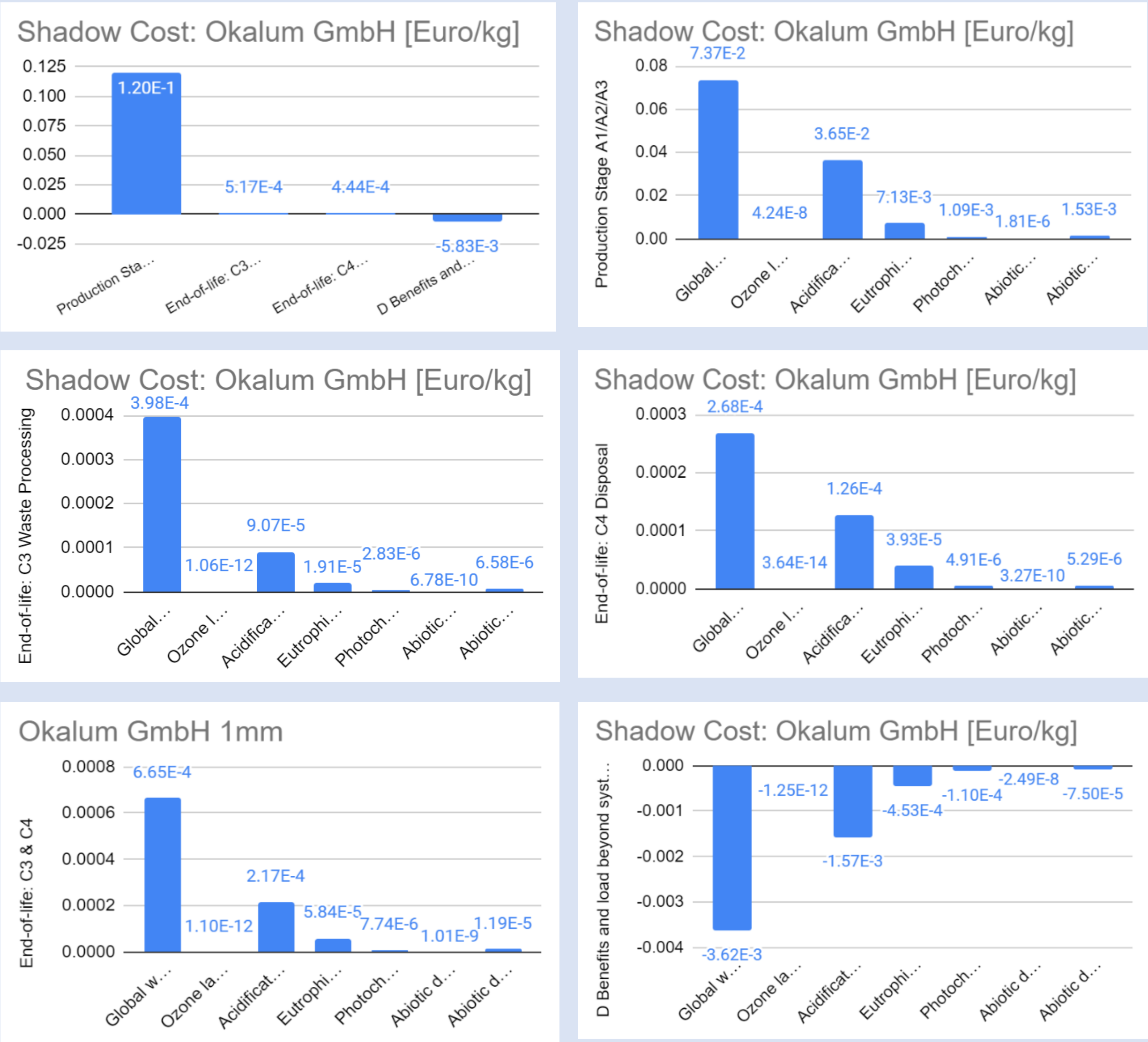

Figure 51. Shadow Cost of Okalum GmbH

8.3.3. Different Configurations of Laminated Glass

In this section, the shadow cost of laminated glass with different glass thickness and different number of interlayer from Saint Gobain and AGC during the production stage (A1 to A3) are analysed. Specifically, the shadow cost of 33.1, 44.1, 33.2, 44.2, 55.2, and 66.2 laminated glass are considered.

Figure 52 shows the shadow cost of laminated glass with different glass thickness and different number of interlayer from Saint Gobain during the production stage (A1 to A3). During the production stage (A1 to A3), for the different configuration of laminated glass from Saint Gobain, it can be seen that, as the thickness of glass and interlayer varies, the shadow cost of these laminated glass only differ slightly. The shadow cost of 55.2 laminated glass is only slightly higher than that of 33.2 laminated glass, and the shadow cost of 33.2 laminated glass is slightly higher than that of 33.1 laminated glass.

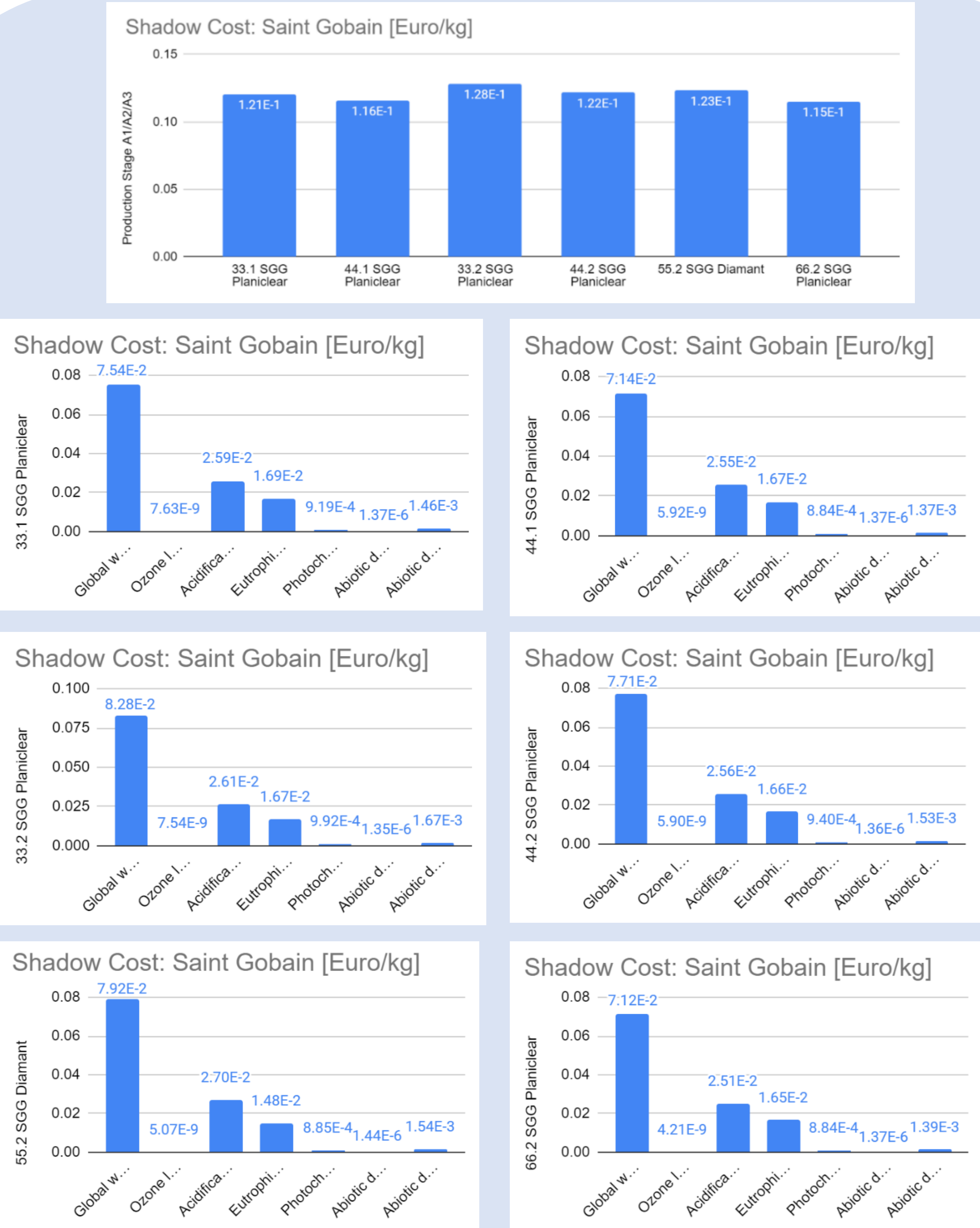

Figure 52. Shadow Cost of Saint Gobain, Different Configuration of Laminated Glass

Figure 53 shows the shadow cost of laminated glass with different glass thickness and different number of interlayer from AGC during the production stage (A1 to A3). The shadow cost of AGC during the production stage (A1 to A3) also confirmed the trend from that of Saint Gobain: as the thickness of glass and interlayer varies, the shadow cost of laminated glass of different configuration only differ slightly. In addition, for all of the different configuration of laminated glass, the shadow cost of Saint Gobain is slightly higher than that of AGC.

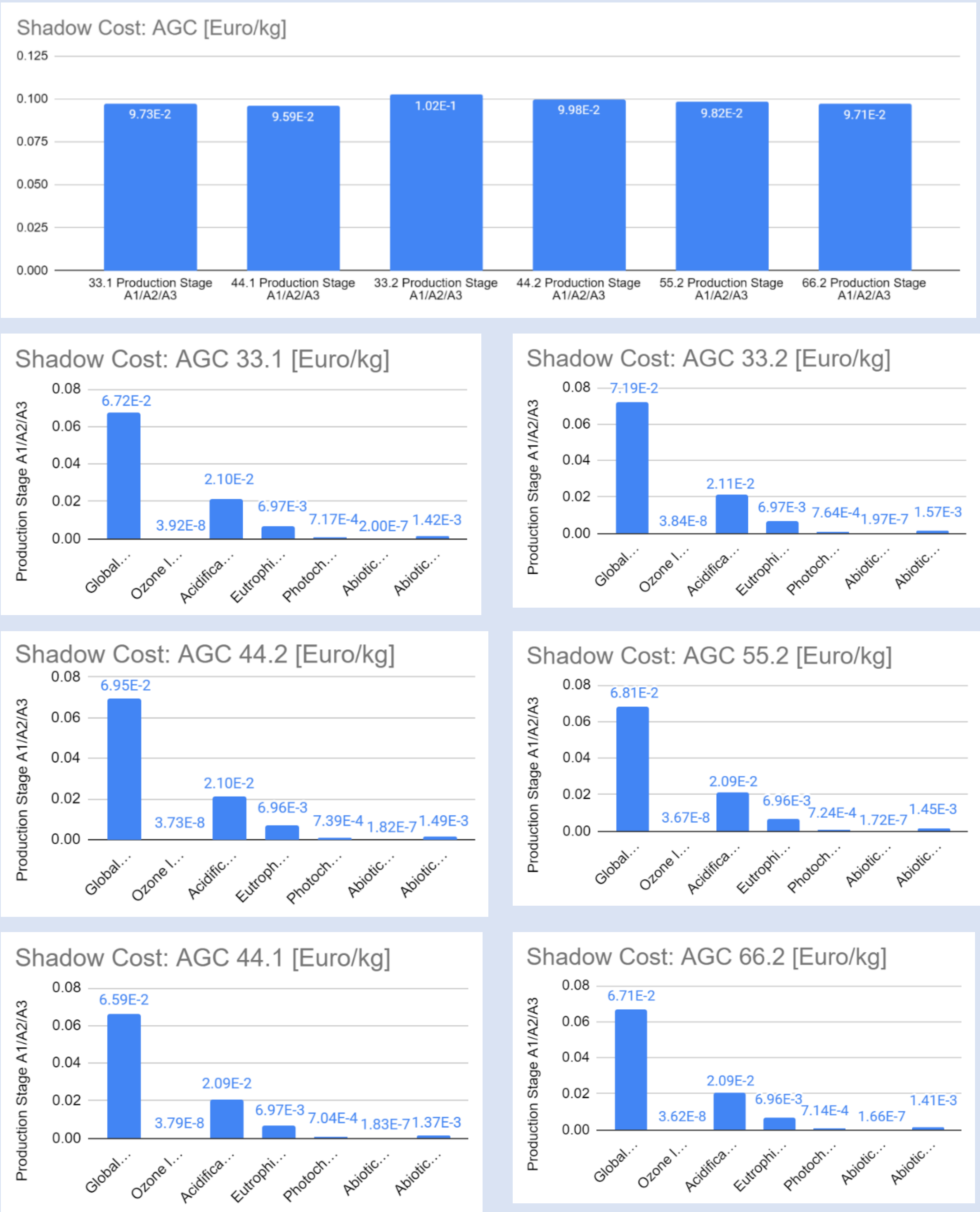

Figure 53. Shadow Cost of AGC, Different Configurations of Laminated Glass

8.3.4. Contribution of the Interlayer, Glass, and Fixed Process

Figure 54 shows the shadow cost of AGC divided into the percentage of contribution by the PVB interlayer, the float glass, and the fixed process, and the this division of shadow cost is provided for the production section (A1/A2/A3), the waste processing section (C3), the disposal section (C4), and the benefits and loads beyond system boundaries section (D).

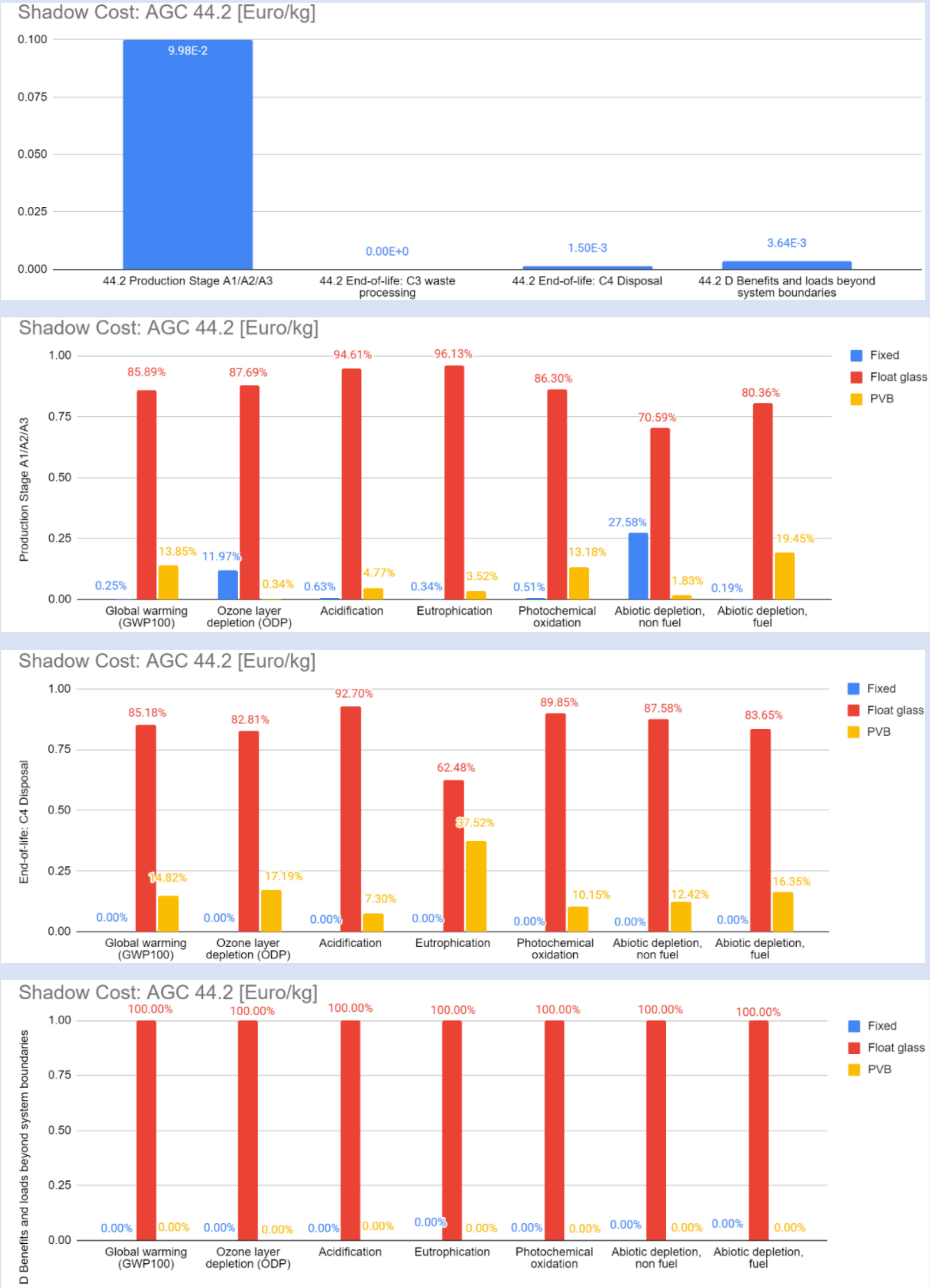

Figure 54. Shadow Cost of AGC, Contribution of Interlayer, Glass, and Fixed Process

In the production section (A1 to A3), the percent contribution of glass in the shadow cost in is always significantly higher than that of the interlayer and the fixed process in all of the 7 impact categories. The percentage contribution of the fixed process is significant in the abiotic depletion (non-fuel) impact and the ozone layer depletion impact. The percentage contribution of the interlayer is the most significant the abiotic depletion (fuel) impact, followed by the global warming impact and the photochemical oxidation impact, which has a lower but still significant percent contribution.

Just like that of the production section (A1 to A3), the percent contribution of glass in the shadow cost in the disposal stage (C4) is always significantly higher than that of the interlayer in all of the 7 impact categories. Comparing the percent contribution of the interlayer in the 7 categories, the percent contribution of the interlayer in the eutrophication impact is significantly higher than that of the other impact categories.

Only the shadow cost of the glass component in laminated glass is considered in the benefits and load beyond system boundaries section (D). The shadow cost of the interlayer component is considered to be zero in section D, and this shows that the interlayer component is not currently being recycled at AGC.

8.3.5. Production Stage

In this section, the shadow cost from Tecnoglass, Laurier Architectural, and Trakya Cam Sanayii A.S. in its production stage A1, A2, and A3 are compared and analysed. Both companies used the TRACI2.1 software and the CML4.1 software to analyse the environmental impact of their laminated glass in its production stage A1, A2, and A3 with respect to the 7 impact categories.

Figure 55 shows the shadow cost of Laurier Architectural in the production stage from the software TRACI2.1 and the software CML4.1. For the laminated glass from Laurier Architectural, the shadow cost of the global warming impact is the highest; the shadow cost of the acidification impact, the eutrophication impact are lower, but they are still a significant amount.

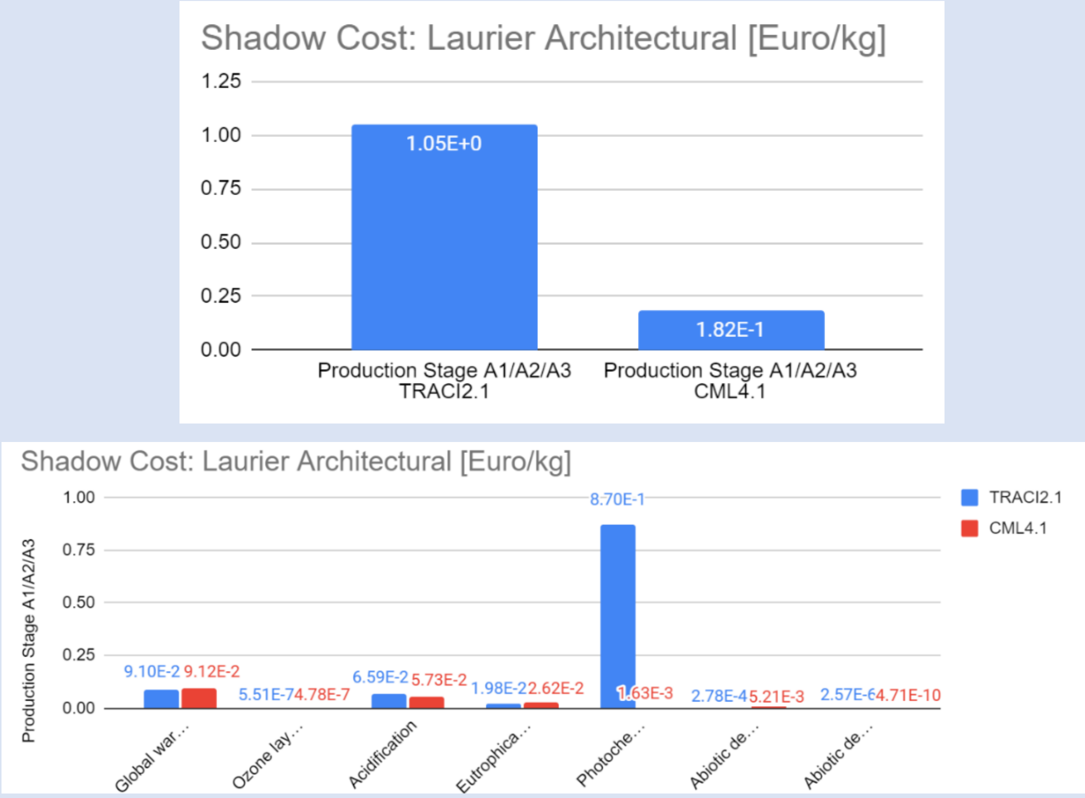

Figure 55. Shadow Cost of Laurier Architectural

Figure 56 shows the shadow cost of Tecnoglass in the production stage from the software TRACI2.1 and the software CML4.1. For the laminated glass from Tecnoglass, for the production stage A1, A2, and A3, the global warming impact has the highest shadow cost, and the shadow cost of the acidification impact, the eutrophication impact, and the abiotic depletion (non-fuel) impact are also considerably high. The shadow cost of production stage A1 and A3 are significantly higher than that of production stage A2. The shadow cost of production stage A3 is the highest; the shadow cost of production stage A1 is slightly lower, but it is still a significant amount.

For both Tecnoglass and Laurier Architectural, for production stage A1, A2, and A3, the shadow cost derived from the TRACI2.1 software is significantly higher than the shadow cost derived from the CML4.1 software. This significant difference in between the shadow cost of these 2 software is caused by the fact that the shadow cost of the photochemical oxidation for TRACI2.1 is extremely high. This extremely high shadow cost is most likely due to the fact that TRACI2.1 considered photochemical impact to be more damaging to your health and weighed this impact more heavily.

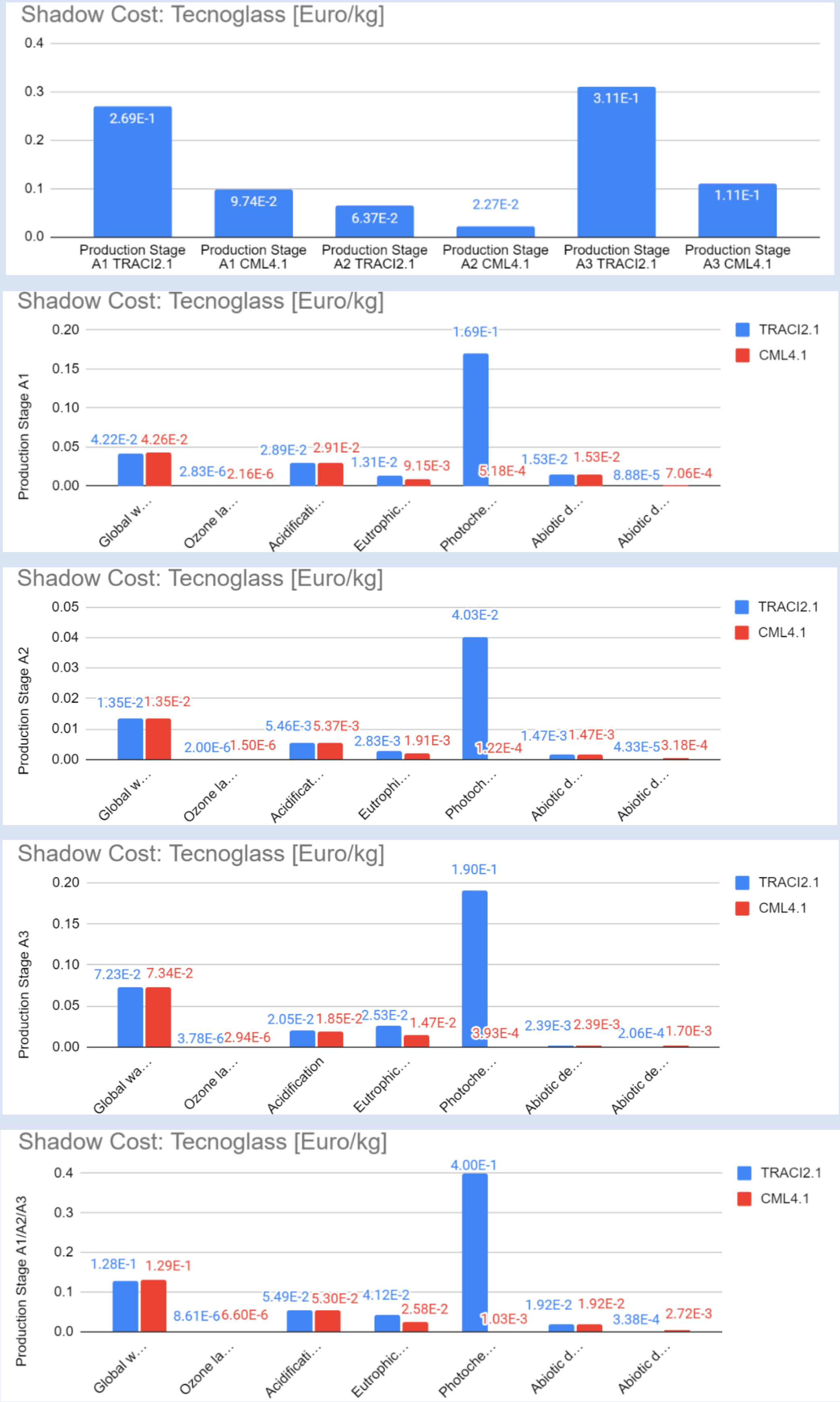

Figure 56. Shadow Cost of Tecnoglass

Figure 57 shows the shadow cost of Trakya Cam Sanayii A.S. in the production stage. The shadow cost information of Trakya Cam Sanayii A.S. further confirms the trend in between production stage A1, A2, and A3 from Tecnoglass and Laurier Architectural. The shadow cost of production stage A1 and A3 are significantly higher than that of production stage A2, and the shadow cost of production stage A3 is slightly higher than that of production stage A1.

Figure 57. Shadow Cost of Trakaya Cam Sanyii

Chapter 9: End-of-Life: Recycling

In this chapter, the recycling options of float glass, interlayer, and laminated glass at the end of their life-time are explored. The current research and industry practices on float glass recycling, interlayer recycling, and laminated glass recycling are included in this section.

9.1. Float Glass Recycling

The most sustainable option of float glass recycling is to recycle the float glass back into the float glass industry; however, it is more common and easier to downcycle the float glass into another product. Downcycling is a recycling practice that involves breaking an item down into its components or materials, and these elements or materials are transformed into a lower-valued product.

9.2. Downcycling

Only 6% of float glass used are being recycled today, and the vast majority of this 6% does not even go back into the float glass industry. Instead, the vast majority of this 6% are downcycled to produce bottles, insulation materials, or embankments. However, these products cannot be recycled again, and so this is not considered closed loop recycling. Figure 58 shows the CO2 savings from different glass recycling alternatives.

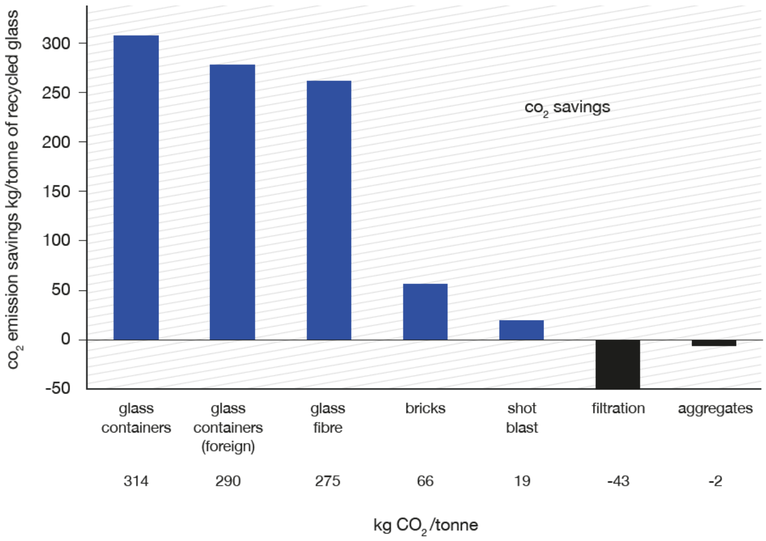

Figure 58. CO2 savings from different glass recycling alternatives (British Glass& GTS, 2017).

It is possible to use glass as an aggregate in concrete, because glass is hard and relatively inert. Concrete with glass aggregate are very aesthetically pleasing (Achintha, 2016). Another reuse possibility is using glass as an alternative aggregate in bituminosus materials in road construction (Achintha, 2016). Figure 59 shows photographs of glass as aggregates in concrete and road construction.

Figure 59. Glass as Aggregate in Concrete and Road Construction (Achintha, 2016)

Other reuse options for glass include as glass beams for reflective paint, pipe cushion for French and storm drain systems, abrasive like sandblasting grits, filter media for swimming pools, golf course sand traps, and aquarium sand (Achintha, 2016).

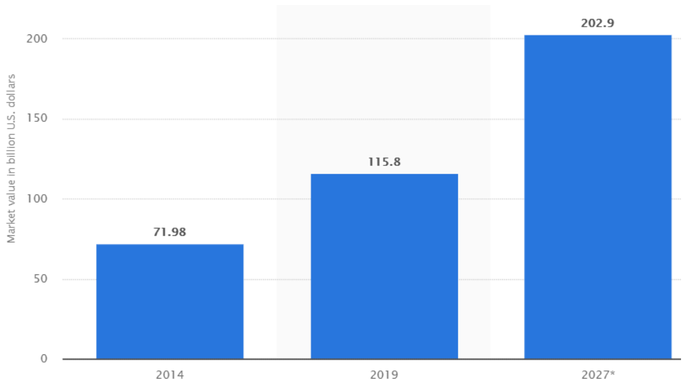

Figure 60. Market value of flat glass worldwide (Garside, 2021)

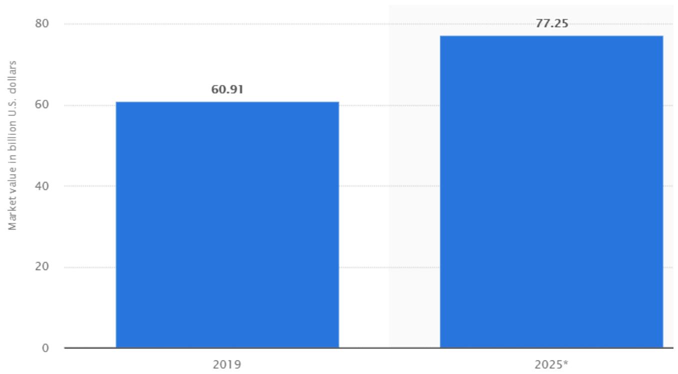

Figure 61. Market value of glass containers and bottles worldwide (Garside, 2021)

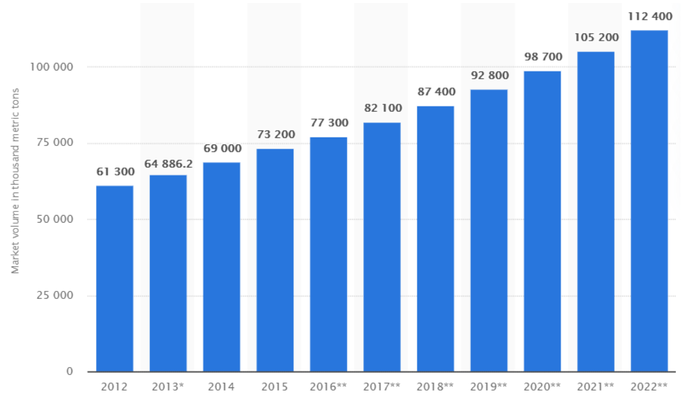

Figure 62. Market volume of flat glass worldwide from 2012 to 2022 (Garside, 2021)

The global production volume of glass bottles and containers was 50.63 million metric tons in 2015, and it is projected that in 2022, this will be 65.42 million metric tons (Garside, 2021). The value for 2019 is interpolated to be 59.08 million metric tons.

The worldwide float glass has a market value of 115.8 billion U.S. dollar in 2019, and the worldwide market volume of float glass is 92,800,000 tons in 2019. The cost of float glass is 1.37551347 dollars/kg. The worldwide glass containers and bottles has a market value of 60.91 billion U.S. dollar in 2019, and the worldwide market volume of glass containers and bottles is 59,080,000 tons in 2019. The cost glass containers and bottles is 1.13645535 dollars/kg. So the amount of downcycling is relatively low at a factor of 1.2.

9.2.1. Upcycling

The problem with upcycling float glass is that glass can only be recycled back into the float glass industry if it do not have any contamination like aluminium or nickel. In addition, coating are applied to control solar gain or thermal performances, and these coating are made from a layer of metal at the surface. These coating are not detrimental to the recycling ability and can be burnt off in the remelting process; however, this is not good for optical characteristics (Achintha, 2016).

Breaking down existing float glass into cullet, and recycling these cullet to create new float glass is practised today. Currently 30% of Saint Gobain's float glass comes from recycled glass. 19% out of this 30% recycled glass is produced from internal factory cullet, and the remaining 11% recycled glass is from pre-consumer cullet from cut-offs. However, this 30% recycled glass from internal factory cullet and cut-off cullet are already at the maximum amount of pre-consumer recyclable glass. So in order to increase the amount of recycled glass in the industry from the 30%, it would be necessary to recycle glass that has been released into the market and installed. However, recycling post-consumer glass has never been done before.

For every tonne of cullet used to produce float glass, 1.2 tonnes of raw material can be saved, which also led to a reduction in mining, quarrying, and transportation (UK Glass Manufacture, 2018). Cullet can melt at a lower temperature than raw materials, so 3% less energy can be used for every 10% cullet used in production (UK Glass Manufacture, 2018). For every tonne of cullet added to the furnace, 250 to 300 kilogram reduction in CO_2 emission (UK Glass Manufacture, 2018). Figure 63 shows the embodied energy of 1 kilogram of flat glass in relation to the percentage of cullet used.

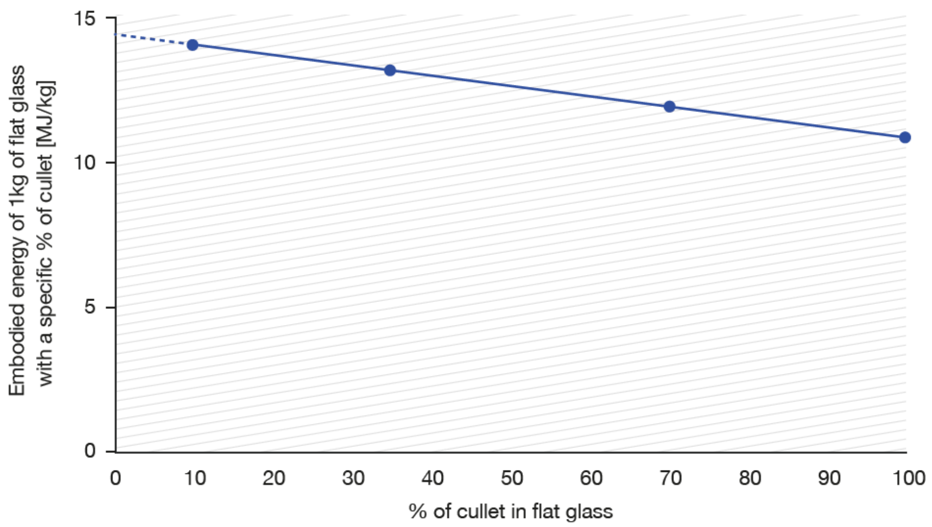

Figure 63. Embodied energy of 1kg of flat glass in relation to % of cullet used (Heesbeen, 2012)

9.2.1.1. Maltha

Maltha is a company that transform glass waste into glass cullet, which can be used to create new glass products. The flat glass that comes in may contain contaminations, like metal, foil, debris, wood, plastic, and rubber; therefore, the glass with contamination needs to be placed through magnets, sieves, cyclones, eddy current separators, laser and camera technology and even x-ray detection facilities. This process results in pure glass cullet that can be used to make new glass products.

9.2.1.2. Structural Properties of Upcycling

9.2.1.2.1. Upcycling: Telesilla's PHD Research

In her PHD research, Telesilla analysed the possibility of transforming everyday waste glass, from beer bottles to mobile phone screens, into casted glass. She recycled different types of non-recyclable silicate glasses into 30 by 30 by 240 mm glass beams, and figure 64 shows the test specimens.

These specimens are then tested with 4-point bending tests, and the resulting flexural strength ranges from 9 to 72 MPa (Telesilla et al, 2020). It was concluded that beam specimens produced from purer cullet and higher forming temperature leads to a distinctly higher strength (Telesilla et al, 2020). She also observed an increase in the strength and young's modulus consecutively from lead silicate, borosilicate, barium silicate, and soda lime silicate family (Telesilla et al, 2020).

It was also concluded that coatings and external contaminants, such as organics and metals, led to defects and low flexural strengths (Telesilla et al, 2020). For the contaminated samples, crystalline formations at the bottom surface in the tensile zone are the cause of facture, leading to lower strength (Telesilla et al, 2020).

Figure 64. Tested Specimens. (Telesilla et al., 2020)

9.2.1.2.2. Upcycling: Rong's Master's Thesis

In her master's thesis, Rong analysed the structural properties of recycled float glass. Rong produced recycled glass from a combination of 3 types of float glass: dark soft-coat glass, light soft-coated glass, and hard-coated glass. Figure 65 shows the recycled glass specimens. Specifically, she analysed the recycled float glass's chemical composition, young's modulus, coefficient of thermal expansion, and the fractural strength.

First, XRF tests are used to compare the composition of the float glass before and after recycling, and she concluded that the silicate dioxide and deposit of alkali moved to the surface after recycling (Yu, 2019). Then, ultrasonic test are used to determine the young's modulus of the recycled glass. The results show that the Young's modulus has slightly decreased after recycling, but it will not make a considerable influence on the structural behaviour (Yu, 2019).

Strain gauges are used find the coefficient of thermal expansion, and she discovered that the CTE value decreased after recycling (Yu, 2019). Lastly, four-point bending test are conducted to find the fracture strength, and the resulting load-displacement curve shows that the recycled glass may have even better structural properties compared to that of the original glass (Yu, 2019).

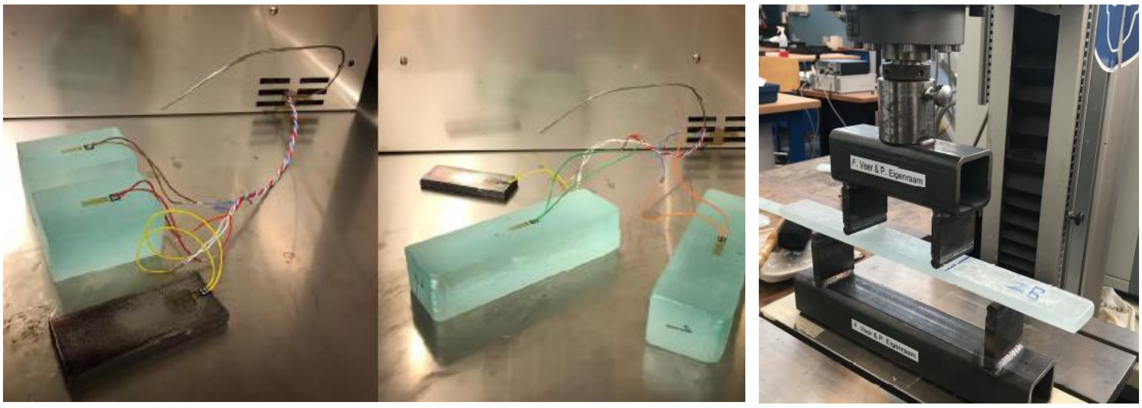

Figure 65. Recycled Glass Specimens (Yu, 2019)

9.3. Interlayer Recycling

The problem with recycling and reusing interlayer as such is that it is difficult to identify the manufacturer and the formulation of the interlayer after a number of years (Achintha, 2016). The design life in Europe is 50 years, so the interlayers are expect last at least 50 years. Regulations may have changed over time, and the different suppliers may have used different grades of interlayer or amount of plasticizer. This small differences in formulation is important, and so its performance cannot guaranteed anymore.

Taking the cut offs generated from the production process and using it to produce new interlayers is practised today. For example, Kuraray offers a product called Butacite G, which are recycled PVB interlayer that are produced from PVB trimmings. Specifically, the manufacturers need to trim off around

10 to 20 cm at the edges, and this lead to a 5 to 10% waste of the PVB produced (Tup, Mnsk, & Kaprkov, 2012).

The interlayer can also be recycled and used in the production of carpet, and figure 66 shows the process for turning PVB into dispersion for carpet tiles. The PVB material can be used as a replacemetn for latex in the precoat of carpets, and the recycled PVB reduce the carbon footprint of precoat by 80% compared to normal latex (Interface, 2020). For example, the company Interface’s microtuft carpet tiles are all produced with recycled PVB precoat.

Figure 66. Using PVB interlayer in carpet production (Interface, 2020)

9.3.1. Shark Solutions

Shark Solutions is a Danish company that recycle PVB interlayers from laminated glass of windshields and buildings. They turn these PVB interlayers into carpet backing, paint and coatings, and sound dampening.

9.3.2. Structural Properties

An experiment was conducted by Dhaliwal and Hay to compare the properties of the recycled PVB with that of the original PVB. The experiment shows that the recycled PVB has similar chemical composition, tensile properites, and weight fraction of plasticizer as that of the original PVB (Dhaliwal & Hay, 2002). In addition, the recycled PVB did not show any loss of optical clarity (Dhaliwal & Hay, 2002).

One problem is that the experiment shows lower amount of plasticizer in the recycled PVB interlayer. However, this problem can be solved by predicting the final plasticizer content with Tg, IR analysis of the carbonyl content, or mass loss measurements below 250 degrees (Dhaliwal & Hay, 2002). Then, dibutyl sebacate can be added to the product to makeup for the plasticizer deficiency (Dhaliwal & Hay, 2002).

9.3.3. Optimal Conditions

Experiments are conducted by Tup, Mnsk, and Kaprkov in order to find the optimal re-processing condition for PVB interlayer that leads to the most optimal the mechanical properties, minimal thermal degradation, and minimal yellowness. Manufacturing conditions that were taken into consideration include its temperature, air oxygen content, and mechanical stress. This experiment determined that the optimal condition for PVB re-processing is at 150 degrees and at a kneader rotational speed of lower than 60rpm (Tup, Mnsk, & Kaprkov, 2012).

9.4. Laminated Glass Recycling

A possibility for recycling laminated glass is grinding it into small pieces, and these small glass pieces that are contaminated with interlayers are placed into a float oven. The interlayer would then be burned off and contribute to the energy consumption of the furnace. This process will also be able to reduce the amount of CO2 pollution, because recycled glass can melt at a lower temperature.

However, the problem with this practise is that there is a limitation on the amount of interlayers in the float oven. Too much interlayers in the oven would lead to an uncontrolled burning, bubbling at the furnace, and glass going all over the furnace. Also, this practise is not as sustainable as reprocessing the interlayer as a material or reusing it altogether.

Pulverizing and separating machinery can be used to grind the glass into small pieces and to remove the laminate layer. However, the size of the cullet cannot be used by the float glass industry, so the resultant cullet has to go into the container glass industry. The PVB interlayer can be used in the carpet tile industry.

Currently it is not possible to fully separate the interlayer component from the glass component and to recycle the two components into new laminated glass. One of the biggest challenge is completely removing the glass shards from the interlayer. The surface of interlayer is not smooth, and this texture is required to remove the air bubbles once the glass panels is in place. This makes it difficult to identify any impurities on the surface of the interlayer, which makes it difficult to identify any residual glass shards in the interlayer.

9.4.1. Delamination

9.4.1.1. Covanord

Covanord is a company that recycle laminated glass with their patented machine. The laminated glass are first aged for 3 months in an outdoor environment, and this is so that the sun and water can attack the PVB interlayer. Over time, the interlayer gets filled with moisture, which make it easier to separate from the glass panels. After separation, these glass panels are grinded into cullet that are 20 by 20 mm2, and these cullet can be integrated in the furnace to create new glass products (Entwistle, 2019).

9.4.1.1.1. Delamination with Humidity and Water Infiltration

In her PhD research, Harwell conducted experiments on laminated glass to see the effect of humidity and water infiltration on the delamination of PVB interlayer from glass. She found that the humidity-aged sample do show a reduction in the interfacial adhesion. In addition, water infiltration at the interface will lead to reduction in peak force and displacement at failure.

9.4.1.2. Delaminating Resources

The company Delaminating Resources (Delam) has developed a patented system for the delamination of laminated glass that utilizes heat, time, and steam, and figure 67 shows the delamination machine. The delamination process can take as little as 5 minutes to complete. If there is nothing wrong with the glass panels after delamination, the glass can then be re-laminated for usage again. The delaminated components of both the glass and the interlayer part can also be 100% recycled.

The current issue is that the system for annealed glass still require additional work. The current system can be used for curved glass, tempered glass, and heat strengthened glass, and this system can be used for PVB, SGP, and EVA interlayers.

Figure 67. Patented Delamination Machine from the Company Delam (Delam, 2020)

9.4.1.3. D201 Nonionic Surfactant

The chemical D201 nonionic surfactant, which was developed by Jeong Chem Ltd Incheon, can be used to separate glass from PVB films. Mechanochemical separation is when waste PVB chunks are mechanically stirred in the nonionic surfactant D201 for a certain period of time, and the glass and PVB components are separated by a stainless steel mesh-screening filter (Swain et al., 2015). Figure 68 shows the mechanochemical seperation machine and its schematics. In this experiment, the separated glass, separated PVB, and residual glasses were weighed to understand the separation process (Swain et al., 2015).

This experiment shows that the most optimal condition is at 60 min reaction time, 400 rpm stirring speed, 30% of surfactant D201, and temperature of 35 degrees (Swain et al., 2015). Figure 69 shows the different conditions and its corresponding separation efficiency. In addition, this experiment shows that recycled PVB contains only C and O; however, the original PVB also contains Si, Ca, Mg, Na, and Al (Swain et al., 2015). The composition of recycled PVB and commercial PVB are shown in figure 70.

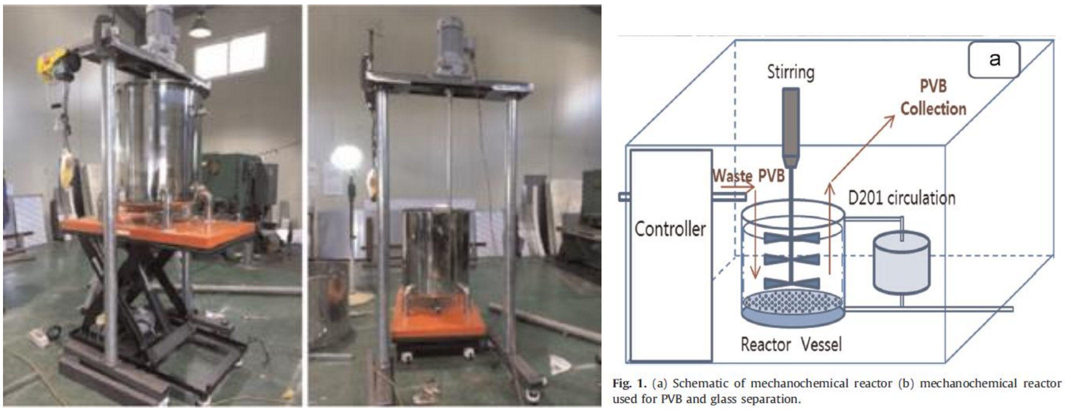

Figure 68. Mechanochemical Separation Machine and its Schematics (Swain et al., 2015)

Time of Reaction (min)	Stirring Speed (rpm)	Concentration (D201) (vol%)	Temperature (°C)	Separation efficiency (%)
60	400	25	25	86
60	400	30	35	100
80	400	25	35	94
80	400	30	35	100

Figure 69. Optimum Condition and its Separation Efficiencies (Swain et al., 2015)

Element	Waste PVB (wt%)	Recycled PVB (wt%)
C	3.96	65.28
O	48.02	34.72
Na	9.30	0
Mg	2.12	0
Al	0.60	0
Si	29.56	0
Ca	6.44	0

Figure 70. Composition of Recycled PVB and Commercial PVB

Part V. Case Study: Glass Floor at Delft Station

This section is on the case study conducted on the glass floor panels at the train station in Delft. This section contains a chapter on the structural aspect of the case study, and the other chapter is on the sustainability aspect of the case study. The structural aspect of the case study contains analytical calculations and computer simulation with DIANA, and the sustainability aspect of the case study contains shadow cost calculations.

Chapter 10. Case Study: Structural Analysis

This chapter is on the structural aspect of the case study on the glass floor panels at the train station in Delft, and figure 71 is a photograph of the laminated glass floor. Specifically, the serviceability limit state and the ultimate limit state of laminated glass with PVB, SGP, and EVA interlayer are considered. The post-breakage situation is also considered. The loading conditions are according to the Eurocode, and the glass calculations are according to the Dutch code NEN2608.

10.1. Laminated Glass Floor at Delft Station

Figure 71 is a photograph of the laminated glass floor. Specifically, the serviceability limit state and the ultimate limit state of laminated glass with PVB, SGP, and EVA interlayer are considered. The post-breakage situation is also considered. The loading conditions are according to the Eurocode, and the glass calculations are according to the Dutch code NEN2608.

Figure 71. Laminated Glass Floor at the Central Station of Delft

- Glass floor plate of 2.7 m by 1 m, supported at all sides
- Consequence class CC2, design life: 50 years
- Imposed floor load of 5.0 kN/m2 for the load duration of 50 years
- Imposed point load of 7 kN at 0.1 m by 0.1 m for the load duration of 50 years
- Glass composition to check: heat strengthened (HS), interlayers of 0.76 mm thickness
- At the temperature of 17°C and load duration of 50 years, $G_{tl,PVB}$=0.05, $G_{tl,SGP}$=6.42, and $G_{tl,EVA}$=1.33

10.2. Tensile Strength Calculations

The tensile strength of heat-strengthened glass loaded by distributed loads and the point load is calculated in 12.1.1 and 12.1.2 respectively. The tensile strength are calculated according to the Dutch code NEN2608.

10.2.1. Distributed Loads

Surface effect factor k_a: $k_a = 1.644 \times A^{-\left(\frac{1}{25}\right)}$ uniformly distributed surface pressure

$$= 1.644 \times (2700mm\ x\ 1000mm)^{-\left(\frac{1}{25}\right)} = 0.909$$

The surface effect factor is typically set to 1; however, in this case, it is equal to $1.644 \times A^{-\left(\frac{1}{25}\right)}$, because the glass pane is subjected to an uniformly distributed surface pressure.

Edge quality factor k_e: k_e=1 for heat-strengthened glass loaded out of pane

Surface texture factor k_{sp}: k_{sp}= 1 for float glass

Characteristic tensile (bending) strength: $f_{g;k}$ = 45 N/mm^2

Glass material factor $\gamma_{m;A}$: $\gamma_{m;A}$=1.8 when wind is not normative

Load Duration factor k_{mod}: $k_{mod} = \left(\frac{5}{t}\right)^{\frac{1}{c}} = \left(\frac{5}{50\ x\ 365\ x\ 24\ x\ 3600}\right)^{\frac{1}{16}} = 0.294$

Zone Factor Kz: Kz = 1 for heat-strengthened glass

Prestress $f_{b;k}$: $f_{b;k}$=70 N/mm2 for heat strengthened float glass

Prestress factor $\gamma_{m;v}$: $\gamma_{m;v}$ = 1.2

Tensile strength for distributed load (t=50 years):

$$f_{mt;u;d} = \frac{k_a \times k_e \times k_{mod} \times k_{sp} \times f_{g;k}}{\gamma_{m;A}} + \frac{k_e \times k_z \times (f_{b;k} - k_{sp} \times f_{g;k})}{\gamma_{m;V}}$$

$$= \frac{0.909 \times 0.8 \times 0.294 \times 1 \times 45 N/mm2}{1.8} + \frac{1 \times 1 \times (70 N/mm2 - 1 \times 45 N/mm2)}{1.2}$$

= 27.523N/mm2

Interlayer	Tensile Strength of Distributed Load (N/mm2)
PVB, SGP, EVA	27.52

10.2.2. Point Loads

Surface effect factor k_a: $k_a = 1.644 \times A^{-\left(\frac{1}{25}\right)}$ uniformly distributed surface pressure

$$= 1.644 \times (100mm \; x \; 100mm)^{-\left(\frac{1}{25}\right)}$$

$$= 1.137$$

The surface effect factor is typically set to 1; however, in this case, it is equal to $1.644 \times A^{-\left(\frac{1}{25}\right)}$, because the glass pane is subjected to a point load

Edge quality factor k_e: k_e=1 for heat-strengthened glass loaded out of pane

Surface texture factor k_{sp}: k_{sp}= 1 for normal surface texture

Characteristic tensile (bending) strength: $f_{g;k}$ = 45 N/mm^2

Glass material factor $\gamma_{m;A}$: $\gamma_{m;A}$=1.8 when wind is not normative

Load Duration factor k_{mod}: $k_{mod} = \left(\frac{5}{t}\right)^{\frac{1}{c}}$

$$= \left(\frac{5}{50 \; x \; 365 \; x \; 24 \; x \; 3600}\right)^{\frac{1}{16}}$$

$$= 0.294$$

Zone Factor Kz: Kz = 1 for heat-strengthened glass

Prestress $f_{b;k}$: $f_{b;k}$=70 N/mm2 for heat strengthened float glass

Prestress factor $\gamma_{m;v}$: $\gamma_{m;v}$ = 1.2

Tensile strength for point load (t=50 years):

$$f_{mt;u;d} = \frac{k_a \times k_e \times k_{mod} \times k_{sp} \times f_{g;k}}{\gamma_{m;A}} + \frac{k_e \times k_z \times (f_{b;k} - k_{sp} \times f_{g;k})}{\gamma_{m;V}}$$

$$= \frac{1.137 \times 0.8 \times 0.294 \times 1 \times 45N/mm2}{1.8} + \frac{1 \times 1 \times (70N/mm2 - 1 \times 45N/mm2)}{1.2}$$

= 29.202 N/mm2

Interlayer	Tensile Strength of Point Load (N/mm2)
PVB, SGP, EVA	29.20

Figure 72. Tensile Strength of Distributed and Point Load

10.3. Equivalent Thickness Calculations

The equivalent thickness of laminated glass with PVB 12.12.12.12 composition, SGP 12.12.10 composition, and EVA 12.12.10.10 are calculated in this section. The equivalent thickness for its ultimate limit state and the serviceability limit state is shown in section 12.2.1 and 12.2.2 respectively.

10.3.1. Ultimate Limit State

Here is a sample calculation for the equivalent thickness of laminated glass with PVB interlayer with 12.12.12.12 composition for its ultimate limit state. The calculations for the other configurations and interlayers are done in the same way in Excel, and only the results are shown below.

$\frac{B}{H} = \frac{2700}{1000}$ = 2.7 → k_w = 0.893 k_σ = 1.697

$z = \frac{B_1+H_1}{2}$

$= \frac{2700mm+1000mm}{2}$

= 1850 mm

a=1000mm

Shape factor ULS: $L_\sigma = k_\sigma \times \left(\frac{2\times a}{z}\right)^{-0.60906}$

$= 1.697 \times \left(\frac{2\times 1000}{1850}\right)^{-0.60906}$

= 1.618

Shape factor determined by geometry: $L_A^2 = \frac{1}{\frac{1}{B^2}+\frac{1}{H^2}}$

$= \frac{1}{\frac{1}{2700^2}+\frac{1}{1000^2}}$

= 879372.738

$$X = \max\begin{pmatrix} \sum_{i=1}^{n-1}(t_{pl;i} \times t_{v;i}) \\ \sum_{i=2}^{n-1}(t_{pl;i} \times t_{v;i-1}) \end{pmatrix}$$

= 11.7 x 0.76 + 11.7 x 0.76 + 11.7 x 0.76

= 26.676 mm^2

$$\beta = \frac{1}{2} \times \frac{\pi^2}{L_A^2} \times \frac{E_g}{1-\nu_g^2} \times \frac{X}{G_{tl}}$$

$= \frac{1}{2} \times \frac{\pi^2}{879372.738^2} \times \frac{70{,}000 \text{ N/mm2}}{1-0.23^2} \times \frac{26.676 \text{ mm2}}{0.05}$

= 221.284

Shear coupling factor of interlayer $\boldsymbol{\omega_\sigma}$: $\omega_\sigma = \frac{1}{1+\frac{\beta}{L_\sigma}}$

$$=\frac{1}{1+\frac{221.284}{1.618}}$$

= 0.00726

Design value ULS (mm): $t_{gg;i;u} = \sqrt{\frac{(1-\omega_\sigma)\times\sum_{j=1}^{n}\left(t_{pl;j}^3\right)+\omega_\sigma\times\left(\sum_{j=1}^{n}\left(t_{pl;j}\right)\right)^3}{t_{pl;i}+2\times\omega_\sigma\times t_{m;i}}}$

Equivalent Glass Thickness ULS (mm):

$$t_{gg;u} = MIN\left(t_{gg;i;u}\right)$$

$$= \sqrt{\frac{(1-\omega_\sigma)\times\left(t_1^3+t_2^3+t_3^3\right)+\omega_\sigma\times(t_1+t_2+t_3)^3}{t_3+2\times\omega_\sigma\times \max\left(t_{m;1},t_{m;2},t_{m;3}\right)}}$$

$$= \sqrt{\frac{(1-0.00726)\times(11.7^3+11.7^3+11.7^3+11.7^3)+0.00726\times(11.7+11.7+11.7+11.7)^3}{11.7+2\times0.00726\times(17.55)}}$$

= 24.38mm

Interlayer	tgg;1;u (mm) Distributed Load	tgg;1;u (mm) Point Load
PVB (12.12.12.12)	24.38	23.57
SGP (12.12.10)	30.76	25.83
EVA (12.12.10.10)	32.14	24.44

Figure 73. ULS Equivalent Thickness

10.3.2. Serviceability Limit State

Here is a sample calculation for the equivalent thickness of laminated glass with PVB interlayer with 12.12.12.12 composition for its serviceability limit state. The calculations for the other configurations and interlayers are done in the same way in Excel, and only the results are shown below.

Shape factor SLS: $L_w = k_w \times \left(\frac{2\times a}{z}\right)^{-0.04354}$

$$= 0.893 \times \left(\frac{2\times1000}{1850}\right)^{-0.04354}$$

= 0.890

Shear Coupling factor ω_w: $\omega_W = \frac{1}{1+\frac{\beta}{L_W}}$

$= \frac{1}{1+\frac{221.284}{0.890}}$

= 0.00401

Equivalent glass thickness SLS (mm):

$$t_{gg;ser} = \sqrt[3]{(1-\omega_w) \times \sum_{i=1}^{n}(t_{pl;i}^3) + \omega_w \times \left(\sum_{i=1}^{n}(t_{pl;i})\right)^3}$$

$$= \sqrt[3]{(1-\omega_w) \times (t_1^3 + t_2^3 + t_3^3) + \omega_w \times (t_1 + t_2 + t_3)^3}$$

$$= \sqrt[3]{(1-0.00401) \times (11.7^3 + 11.7^3 + 11.7^3 + 11.7^3) + 0.00401 \times (11.7 + 11.7 + 11.7 + 11.7)^3}$$

= 18.94mm

Interlayer	Distributed Load tgg,ser (mm)	Point Load tgg,ser (mm)
PVB (12.12.12.12)	18.94	18.89
SGP (12.12.10)	26.28	26.14
EVA (12.12.10.10)	23.21	22.95

Figure 74. SLS Equivalent Thickness

10.4. Load Cases

The load combination in the ultimate limit state and serviceability limit state are calculated in this section, and the load taken into consideration include the self-weight, the distributed loads, and the point load.

Weight of laminated glass = $4 * 11.7mm * 10^{-3} * 25\,\text{kN}/m^3$

$= 1.17\,\text{kN}/m^2$

ULS load case for distributed load: $p_{d;z} = 1.2 * 1.17\,\text{kN}/m^2 + 1.5 * 5\,\text{kN}/m^2$

$= 8.904\,\text{kN}/m^2$

SLS load case for distributed load: $p_{d;z} = 1.17\,\text{kN}/m^2 + 5\,\text{kN}/m^2$

$= 6.17\,\text{kN}/m^2$

ULS load case for point load: $p_{d;z} = 1.5 * 7\text{kN}$

$= 10.5\text{kN}$

SLS load case for point load: $p_{d;z}$ = 7 kN

10.5. Unity Checks of Ultimate Limit States

10.5.1. Distributed Load

The theory of elasticity is used to calculate design stress of the ULS load case for the distributed load, and this design stress compared with the tensile strength of heat-strengthened glass to obtain the ULS unity check.

	l_y/l_x		1,0	1,2	1,4	1,6	1,8	2,0	2,5	3,0
I	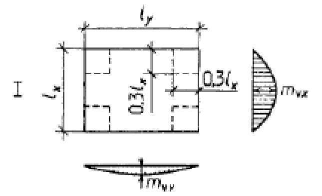	$m_{vx} = 0{,}001\, p_d l_x^2$	41	54	67	79	87	97	110	117
		$m_{vy} = 0{,}001\, p_d l_x^2$	41	35	31	28	26	25	24	23
		$w = 0.001 \frac{p_d l_x^4}{EI}$	4,1	5,6	7,0	8,2	9,2	10		12.2

Figure 75. Theory of Elasticity: Governing Bending Moment and Deflection Coefficient (NEN6720)

Maximum bending moment per unit width m_x: $m_x = 0.001 * 112.8 * p_d(l_x)^2$

$= 0.001 * 112.8 * 8.904kN/m2 * (1m)^2$

= 1.00 kNm/m

Elastic section modulus w_y: $w_y = b * \frac{\mathrm{tgg;u}^2}{6}$

$= 1\mathrm{m} * \frac{(0.02438\mathrm{m})^2}{6}$

= 0.0000990 m^3

Design Stress σ_{ed}: $\sigma_{ed} = \frac{m_x}{W_y}$

$= \frac{1.00\ \mathrm{kNm/m}}{0.0000990\ \mathrm{m3}}$

= 10140.937 kN/m2

= 10.14 N/mm^2

Interlayer	σ_{ed} (N/mm2) Distributed Load
PVB (12.12.12.12)	10.14
SGP (12.12.10)	6.07
EVA (12.12.10.10)	5.76

Figure 76. ULS Unity Check of Distributed Load

10.5.2. Point Load

The maximum stress of the point load was calculated using the information from Table 11.4 from the textbook Roark's Formula for Stress and Strain by Warren Young and Richard Budynas.

Uniform over central rectangular area

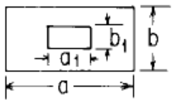

(At center) $\sigma_{max} = \sigma_b = \frac{\beta W}{t^2}$ where $W = qa_1b_1$

b_1/b \ a_1/b	$a = b$: 0	0.2	0.4	0.6	0.8	1.0
0		1.82	1.38	1.12	0.93	0.76
0.2	1.82	1.28	1.08	0.90	0.76	0.63
0.4	1.39	1.07	0.84	0.72	0.62	0.52
0.6	1.12	0.90	0.72	0.60	0.52	0.43
0.8	0.92	0.76	0.62	0.51	0.42	0.36
1.0	0.76	0.63	0.52	0.42	0.35	0.30

$a = 1.4b$: 0	0.2	0.4	0.8	1.2	1.4	$a = 2b$: 0	0.4	0.8	1.2	1.6	2.0
	2.0	1.55	1.12	0.84	0.75		1.64	1.20	0.97	0.78	0.64
1.78	1.43	1.23	0.95	0.74	0.64	1.73	1.31	1.03	0.84	0.68	0.57
1.39	1.13	1.00	0.80	0.62	0.55	1.32	1.08	0.88	0.74	0.60	0.50
1.10	0.91	0.82	0.68	0.53	0.47	1.04	0.90	0.76	0.64	0.54	0.44
0.90	0.76	0.68	0.57	0.45	0.40	0.87	0.76	0.63	0.54	0.44	0.38
0.75	0.62	0.57	0.47	0.38	0.33	0.71	0.61	0.53	0.45	0.38	0.30

Figure 77. Maximum Stress of Uniform Load over Central Rectangular Area (Young & Budynas, 2002)

Design Stress σ_{ed}: $\sigma_{ed} = \frac{\beta W}{t^2}$

$= \frac{1.73 * 10.5kN}{(23.57\text{mm})^2}$

= 32.69 N/mm^2

Interlayer	σ_{ed} (N/mm2) Point Load
PVB (12.12.12.12)	32.69
SGP (12.12.10)	27.22
EVA (12.12.10.10)	30.40

Figure 78. ULS Unity Check of Point Load

10.6. Unity Checks of Serviceability Limit States

10.6.1. Distributed Load

The theory of elasticity is used to calculate the deflection for the distributed load, and this deflection compared with the maximum deflection of glass to obtain the SLS unity check.

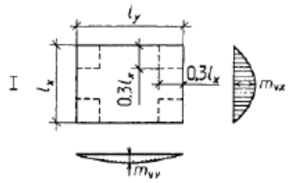

	l_y/l_x	1,0	1,2	1,4	1,6	1,8	2,0	2,5	3,0
I	$m_{vx} = 0{,}001\, p_d l_x^2$	41	54	67	79	87	97	110	117
	$m_{vy} = 0{,}001\, p_d l_x^2$	41	35	31	28	26	25	24	23
	$w = 0.001 \dfrac{p_d l_x^4}{EI}$	4,1	5,6	7,0	8,2	9,2	10		12,2

Figure 79. Theory of Elasticity: Governing Bending Moment and Deflection Coefficient (NEN6720)

Moment of Inertia I_y: $I_y = \frac{1}{12} * l \times tgg, ser^3$

$= \frac{1}{12} * 2700mm \times (18.94mm)^3$

= 1528063.25 mm^4

Design value of the uniformly distributed load p_d: $p_d = p_{d;z} * l_y$

= 6.17 kN/m^2* 2.7m

= 16.659 kN/m

$l_y/l_x = \frac{2700\text{mm}}{1000\text{mm}}$

=2.7

Deflection coefficient = $\frac{(12.2-10)*(2.7-2)}{3-2}$ +2

=11.54

Deflection w: $w = \frac{0.001 \times pd \times Lx^4}{E \times I_y}$

= 0.001*11.54*$\frac{16.659kN/m \times (1000mm)^4}{70{,}000\ N/mm2 \times 1528063.25\ mm4}$

= 1.80 mm

Maximum deflection U_{max}: $U_{max} = \frac{1000\text{mm}}{250}$

= 4 mm

Interlayer	w (mm) Distributed Load
PVB (12.12.12.12)	1.80
SGP (12.12.10)	0.64
EVA (12.12.10.10)	0.96

Figure 80. ULS Unity Check of Point Load

10.6.2. Point Load

The maximum deflection of the point load was calculated using the information from the textbook Roark's Formula for Stress and Strain, and this deflection compared with the maximum deflection of glass to obtain the SLS unity check.

Rectangular plate; all edges simply supported 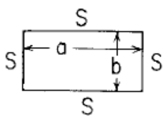	Uniform over small concentric circle of radius r_o (note definition of r'_o)	(At center) $\sigma_{max} = \frac{3W}{2\pi t^2}\left[(1+\nu)\ln\frac{2b}{\pi r'_o}+\beta\right]$ $y_{max} = \frac{-\alpha W b^2}{Et^3}$

a/b	1.0	1.2	1.4	1.6	1.8	2.0	∞
β	0.435	0.650	0.789	0.875	0.927	0.958	1.0
α	0.1267	0.1478	0.1621	0.1715	0.1770	0.1805	0.1

Figure 81. Maximum Stress of Uniform Load over Central Rectangular Area (Young & Budynas, 2002)

Deflection w: $w = \frac{\alpha W b^2}{Et^3}$

$$= \frac{0.1805 * 7kN * (1000mm)^2}{70{,}000\ N/mm2 * (18.89mm)^3}$$

= 2.68 mm

Maximum deflection U_{max}: $U_{max} = \frac{1000\text{mm}}{250}$

= 4mm

Interlayer	w (mm) Point Load
PVB (12.12.12.12)	2.68
SGP (12.12.10)	1.01
EVA (12.12.10.10)	1.49

Figure 82. SLS Unity Check of Point Load

10.7. Post-Breakage Behaviour

The post-breakage behaviour was analysed with the Method of Fine and Kinney from NEN 2608 Annex D, and the results showed that lateral breakage on 1 side should be assumed during the post-breakage situation.

Probability of damage with or without intent WS: WS=1 assume that the probability of damage with or without intent is only possible in the long term

Exposure of structural element BS: BS=10 assume constant exposure of the structural element

Consequence of complete break ES: ES=3 Heat-strengthened glass is applied, and so it would stay in its play after breakage. So minor injury can be assumed.

Risk of the Damage RS: RS = WS x BS x ES

= 1 x 10 x 3

= 30

RS < 70, so lateral breakage on one side is assumed during post-breakage situation.

10.7.1. Equivalent Thickness

Since these laminated glass panels is assumed to be used in a glass floor, the top glass panel is assumed to be broken during post-breakage. The post-breakage situation is assumed to have the strength of a 12.12.12 laminated glass with the self-weight of all 4 glass panels. The load combinations are assumed to be in serviceability limit state.

$$X = \max\begin{pmatrix} \sum_{i=1}^{n-1}(t_{pl;i} \times t_{v;i}) \\ \sum_{i=2}^{n-1}(t_{pl;i} \times t_{v;i-1}) \end{pmatrix}$$

= 11.7 x 0.76 + 11.7 x 0.76

= 17.784 mm2

$$\beta = \frac{1}{2} \times \frac{\pi^2}{L_A^2} \times \frac{E_g}{1-\nu_g^2} \times \frac{X}{G_{tl}}$$

$$= \frac{1}{2} \times \frac{\pi^2}{879372.738^2} \times \frac{70{,}000 \text{ N/mm2}}{1-0.23^2} \times \frac{17.784\text{mm2}}{0.05}$$

= 147.523

Shear coupling factor of interlayer SLS $\boldsymbol{\omega_\sigma}$: $\omega_\sigma = \frac{1}{1+\frac{\beta}{L_\sigma}}$

$$= \frac{1}{1+\frac{147.523}{1.618}}$$

= 0.0109

Design value ULS (mm): $t_{gg;i;u} = \sqrt{\frac{(1-\omega_\sigma)\times\sum_{j=1}^{n}\left(t_{pl;j}^3\right)+\omega_\sigma\times\left(\sum_{j=1}^{n}\left(t_{pl;j}\right)\right)^3}{t_{pl;i}+2\times\omega_\sigma\times t_{m;i}}}$

Equivalent Glass Thickness ULS (mm):

$$t_{gg;u} = MIN(t_{gg;i;u})$$

$$= \sqrt{\frac{(1-\omega_\sigma)\times(t_1^3+t_2^3)+\omega_\sigma\times(t_1+t_2)^3}{t_3+2\times\omega_\sigma\times\max\,(t_{m;1},t_{m;2})}}$$

$$= \sqrt{\frac{(1-0.0109)\times(11.7^3+11.7^3+11.7^3)+0.0109\times(11.7+11.7+11.7)^3}{11.7+2\times0.0109\times(11.7)}}$$

= 20.90 mm

Interlayer	Post-Breakage Distributed Load tgg;1;u (mm)	Post-Breakage Point Load tgg;1;u (mm)
PVB (12.12.12.12)	20.90	20.38
SGP (12.12.10)	22.50	20.18
EVA (12.12.10.10)	26.23	22.83

Figure 83. Equivalent Thickness during Post-breakage

10.7.2. Ultimate Limit States

10.7.2.1. Distributed Load

For the post-breakage unity check, the strip method of load transfer is used to calculate design stress of the SLS load case for the distributed load, instead of the ULS load case from before. This design stress then compared with the tensile strength of heat-strengthened glass to obtain the post-breakage unity check.

	l_y/l_x	1,0	1,2	1,4	1,6	1,8	2,0	2,5	3,0
I 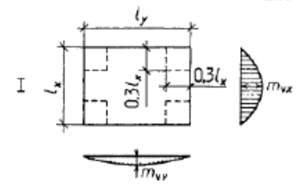	$m_{vx} = 0{,}001\, p_d l_x^2$	41	54	67	79	87	97	110	117
	$m_{vy} = 0{,}001\, p_d l_x^2$	41	35	31	28	26	25	24	23
	$w = 0.001 \dfrac{p_d l_x^4}{EI}$	4,1	5,6	7,0	8,2	9,2	10		12.2

Figure 84. Theory of Elasticity: Governing Bending Moment and Deflection Coefficient (NEN6720)

Maximum bending moment per unit width m_x: $m_x = 0.001 * 112.8 * p_d(l_x)^2$

$= 0.001 * 112.8 * 5.8775kN/m2 * (1m)^2$

= 0.66 kNm/m

Elastic section modulus w_y: $w_y = b * \frac{\text{tgg;u}^2}{6}$

$= 1\text{m} * \frac{(0.02090\text{m})^2}{6}$

$= 0.0000728\ \text{m}^3$

Design Stress σ_{ed}: $\sigma_{ed} = \dfrac{m_x}{W_y}$

$$= \frac{0.66\ \text{kNm/m}}{0.0000728\ \text{m3}}$$

$= 9106.087$ kN/m2

$= 9.11\ \text{N/mm}^2$

Interlayer	σ_{ed} (N/mm2) Distributed Load
PVB (12.12.12.12)	9.11
SGP (12.12.10)	7.47
EVA (12.12.10.10)	5.73

Figure 85. Unity Check of Distributed Load during Post-Breakage

10.7.2.2. Point Load

For the post-breakage situation, the maximum deflection of the point load was calculated using the information from the textbook Roark's Formula for Stress and Strain. The SLS load case for the point load was used instead of the ULS load case.

Uniform over central rectangular area

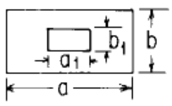

(At center) $\sigma_{\max} = \sigma_b = \dfrac{\beta W}{t^2}$ where $W = q a_1 b_1$

b_1/b \ a_1/b ($a = b$)	0	0.2	0.4	0.6	0.8	1.0
0		1.82	1.38	1.12	0.93	0.76
0.2	1.82	1.28	1.08	0.90	0.76	0.63
0.4	1.39	1.07	0.84	0.72	0.62	0.52
0.6	1.12	0.90	0.72	0.60	0.52	0.43
0.8	0.92	0.76	0.62	0.51	0.42	0.36
1.0	0.76	0.63	0.52	0.42	0.35	0.30

b_1/b \ a_1/b ($a = 1.4b$)	0	0.2	0.4	0.8	1.2	1.4
0		2.0	1.55	1.12	0.84	0.75
0.2	1.78	1.43	1.23	0.95	0.74	0.64
0.4	1.39	1.13	1.00	0.80	0.62	0.55
0.6	1.10	0.91	0.82	0.68	0.53	0.47
0.8	0.90	0.76	0.68	0.57	0.45	0.40
1.0	0.75	0.62	0.57	0.47	0.38	0.33

b_1/b \ a_1/b ($a = 2b$)	0	0.4	0.8	1.2	1.6	2.0
0		1.64	1.20	0.97	0.78	0.64
0.2	1.73	1.31	1.03	0.84	0.68	0.57
0.4	1.32	1.08	0.88	0.74	0.60	0.50
0.6	1.04	0.90	0.76	0.64	0.54	0.44
0.8	0.87	0.76	0.63	0.54	0.44	0.38
1.0	0.71	0.61	0.53	0.45	0.38	0.30

Figure 86. Maximum Stress of Uniform Load over Central Rectangular Area (Young & Budynas, 2002)

Design Stress σ_{ed}: $\sigma_{ed} = \dfrac{\beta W}{t^2}$

$$= \frac{1.73 * 7kN}{(20.38\text{mm})^2}$$

$= 29.17\ \text{N/mm}^2$

Interlayer	σ_{ed} (N/mm2) Point Load
PVB (12.12.12.12)	29.17
SGP (12.12.10)	29.73
EVA (12.12.10.10)	23.24

Figure 87. Unity Check of Point Load during Post-Breakage

10.8. Summary of the Results

The unity check for the ultimate limit state, the serviceability limit state, and the post-breakage situation are first calculated for laminated glass with all 3 types of interlayers with the 12.12.12 configuration. The unity check for laminated glass with PVB interlayer with the 12.12.12 configuration exceeds 1; therefore, the configuration needs to be increased. The 12.12.12.12 configuration ended up being sufficient.

The unity checks for laminated glass with SGP interlayer with the 12.12.12 configuration are extremely low, so the configuration is lowered to save material. In the end, the 12.12.10 configuration was enough.

Just like that of laminated glass with PVB interlayer, laminated glass with EVA interlayer with the 12.12.12 configuration has the unity check of over 1. So the configuration needs to be increased, and my hand calculations show that a configuration of 12.12.10.10 is enough.

Figure 88 shows the maximum stress for the distributed load condition and point load condition for the ultimate limit state and the post-breakage scenario. The maximum stress for the point load condition is significantly higher than that of the distributed load condition, so the determining condition for the design will be the point load condition.

Four glass panels are required for laminated glass with PVB and EVA interlayer, so their critical scenario is the post-breakage scenario with the point load condition. Only 3 panels are necessary for laminated glass with SGP interlayer, so the critical scenario is the ultimate limit state with the point load condition.

Figure 88 shows the deflection for the distributed load condition and the point load condition for the serviceability limit state. The deflection for laminated glass with PVB interlayer is the highest and the deflection for laminated glass with SGP interlayer is the lowest.

Interlayer	σ_{ed} Distributed Load (N/mm2)	σ_{ed} Point Load (N/mm2)	σ_{ed} Post-Breakage Distributed Load (N/mm2)	σ_{ed} Post-Breakage Point Load (N/mm2)	w Distributed Load (mm)	w Point Load (mm)
PVB (12.12.12.12)	10.14	32.69	9.11	29.17	1.80	2.68
SGP (12.12.10)	6.07	27.22	7.47	29.73	0.64	1.01
EVA (12.12.10.10)	5.76	30.40	5.73	23.24	0.96	1.49

Figure 88. Stress and deflection for Distributed and Point Load

10.9. DIANA Simulations

A 2D linear static analysis is first conducted in DIANA to confirm the hand calculations. Then, a 2D structurally nonlinear analysis is conducted to compare with the results from the 2D linear static analysis. Both 2D analysis are conducted with the equivalent thickness from NEN2608. Finally, a 3D linear static analysis is conducted to confirm the results from the previous two analysis. The 3D analysis is conducted with stacked glass elements and interface elements in between those stacked elements.

10.9.1. 2D Model: Linear Static

First, a 2D linear static analysis is first conducted in DIANA to confirm the hand calculations. Figure 89 shows the setup of the model for the distributed load condition and the point load condition for the 2D linear static model. The geometry of the model is 1m by 2.7m, and the equivalent thickness from NEN2608 is used. The glass plate is modelled with translational fixity in the z-direction on all 4 edges, translational fixity in the x and y-direction at 1 vortex, and translational fixity in the x-direction at another vortex. Figure 90 shows the properties of glass that is used for the model. The point load situation is modelled with a distributed load at the centre of the plate over an 100mm by 100mm area. A mesh with the element size of 0.05m is used for the analysis.

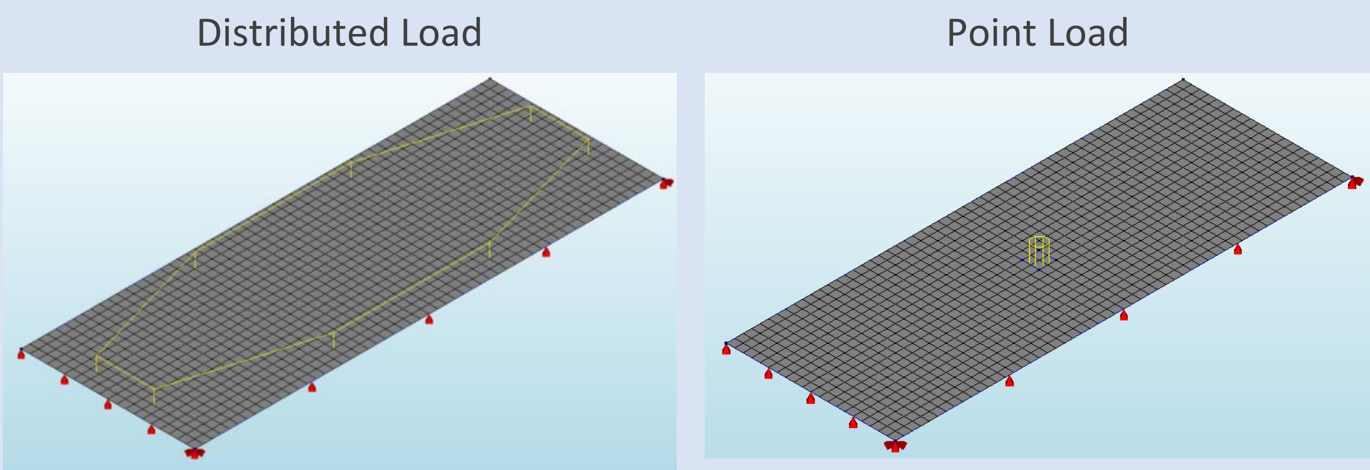

Figure 89. DIANA Setup with Distributed and Point Load

	Glass
Young's modulus	70,000 N/mm2
Poisson's ratio	0.22
Thermal expansion coefficient	9e-06 1/k
Mass density	2.5e-09 T/mm2
Characteristic strength at 28 days	27.5 N/mm2
Mean compressive strength	1000 N/mm2

Figure 90. Properties of Glass (Physical properties of Glass, 2021)

As for the results of the simulation, the total Cauchy principal stress (S1) and the maximum deflection are looked at in detail. Figure 91 shows the formula for calculating the principal stresses as well as the Mohr circle that is used to create the formulas. Principal stresses are the maximum and minimum value of the normal stresses on a plane, and they are represented with σ_1 and σ_2. The Mohr circle is a graphical representation of the transformation law for the Cauchy stress tensor.

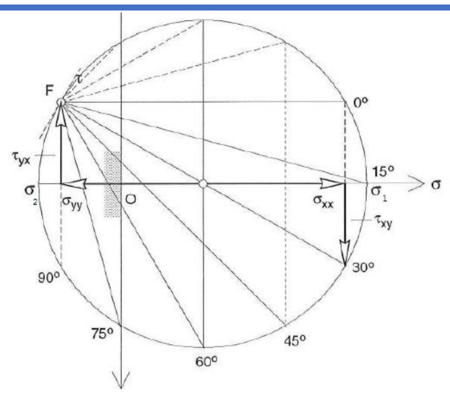

$$\sigma_{1,2} = \frac{\sigma_{xx} + \sigma_{yy}}{2} \pm \sqrt{\left(\frac{\sigma_{xx} - \sigma_{yy}}{2}\right)^2 + \tau_{xy}^2}$$

Figure 91. Mohr Circle and Principal Stress.

Figure 92 shows the stress pattern for the top layer and the bottom layer for the distributed load condition, and the stress pattern are quite logical. For the bottom layer, the highest stress appear at the centre, and the amount of stress decreases as you move outwards from the centre. For the top layer, the lowest stress appear at the centre of the panel, and the stress increases as you move outwards.

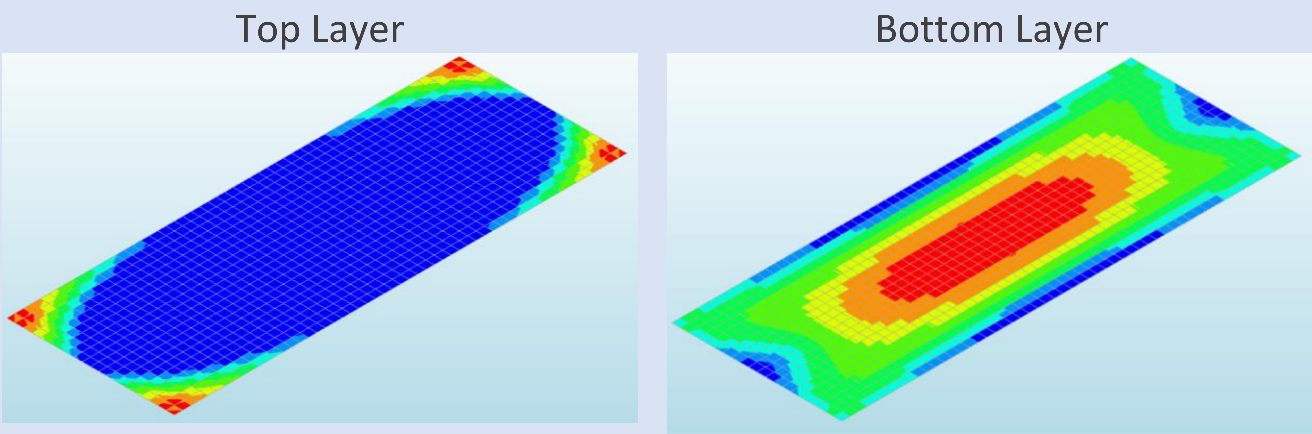

Figure 92. DIANA Setup with a Distributed Load (PVB 12.12.12.12)

Figure 93 shows the stress pattern for the top layer and the bottom layer for the point load condition., and the stress pattern also appears logical. For the bottom layer, the highest stress appear at the centre of the panel, and the amount of stress decreases as you move outwards. It is also logical that the stress at the centre of the bottom layer for the point load condition is higher and more concentrated than that of the distributed load condition. For the top layer, the lowest stress is located at the centre of the panel, and there are high stress concentrations along the long edge of the top layer.

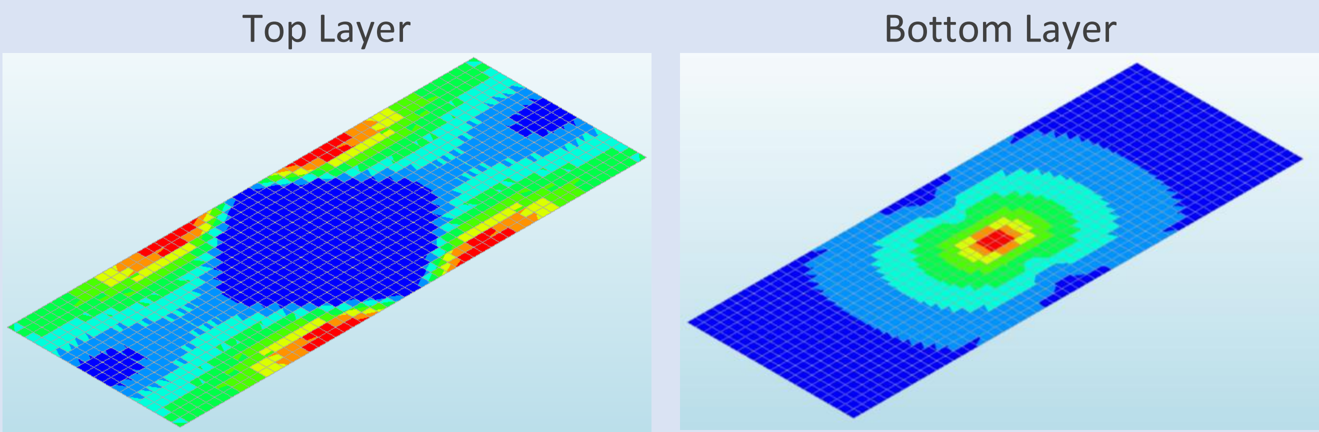

Figure 93. DIANA Setup with a Point Load (PVB 12.12.12.12)

A 2D linear static analysis for the serviceability limit state is also performed in DIANA. The maximum translational distance in the z-direction was compared with the displacement from the simple calculations. Figure 94 shows the deformed shape for the distributed load condition and the point load condition, and the deformed shape appears logical.

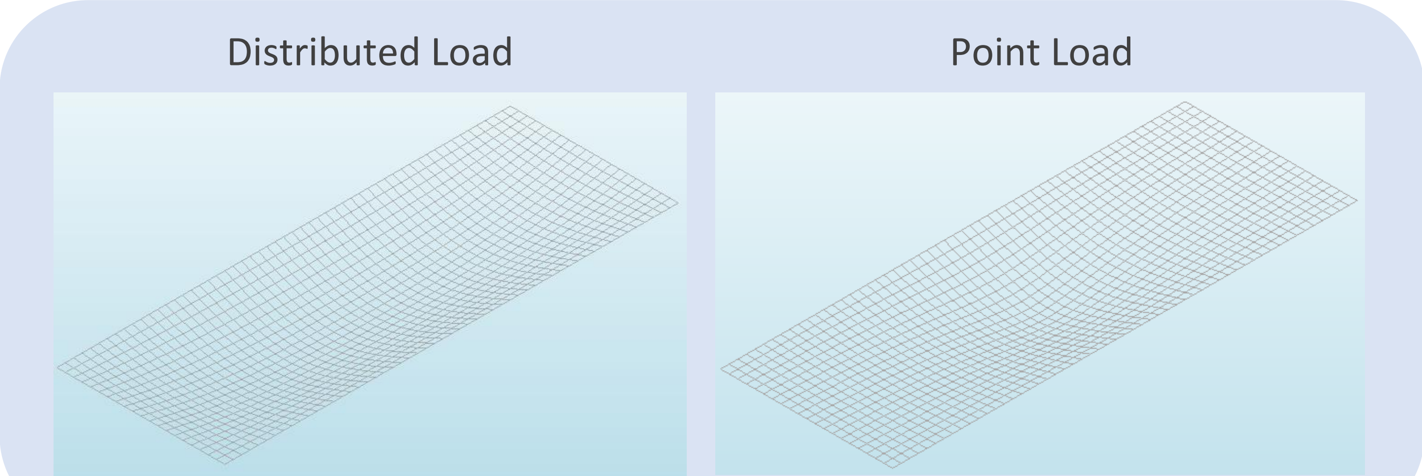

Figure 94. Deformed shape for the Distributed and Point Load

Figure 95 shows the value of the maximum stress and maximum deformation from the linear static model in comparison with that of the hand-calculation for the distributed load condition. Figure 96 shows the stress and deformation of the linear static model in comparison with that of the hand-calculation for the point load condition. The value of the maximum stress and the maximum deflection for the linear static scenario are almost the same as that of the hand calculation: all the scenarios and load conditions have a difference of less than 3%.

Interlayer	σ_{ed} Hand Calculation (N/mm2)	σ_{ed} 2D Linear Static (N/mm2)	σ_{ed} Post-Breakage Hand Calculation (N/mm2)	σ_{ed} Post-Breakage 2D Linear Static (N/mm2)	w Hand Calculation (mm)	δ 2D Linear Static (mm)
PVB (12.12.12.12)	10.14	10.33	9.11	9.28	1.80	1.75
SGP (12.12.10)	6.07	6.13	7.47	7.61	0.64	0.62
EVA (12.12.10.10)	5.76	5.76	5.73	5.84	0.96	0.94

Figure 95. stress and deformation of the hand-calculation vs. linear static model for distributed load

Interlayer	σ_{ed} Hand Calculation (N/mm2)	σ_{ed} 2D Linear Static (N/mm2)	σ_{ed} Post-Breakage Hand Calculation (N/mm2)	σ_{ed} Post-Breakage 2D Linear Static (N/mm2)	w Hand Calculation (mm)	δ 2D Linear Static (mm)
PVB (12.12.12.12)	32.69	32.64	29.17	29.09	2.68	2.82
SGP (12.12.10)	27.22	27.19	29.73	29.67	1.01	1.07
EVA (12.12.10.10)	30.40	30.36	23.24	23.19	1.49	1.57

Figure 96. stress and deformation of the hand-calculation vs. linear static model for point load

10.9.2. 2D Model: Structurally Nonlinear

After the 2D linear static analysis, a 2D structural nonlinear analysis is conducted on the model. 10 load steps with 10% loading on each step is used, and the maximum number of iterations is set to 30. The stress pattern for the structurally nonlinear analysis are the same as that of the linear static analysis.

Figure 97 shows the amount of maximum stress and maximum deformation from the structurally nonlinear analysis in comparison with that of the linear static analysis for the distributed load condition. For the distributed load condition, the value of the maximum stress and the maximum deflection for the structurally nonlinear analysis are exactly the same as that of the linear static analysis.

Figure 98 shows the value of the maximum stress and the maximum deformation of the structurally nonlinear model in comparison with that of the linear static model for the point load condition. The value of the maximum stress for the structurally nonlinear analysis is slightly higher than that of the linear static analysis, but the difference is only less than 1%. The value of the maximum deflection from the structurally nonlinear analysis are exactly the same as that of the linear static analysis.

Interlayer	σed 2D Linear Static (N/mm2)	σed 2D Struct. Nonlinear (N/mm2)	δ 2D Linear Static (mm)	δ 2D Struct. Nonlinear (mm)	σed post-breakage 2D Linear Static (N/mm2)	σed post-breakage 2D Struct. Nonlinear (N/mm2)
PVB (12.12.12.12)	10.33	10.33	1.75	1.75	9.28	9.27
SGP (12.12.10)	6.13	6.13	0.62	0.62	7.61	7.61
EVA (12.12.10.10)	5.76	5.76	0.94	0.94	5.84	5.84

Figure 97. stress and deformation of the linear static vs. structurally nonlinear model for the distributed load

Interlayer	σed 2D Linear Static (N/mm2)	σed 2D Struct. Nonlinear (N/mm2)	δ 2D Linear Static (mm)	δ 2D Struct. Nonlinear (mm)	σed post-breakage 2D Linear Static (N/mm2)	σed post-breakage 2D Struct. Nonlinear (N/mm2)
PVB (12.12.12.12)	32.64	32.87	2.82	2.81	29.09	29.33
SGP (12.12.10)	27.19	27.33	1.07	1.07	29.67	29.92
EVA (12.12.10.10)	30.36	30.55	1.57	1.57	23.19	23.32

Figure 98. stress and deformation of the linear static vs. structurally nonlinear model for the point load

10.9.3. 3D Model: Linear Static

After the 2D linear static analysis and the 2D structural nonlinear analysis, a 3D linear static model is created and analysed. Figure 99 shows the setup of the 3D linear static model for the distributed load condition and the point load condition. The geometry of the model is 1m by 2.7m, and the glass elements with the thickness of either 9.7mm or 11.7mm are stacked on top of each other. Interface elements are created in between the glass elements, and the elastic and shear modulus are defined for those interface elements.

Stacked shell elements with interface elements that was used in the end for the 3D model. Layered shell element was also considered, but it was concluded that it would not be a good option to model laminated glass. This is because the layered shell element assumes the same strain and displacement for all the different sections, so the resultant model would not allow for any shear deformation in the interlayer.

Figure 100 shows the properties of the interface elements that is used for the model, and the values of the shear modulus and the elastic modulus are taken for 20 degree and for the load duration of 10 years. The young's modulus is changed to 1e+12 N/m3 for the point load situation, and this is because the interlayer should behave very stiffly under a point load. The interlayer won't expand sideways, because it is surrounded by other interlayer are not are moving.

The glass plate was setup with translational fixity in the z-direction on all four edges, translational fixity in the x and y-direction at 1 vortex, and translational fixity in the x-direction at another vortex. The translational fixity are all defined at the bottom edge of the stacked elements. The point load condition are modelled with a distributed load at the centre of the top layer over a 100mm by 100mm area. A mesh with 0.05m element size is used.

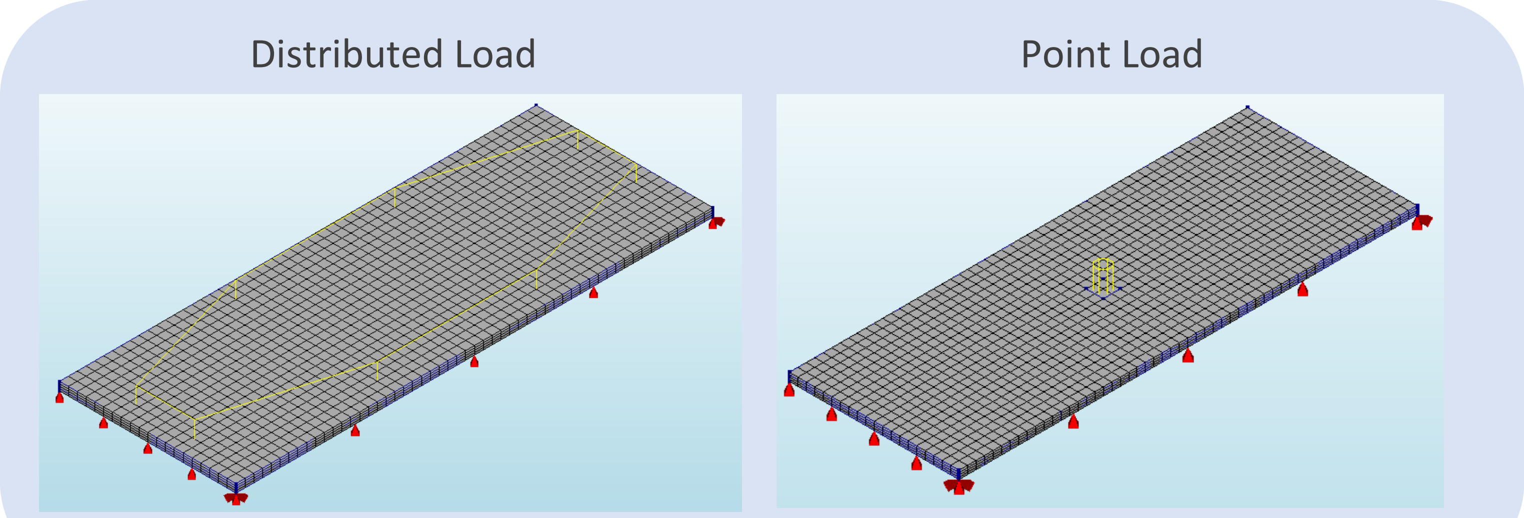

Figure 99. DIANA Setup with Distributed and Point Load

	PVB	SGP	EVA
Young's modulus	0.19 N/mm2 0.25 N/mm3	256 N/mm2 336.8eN/mm3	5N/mm2 6.579N/mm3
Shear Modulus	0.05 N/mm2 0.0658 N/mm3	6.42N/mm2 8.447N/mm3	1.33N/mm2 1.75N/mm3

Figure 100. Properties of PVB, SGP, and EVA Interlayer (Kuraray, 2020) (SWM, 2017)

Figure 101 shows the stress pattern for the top layer and the bottom layer of the distributed load condition, and the stress pattern looks quite logical. The deformation pattern at the bottom layer of the 3D model is similar to that of the 2D model. For the bottom layer, the highest stress appears at the centre, and the value of the stress decreases as you move outwards. For the top layer, the 3D model has lower stress than that of the 2D model.

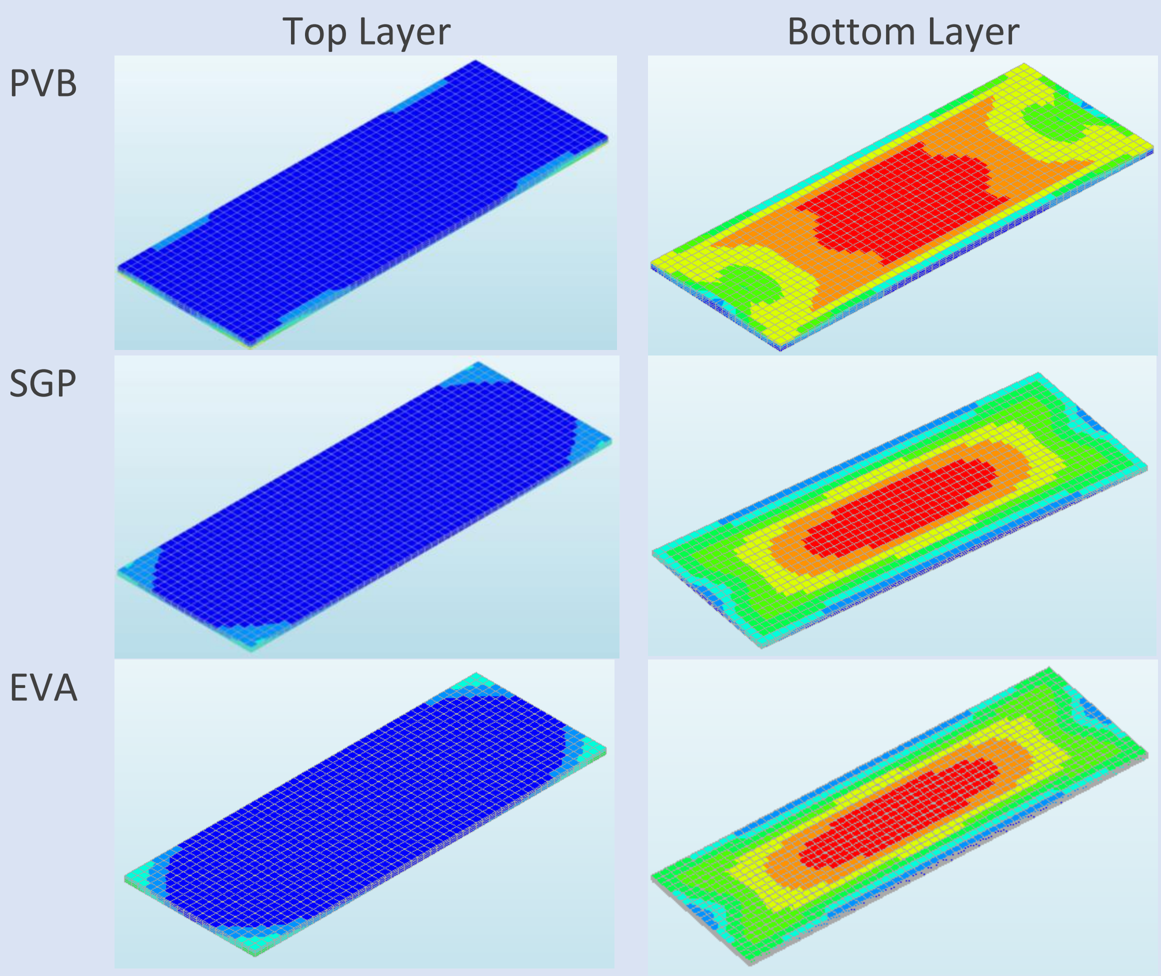

Figure 101. DIANA Setup with a Distributed Load (PVB, SGP, and EVA)

Figure 102 shows the stress pattern for the top layer and the bottom layer for the point load condition, and the stress pattern are quite logical. At the bottom layer, the deformation pattern for the 3D model is similar to that of the 2D model. For the bottom layer, the highest stress appear at the centre, and the amount of stress decreases as you move outwards. It is also logical that the stress at the centre of the bottom layer for the point load conditions has a higher value and is more concentrated than that of the distributed load condition. Just like the situation with the distributed load condition, the 3D model for the point load condition has lower stress at the top layer than that of the 2D model.

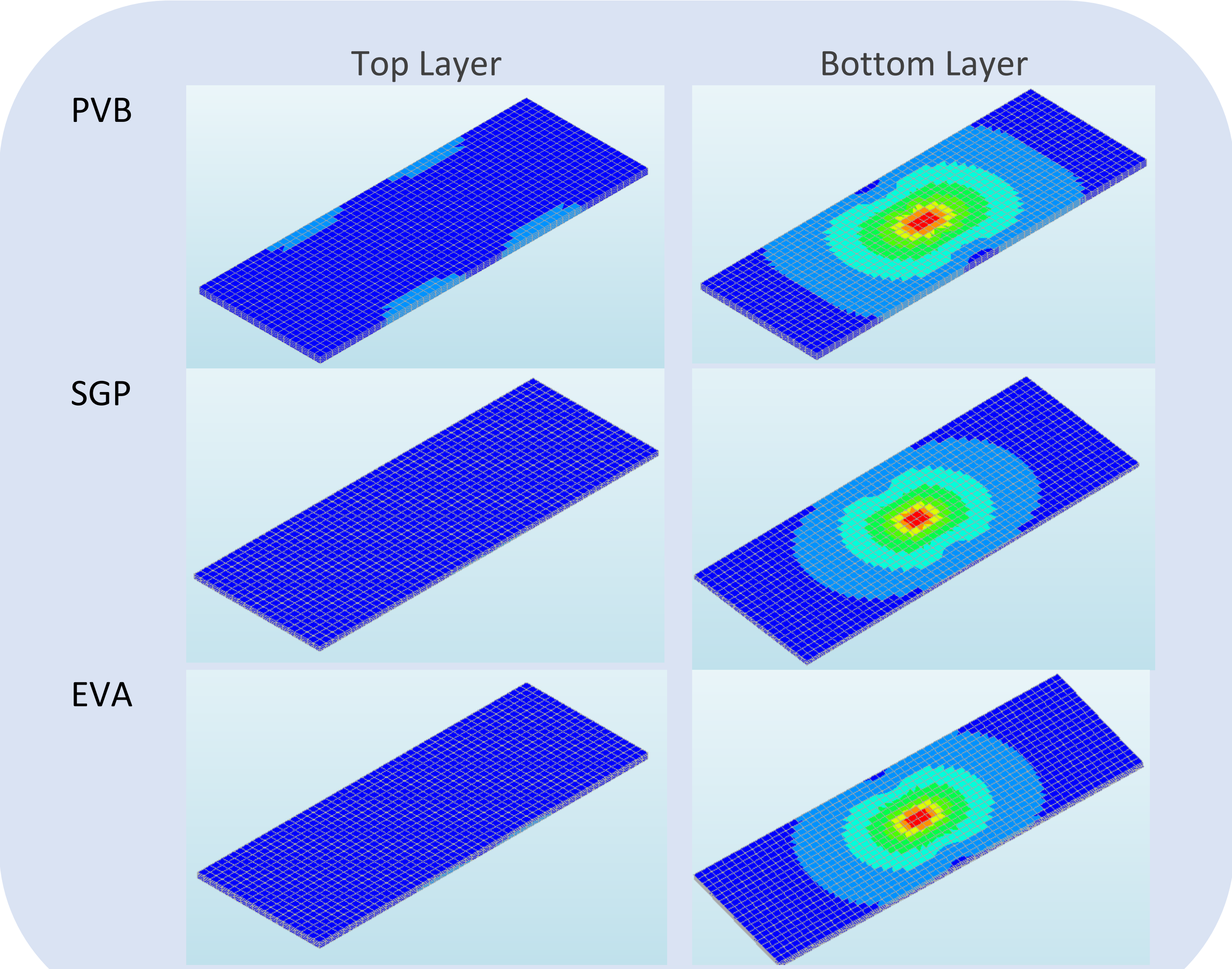

Figure 102. DIANA Setup with a Point Load (PVB, SGP, and EVA)

A 3D linear static analysis for the serviceability limit state is performed in DIANA, and the deformed shape of the 3D model is compared with that of 2D model. Figure 103 shows the deformed shape for the distributed load condition and the point load condition, and the deformed shapes appear logical.

Distributed Load Point Load

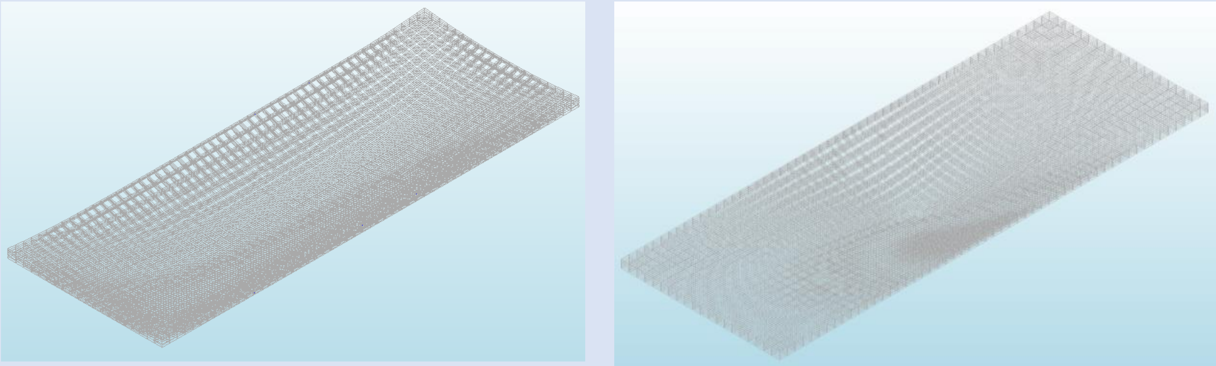

Figure 103. Deformation with Distributed and Point Load

Distributed Load: PVB Interlayer 12.12.12.12

Hand Calculation

$$\sigma_{ed} = 10.14\ \mathrm{N/mm^2}$$
$$w = 1.80\ \mathrm{mm}$$

2D Linear Static

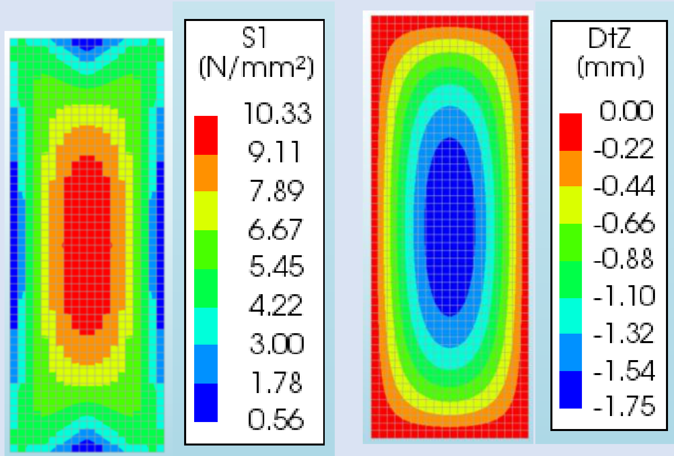

2D Structurally Nonlinear

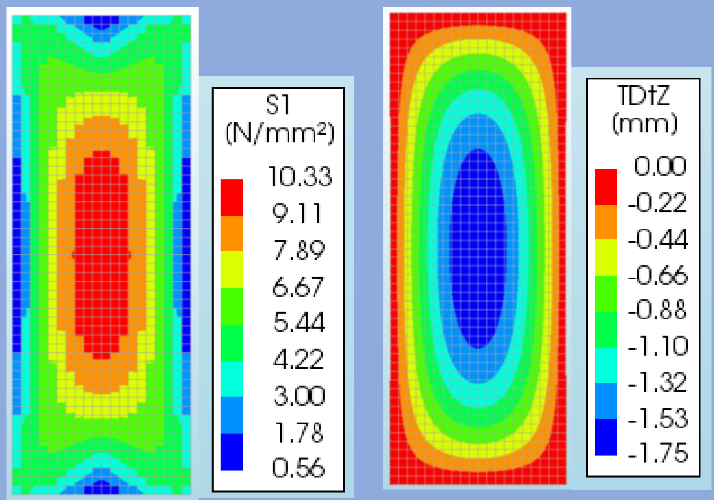

3D Linear Static

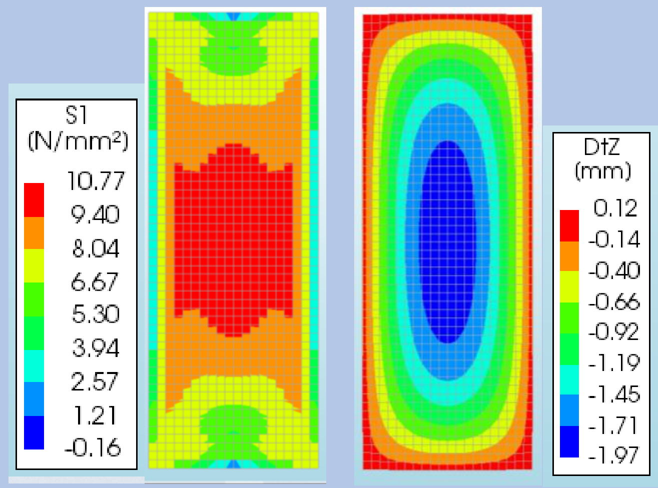

Distributed Load: SGP Interlayer 12.12.10

Hand Calculation

$$\sigma_{ed} = 6.07 \text{ N/mm2}$$
$$w = 0.64 \text{ mm}$$

2D Linear Static

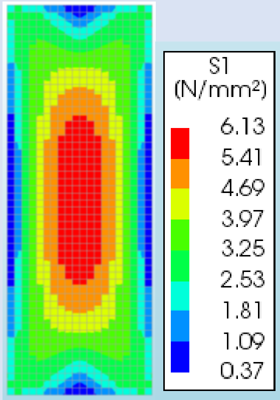

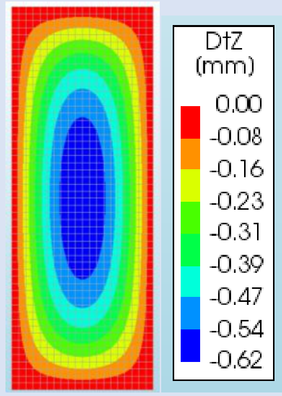

2D Structurally Nonlinear

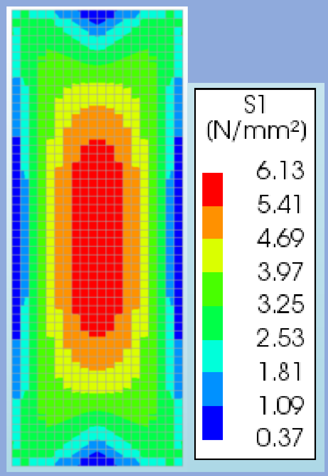

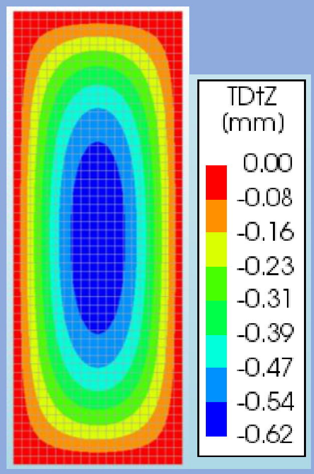

3D Linear Static

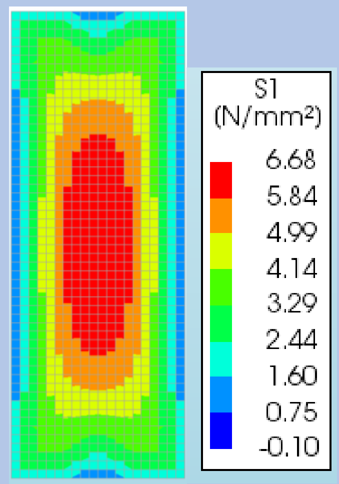

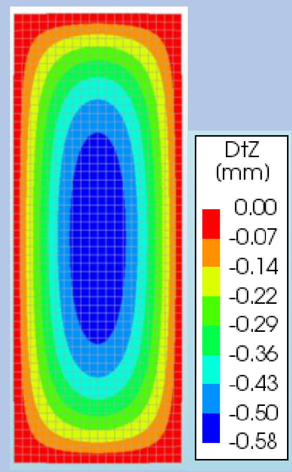

Distributed Load: EVA Interlayer 12.12.10.10

Hand Calculation

$$\sigma_{ed} = 5.76\ \text{N/mm2}$$
$$w = 0.96\ \text{mm}$$

2D Linear Static

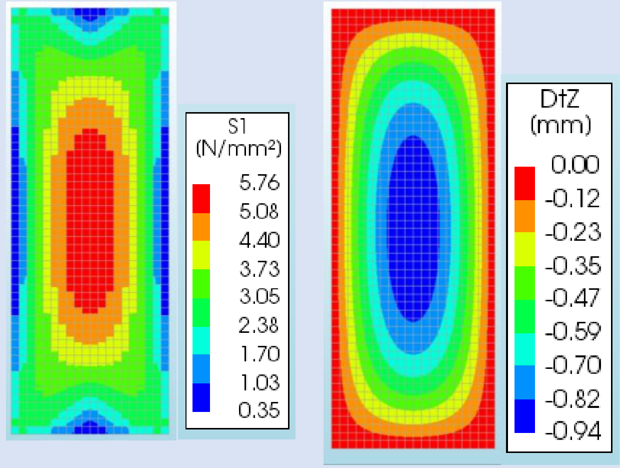

2D Structurally Nonlinear

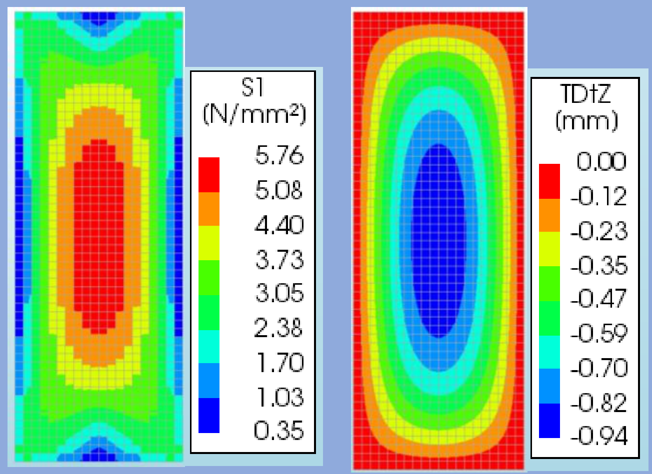

3D Linear Static

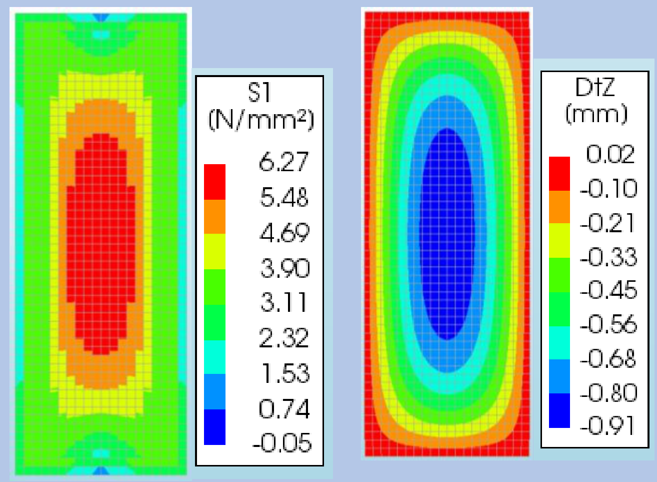

Point Load: PVB Interlayer 12.12.12.12

Hand Calculation

$$\sigma_{ed} = 32.69 \text{ N/mm2}$$
$$w = 2.68 \text{ mm}$$

2D Linear Static

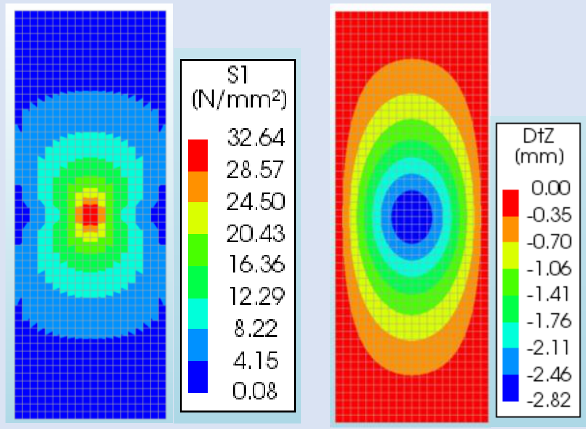

2D Structurally Nonlinear

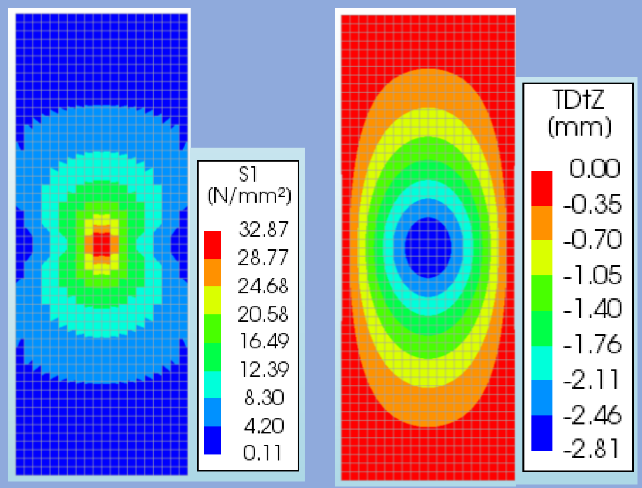

3D Linear Static

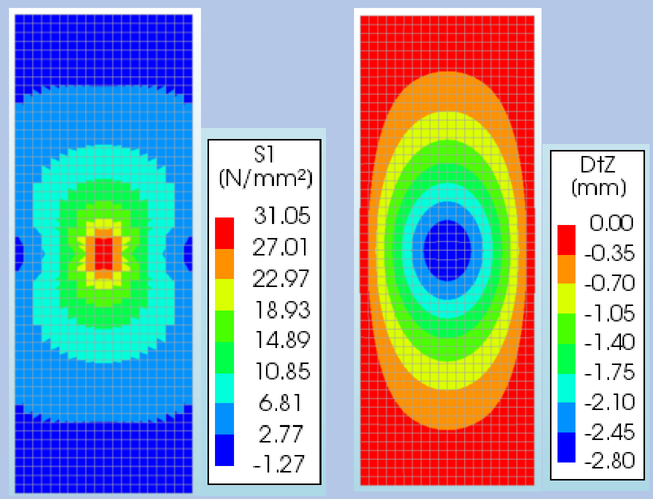

Point Load: SGP Interlayer 12.12.10

Hand Calculation

$$\sigma_{ed} = 27.22 \text{ N/mm2}$$
$$w = 1.01 \text{ mm}$$

2D Linear Static

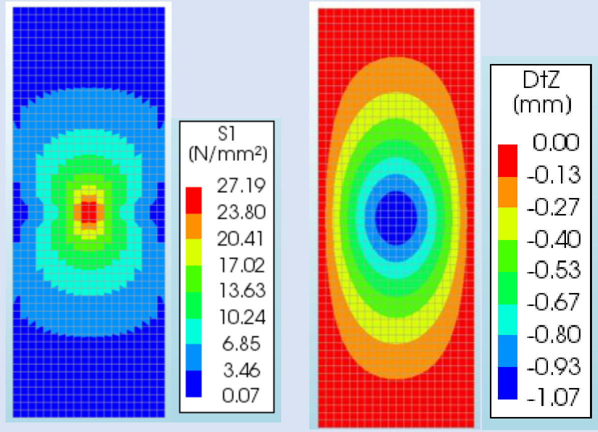

2D Structurally Nonlinear

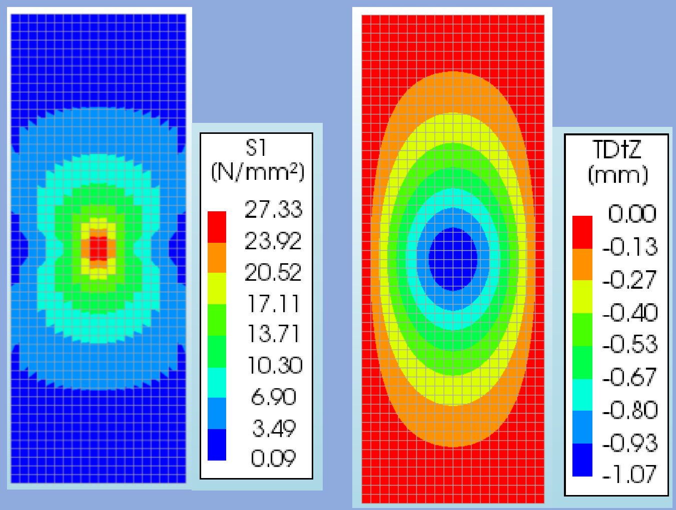

3D Linear Static

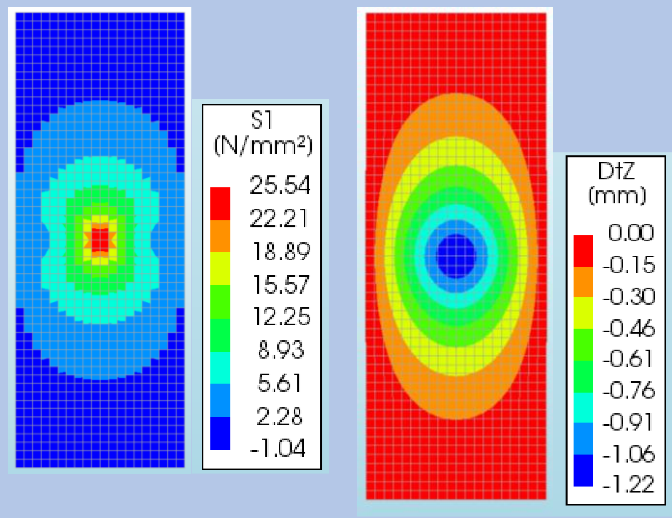

Point Load: EVA Interlayers 12.12.10.10

Hand Calculation

$$\sigma_{ed} = 30.40 \text{ N/mm2}$$
$$w = 1.49 \text{ mm}$$

2D Linear Static

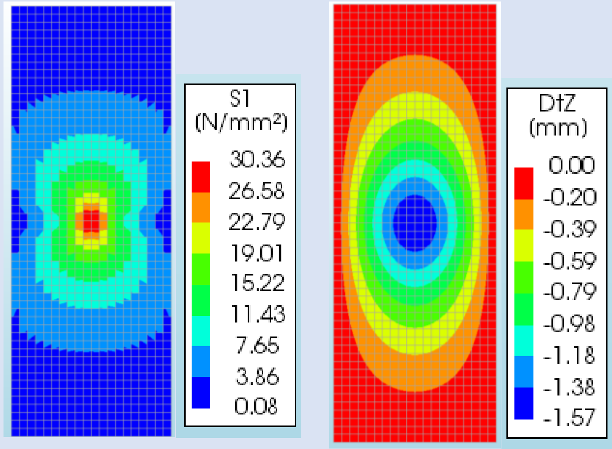

2D Structurally Nonlinear

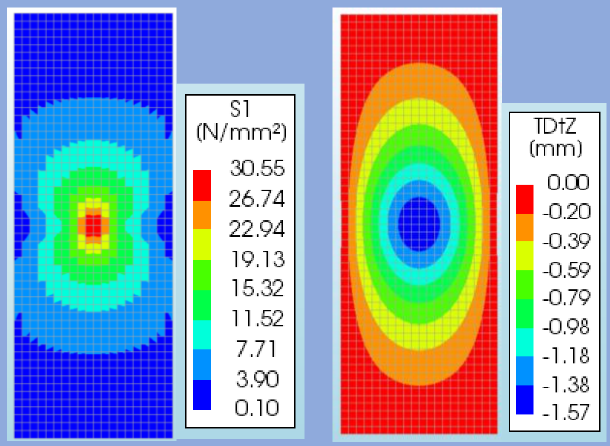

3D Linear Static

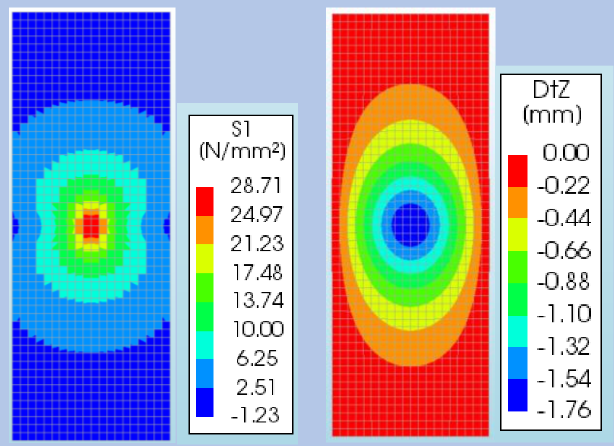

Post-Breakage Distributed Load PVB Interlayers 12.12.12.12

Hand Calculation

$\sigma_{ed} = 9.11 \text{ N/mm}^2$

2D Linear Static

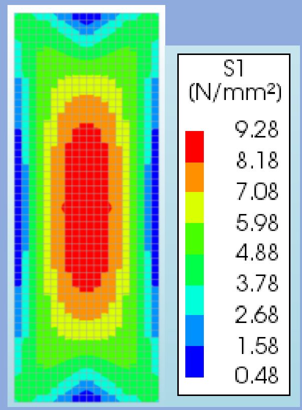

2D Structurally Nonlinear

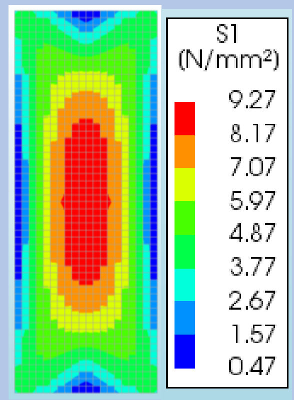

3D Linear Static

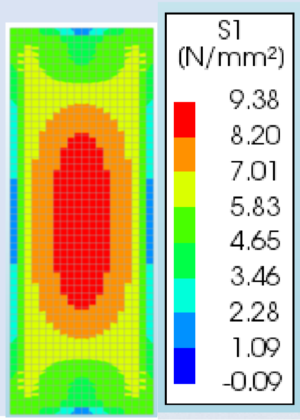

Post-Breakage Distributed Load SGP Interlayers 12.12.10

Hand Calculation

$\sigma_{ed} = 7.47 \text{ N/mm}^2$

2D Linear Static

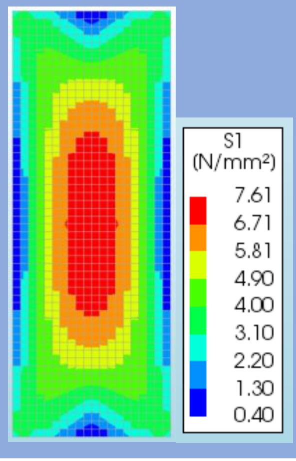

2D Structurally Nonlinear

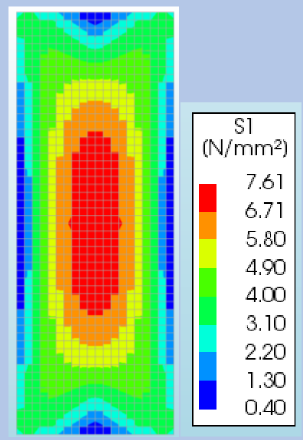

3D Linear Static

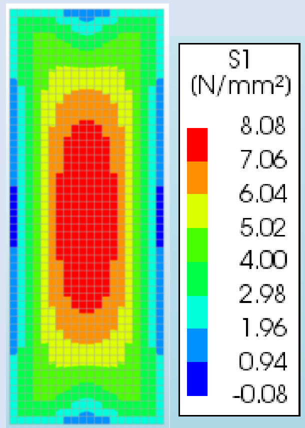

Post-Breakage: Distributed Load EVA Interlayers 12.12.10.10

Hand Calculation

$\sigma_{ed} = 5.73\ \mathrm{N/mm^2}$

2D Linear Static

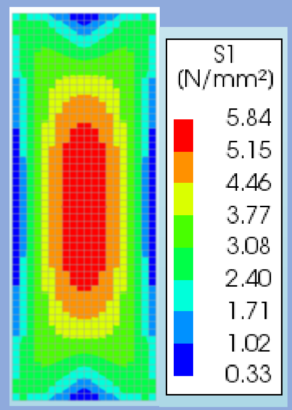

2D Structurally Nonlinear

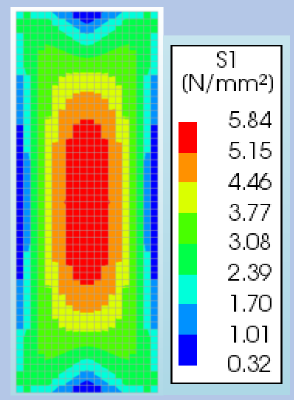

3D Linear Static

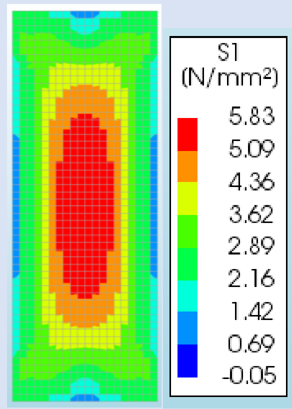

Post-Breakage Point Load PVB Interlayers 12.12.12.12

Hand Calculation

$\sigma_{ed} = 29.17\ \mathrm{N/mm^2}$

2D Linear Static

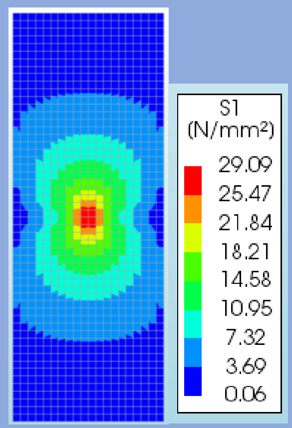

2D Structurally Nonlinear

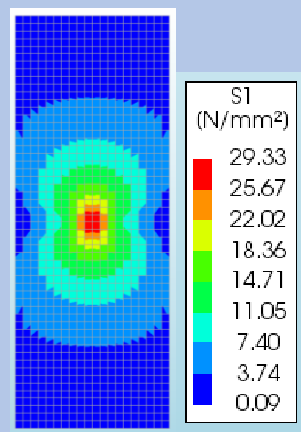

3D Linear Static

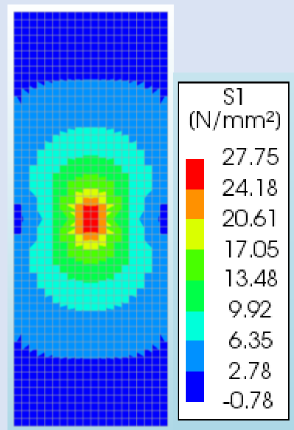

Post-Breakage Point Load SGP Interlayers 12.12.10

Hand Calculation

$\sigma_{ed} = 29.73\ \mathrm{N/mm^2}$

2D Linear Static

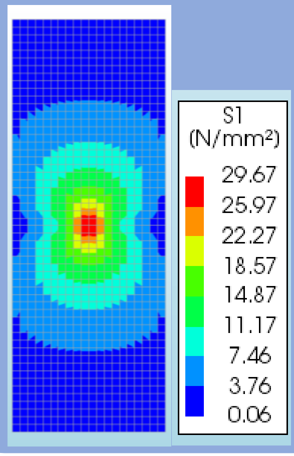

2D Structurally Nonlinear

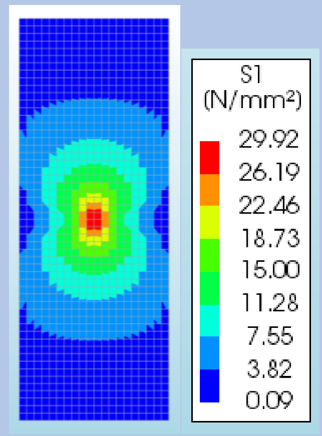

3D Linear Static

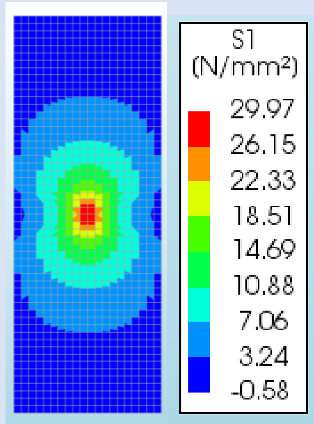

Post-Breakage: Point Load EVA Interlayers 12.12.10.10

Hand Calculation

$\sigma_{ed} = 23.24\ \mathrm{N/mm^2}$

2D Linear Static

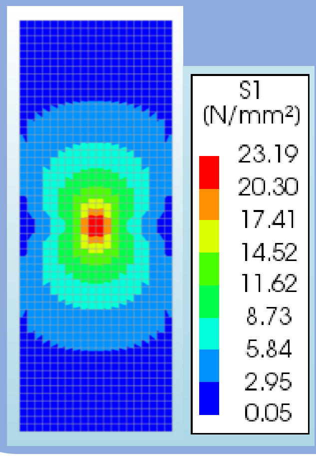

2D Structurally Nonlinear

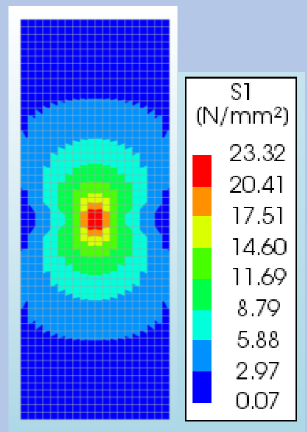

3D Linear Static

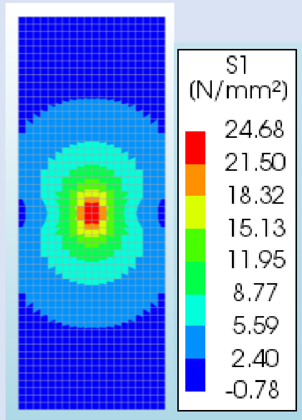

10.10. Summary of the Results

The percent difference in between the hand calculations, the 2D linear static analysis, the 2D geometrically nonlinear analysis, and the 3D linear static analysis are within 10% for all the ultimate limit state and post-breakage scenarios, so both the hand calculations and the DIANA simulations can be considered acceptable.

However, the percent difference in between the amount of deflection for SGP 12.12.10 and EVA 12.12.10.10 from the 3D model doesn't align with that from the hand calculations and the 2D models. The percent difference for the serviceability limit state of SGP 12.12.10 and EVA 12.12.10.10 are 17% and 15% respectively.

For SGP 12.12.10 and EVA 12.12.10.10, the glass panels are first modelled in 3D with the thinner panels at the top and the thicker panels at the bottom. This means that the 11.7mm are placed on the top and the 9.7mm are placed at the bottom. However, with this type of configuration, the amount of stress for EVA 12.12.10.10 from the 3D model doesn't align with that from the hand calculations and the 2D models. So the configuration with thicker panels at the top and thinner panels at the bottom are modelled in 3D for EVA 12.12.10.10, and the amount of stress from the 3D model with this configuration do align with that from the hand calculations and the 2D models.

Interlayer	σ_{ed} Hand Calculation (N/mm2)	σ_{ed} 2D Linear Static (N/mm2)	σ_{ed} 2D Structurally Nonlinear (N/mm2)	σ_{ed} 3D Linear Static (N/mm2)
PVB 12.12.12.12	10.14	10.33	10.33	10.77
SGP 12.12.10	6.07	6.13	6.13	6.68
EVA 12.12.10.10	5.76	5.76	5.76	6.27

Figure 104. Distributed Load ULS

Interlayer	w Hand Calculation (mm)	δ 2D Linear Static (mm)	δ 2D Structurally Nonlinear (mm)	δ 3D Linear Static (mm)
PVB 12.12.12.12	1.80	1.75	1.75	1.97
SGP 12.12.10	0.64	0.62	0.62	0.58
EVA 12.12.10.10	0.96	0.94	0.94	0.91

Figure 105. Distributed Load SLS

Interlayer	σ_{ed} Hand Calculation (N/mm2)	σ_{ed} 2D Linear Static (N/mm2)	σ_{ed} 2D Structurally Nonlinear (N/mm2)	σ_{ed} 3D Linear Static (N/mm2)
PVB 12.12.12.12	9.11	9.28	9.27	9.38
SGP 12.12.10	7.47	7.61	7.61	8.08
EVA 12.12.10.10	5.73	5.84	5.84	5.83

Figure 106. Distributed Load Post breakage

Interlayer	σ_{ed} Hand Calculation (N/mm2)	σ_{ed} 2D Linear Static (N/mm2)	σ_{ed} 2D Structurally Nonlinear (N/mm2)	σ_{ed} 3D Linear Static (N/mm2)
PVB 12.12.12.12	32.69	32.64	32.87	31.05
SGP 12.12.10	27.22	27.19	27.33	25.54
EVA 12.12.10.10	30.40	30.36	30.55	28.71

Figure 107. Point Load ULS

Interlayer	w Hand Calculation (mm)	δ 2D Linear Static (mm)	δ 2D Structurally Nonlinear (mm)	δ 3D Linear Static (mm)
PVB 12.12.12.12	2.68	2.82	2.81	2.80
SGP 12.12.10	1.01	1.07	1.07	1.22
EVA 12.12.10.10	1.49	1.57	1.57	1.76

Figure 108. Point Load SLS

Interlayer	σ_{ed} Hand Calculation (N/mm2)	σ_{ed} 2D Linear Static (N/mm2)	σ_{ed} 2D Structurally Nonlinear (N/mm2)	σ_{ed} 3D Linear Static (N/mm2)
PVB 12.12.12.12	29.17	29.09	29.33	27.62
SGP 12.12.10	29.73	29.67	29.92	29.97
EVA 12.12.10.10	23.24	23.19	23.32	24.68

Figure 109. Point Load Post breakage

Chapter 11. Case Study: Sustainability Analysis

This chapter is on the sustainability aspect of the case study on the glass floor panels at the train station in Delft. Specifically, the shadow costs of laminated glass with different types of interlayer are considered.

11.1. Shadow Cost of Glass Floor

In this section, the shadow cost of the laminated glass configuration that would satisfy the structural requirements of the laminated glass floor at Delft Station are calculated. These configurations include 12.12.12.12 laminated glass with PVB interlayer, 12.12.10 laminated glass with SGP interlayer, and 12.12.10.10 laminated glass with EVA interlayer

11.1.1. Sample Calculations

Figure 110 shows an sample calculation of how the shadow cost of the glass floor at Delft Station is calculated. The first column in the table below shows the environmental impact in kilogram for 1m2 of laminated glass; for example, the global warming impact for 1m2 of 12.12.12.12 laminated glass is 160.874 kg of CO2, and this information is found in the Environmental Product Declaration of laminated glass.

The second column shows the environmental cost in euro per kilogram of impact. The third column shows the shadow cost in euro per 1m2 laminated glass, which is calculated by multiplying the first column by the second column. The last column shows the shadow cost of the functional unit, which is calculated by multiplying the shadow cost per 1m2 laminated glass by the area of the functional unit. The function unit is 2.7 m2 of laminated glass. After the shadow cost of the each of the 7 impact categories are found, the total shadow cost of the laminated glass is found by adding the shadow cost of the 7 impact categories.

Impact Category	Env. Impact of Laminated glass [kg X/1m2Glass]	Environmental cost [euro/kg X]	Shadow Cost of Laminated Glass [Euro/1m2Glass]	Shadow Cost of Laminated Glass [Euro/FU]
Global warming (GWP100) [kg CO2]	160.874	0.05	8.044	21.718
Ozone layer depletion (ODP) [kg CFC-11]	0.000	30	0.000	0.000
Acidification [kg SO2]	0.635	4	2.542	6.863
Eutrophication [kg (PO4)3-]	0.094	9	0.850	2.294
Photochemical oxidation [kg Ethene]	0.043	2	0.086	0.231
Abiotic depletion, non fuel [kg Antimone]	0.000	0.16	0.000	0.000
Abiotic depletion, fuel [MJ]	1.049	0.16	0.168	0.453
Total Shadow Cost				**31.559**

Figure 110. Sample Shadow Cost Calculation of 12.12.12 during Production Stage (A1 to A3)

GWP100 Impact per 1m² glass = 160.874 $kgCO_2/1m^2$ glass

Environmental cost of GWP100= 0.05 euro/$kgCO_2$

Shadow cost of GWP100 per 1m² glass = Global Warming Impact per 1m² glass * env. cost

$$= 160.874\ kgCO_2/1m^2\ glass * \frac{0.05\ euro}{kgco2}$$

= 8.044 euro/1m² glass

Shadow cost of GWP100 per glass floor = shadow cost of GWP100 per 1m² glass * area of glass

= 8.044 euro/1m² glass * 2.7 m²/FU

= 21.718 euro/FU

Total shadow cost = cost of GWP100 + cost of ODP + cost of acidification + cost of eutr.

+ cost of photochemical oxidation + cost of abiotic depletion (non-fuel)

+ cost of abiotic depletion (fuel)

= 21.718 euro/FU + 0.000 euro/FU + 6.863 euro/FU + 2.294 euro/FU

+ 0.231 euro/FU + 0.000 euro/FU + 0.453 euro/FU

= 31.559 euro/FU

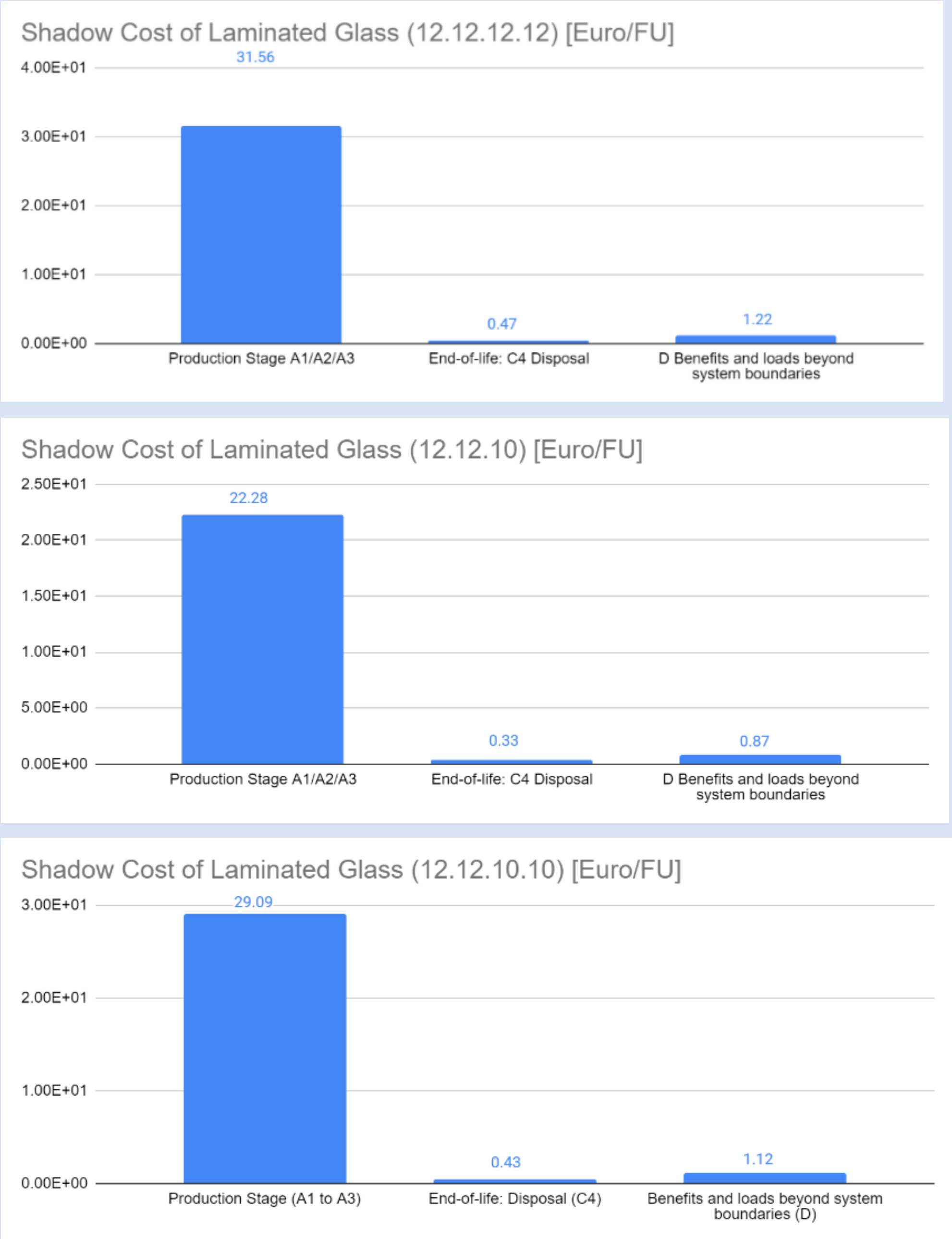

Figure 111. Shadow Cost of Glass Floor: Production Stage (A1 to A3)

11.1.2. Production Stage (A1 to A3)

The shadow cost of the glass floor during its production stage (A1 to A3) was calculated for the 7 impact categories.

During the production of float glass, CO2 is generated through electricity generation or natural gas combustion to heat the furnace as well as the glassmaking chemical process which release CO2 from carbonate raw materials. The release of CO2 bubbles help to remove air bubble during the refining process, so the release of CO2 help with produce glass without bubbles. 1m2 of low-e double glazing lead to 25 kilogram of CO2 emission [10]. Across the EU, recycling of all building glass waste would reduce carbon emissions by 230,000 tonnes per year [2].

There is no sign of impending shortage of the raw materials required to produce glass. 70% of the raw material required to produce glass is high quality silica sand. Other raw materials include soda ash, which are used to help with the melting process, and limestone and dolomite, which are added for durability and weather performances. Across the EU, recycling of all building glass waste would save 1.23 million tonnes of raw material per year [2].

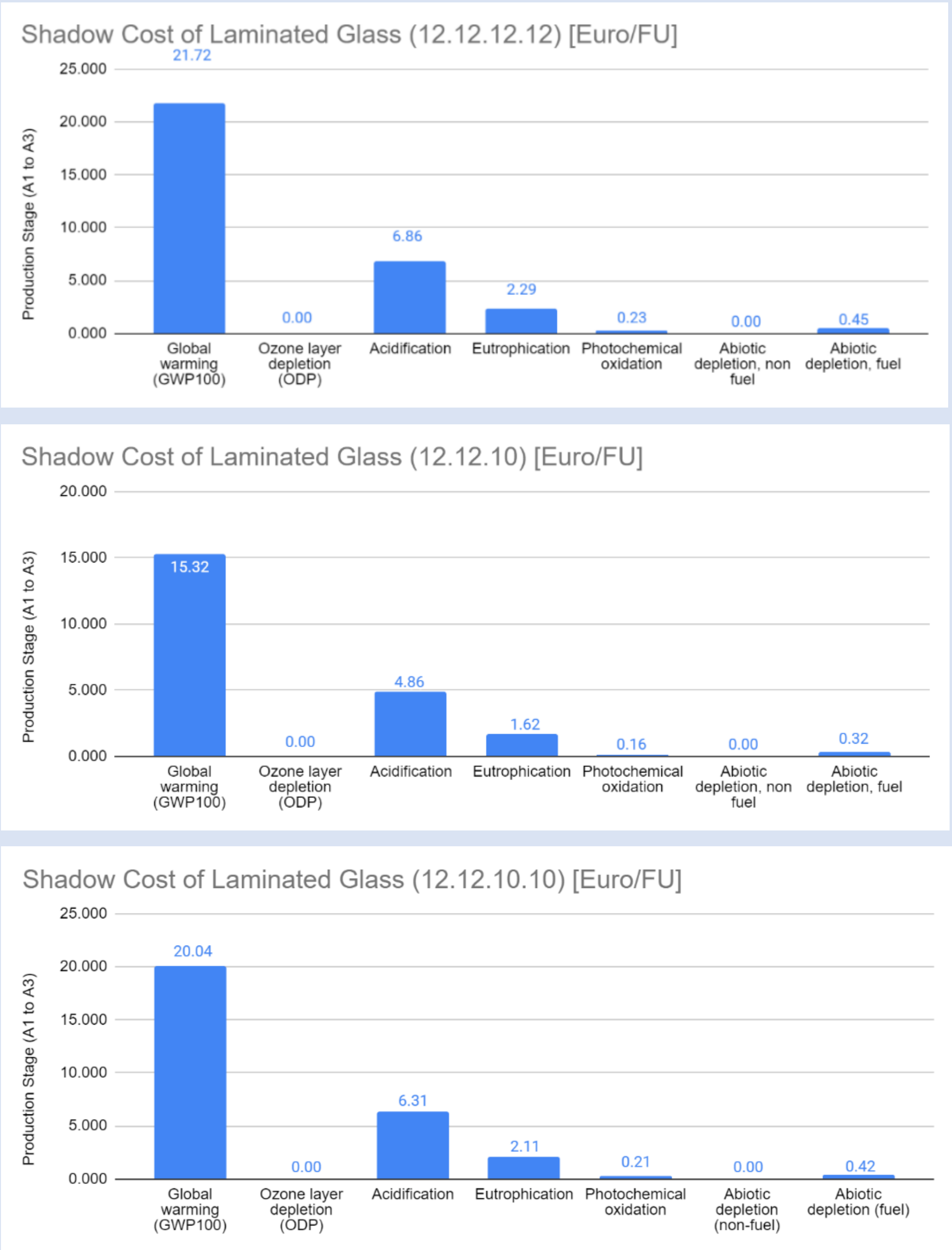

Figure 112. Shadow Cost of Glass Floor: Production Stage (A1 to A3)

11.1.3. End-of-life Stage: Disposal (C4)

The shadow cost of the glass floor during its end-of-life stage: disposal stage (C4) was calculated for the 7 impact categories. This shadow cost information was calculated based on the information found in AGC's Environmental Product Declaration from 2018, and Environmental Product Declaration assumed total disposal of the product without any recycling or reuse option.

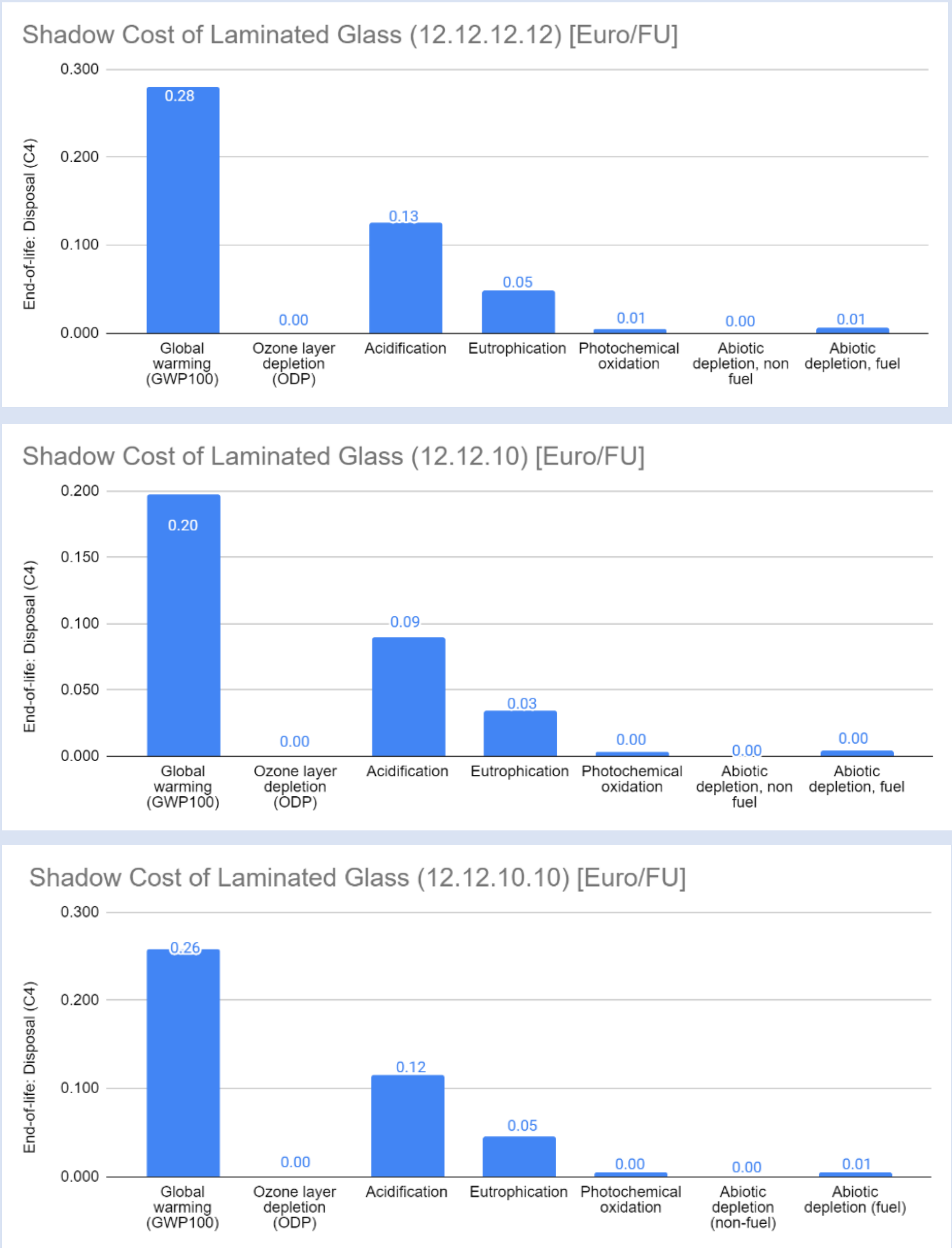

Figure 113. Shadow Cost of Glass Floor: End-of-life Stage: Disposal (C4)

11.1.4. Benefits and Loads Beyond System Boundaries (D)

The shadow cost of the glass floor during benefits and loads beyond system boundaries (D) was calculated for the 7 impact categories. Only the float glass component provides benefits and load beyond system boundaries; the shadow cost of the PVB interlayer and the fixed processes are not recovered in this section.

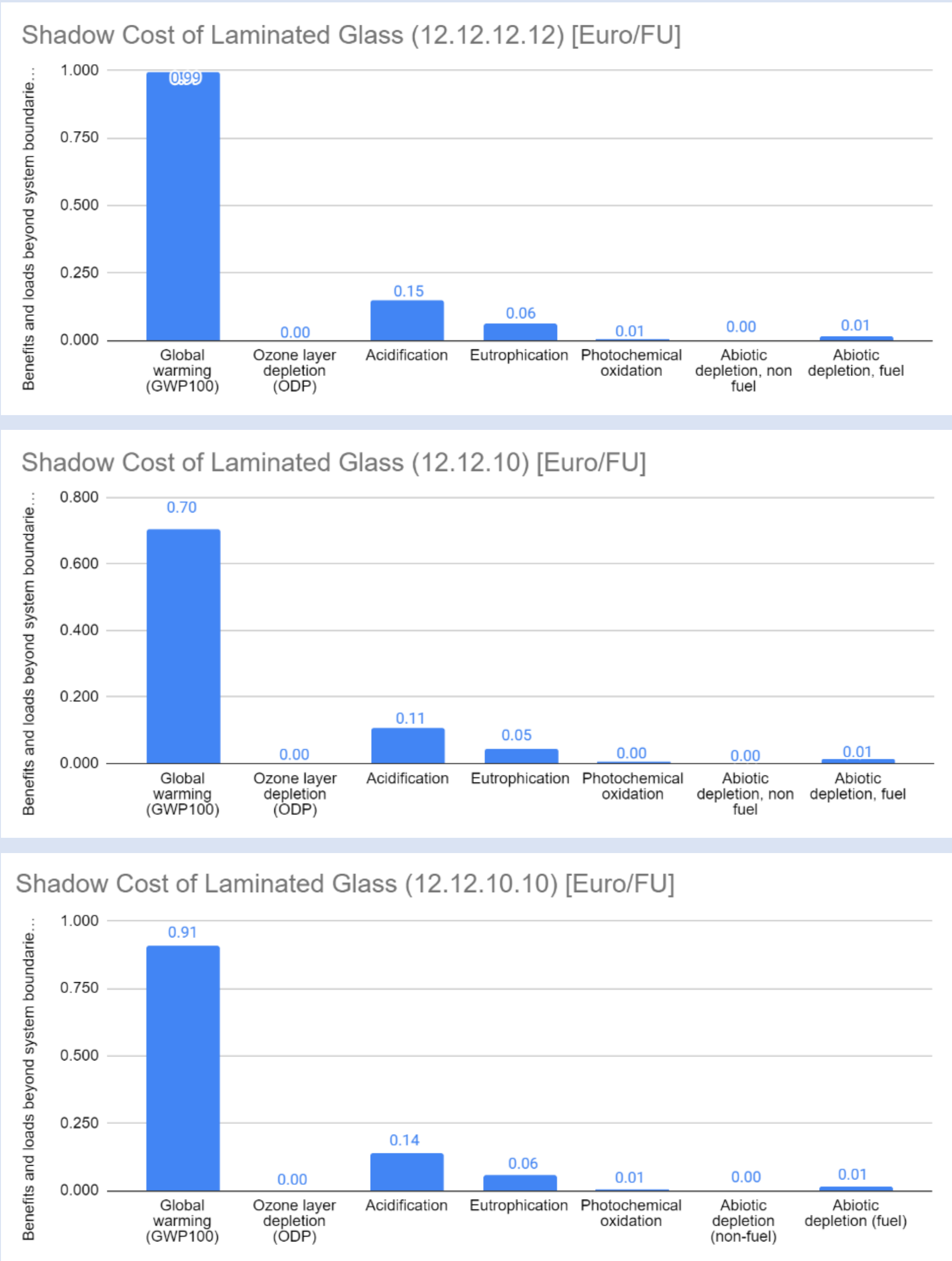

Figure 114. Shadow Cost of Glass Floor: Benefits and Loads Beyond System Boundaries (D)

Interlayer	Shadow Cost (€): Production Stage (A1 to A3)	Shadow Cost (€): End-of-life: Disposal (C4)	Shadow Cost (€): Benefits and loads beyond system boundaries (D)
PVB 12.12.12.12	31.6	0.466	1.22
SGP 12.12.10	22.3	0.328	0.867
EVA 12.12.10.10	29.1	0.430	1.12

Figure 115. Shadow cost in the Different Stage

		Shadow Cost (€):						
Interlayer		Global warming	Ozone layer depletion	Acidif.	Eutroph.	Photoch. oxidation	Abiotic depl. (non-fuel)	Abiotic depl. (fuel)
Production Stage (A1 to A3)	PVB 12.12.12.12	21.718	0.000	6.863	2.294	0.231	0.000	0.453
	SGP 12.12.10	15.319	0.000	4.857	1.623	0.163	0.000	0.319
	EVA 12.12.10.10	20.044	0.000	6.306	2.106	0.213	0.000	0.419
End-of-life: Disposal (C4)	PVB 12.12.12.12	0.280	0.000	0.126	0.049	0.005	0.000	0.006
	SGP 12.12.10	0.198	0.000	0.089	0.034	0.004	0.000	0.004
	EVA 12.12.10.10	0.259	0.000	0.116	0.046	0.005	0.000	0.005
Benefits and loads beyond system boundaries (D)	PVB 12.12.12.12	0.991	0.000	0.149	0.064	0.006	0.000	0.015
	SGP 12.12.10	0.702	0.000	0.105	0.045	0.004	0.000	0.011
	EVA 12.12.10.10	0.909	0.000	0.136	0.058	0.005	0.000	0.014

Figure 116. Shadow Cost of the Different Impact Categories

Part V. Conclusion

Chapter 12. Conclusion

12.1. Structural Performance

Tensile tests from literature on PVB, SGP, and EVA interlayers are compared for their initial stiffness, maximum stress, and ductility. The results show that SGP interlayer has the highest maximum allowable stress at 45 MPa in comparison with the maximum stress of 43 MPa for PVB and the maximum stress of 10 MPa for EVA. EVA interlayer has the highest ductility with a strain value of 7 in comparison with a strain value of 2 for SGP and a strain value of 5 for PVB. PVB interlayer has a lower initial stiffness as well as lower ductility, and SGP interlayer has the highest initial stiffness. These tensile tests are conducted under the same condition, so they are comparable.

However, it should be noted that “Extra Strength PVB” has similar initial stiffness, maximum stress, and ductility to that of SGP interlayer, so it is important to distinguish between PVB interlayer and “PVB Extra Strength”.

In the DIANA simulation from the case study, the maximum stress at the second lowest glass panel of laminated glass with PVB, SGP, and EVA interlayer are 30.90N/mm2, 21.79N/mm2, and 25.41N/mm2 respectively. The maximum stress at the second lowest glass panel can give some indication for the amount of stress experienced by the interlayer, and these stress values are all taken from the governing scenario, or the ultimate limit state of the point load situation. These maximum stress values from the DIANA simulation from the case study are lower than the maximum stress before breakage from the tensile tests from for PVB and SGP interlayer, so it is not important that SGP interlayer has a higher maximum stress than that of PVB interlayer in this case.

The tensile tests from literature shows that the elastic modulus of SGP is the highest, and the elastic modulus of PVB is the lowest. This is in line with the elastic modulus value from the interlayer companies, and this is also in line with the values used in the DIANA simulations. However, the elastic modulus values should not be very important in my case study, because the point load conditions are the governing conditions, and the elastic modulus value is not important in the point load condition. This is because the interlayer should behave very stiffly under a point load, because it is surrounded by other interlayer that are not moving.

From the DIANA simulation of the case study, the maximum deformation for laminated glass with PVB, SGP, and EVA interlayer are 2.80mm, 1.22mm, and 1.76mm respetively. Since laminated glass with PVB interlayer will deform more, PVB will need to be more ductile. By the same logive, laminated glass with SGP interlayer will deform less, so SGP will not need to be as ductile. The tensile test from literature shows that EVA is the most ductile material, and SGP is the most brittle. Strenth and stiffness could be important in a scenario where all the glass are broken; however, this scenario is not considered in this analysis.

In addition to the tensile tests, four-point bending tests from literature on laminated glass with PVB, SGP, and EVA interlayer are compared. The results show that laminated glass with SGP will break at a larger force of 1500N in comparison with a force of 1200N for PVB and a force of 1000N for EVA. The results also show that laminated glass with SGP will break at a large displacement of 18mm in comparison with 16mm for PVB and 15mm for EVA.

The four-point bending tests should be a more realistic and should be a better indication of the behaviour of interlayer in a real-life scenario. With the same configuration, laminated glass with SGP can take more load and displacement before the bottom panel breaks. Laminated glass with EVA can take the least load and displacement before the bottom panel breaks, but the difference between PVB and EVA is quite small. This shows that laminated glass with SGP interlayer would perform better structurally.

If a load is applied onto laminated glass, the bottom panel will fracture first, and the top panel and middle panel will need to take all the load. The interlayer will be in tension and will lock the broken glass pieces together. At this time, the ability of the interlayer to hold the broken pieces together is dependent on the tensile strength of the interlayer. It is common to use heat-strengthened glass in laminated glass because of its the post-breakage patterns; however, perhaps it would be possible to use an interlayer with higher tensile strength in combination with fully-tempered.

In addition to the tensile tests and the four-point bending tests from literature, hand calculations are used to analyse a case study of the glass floor at Delft Station. It was concluded from the hand calculations that laminated glass with PVB, SGP, and EVA interlayer requires a configuration of 12.12.12.12, 12.12.10, and 12.12.10.10 respectively.

From the hand calculations, it was found that the maximum stress for the point load condition is significantly higher than that of the distributed load condition, so the determining condition will be the point load condition. Four glass panels are required for laminated glass with PVB and EVA interlayer, and their critical scenario is the ultimate limit state with a point load. Only 3 panels are necessary for laminated glass with SGP interlayer, and its critical scenario is the post-breakage scenario with a point load.

From the hand calculations, it was found that the deflection for laminated glass with PVB interlayer is the highest, and the deflection for laminated glass with SGP interlayer is the lowest. This is very reasonable. SGP interlayer has the highest shear modulus, so the glass panels would be able to work together more, which lead to lower deflection. PVB, on the other hand, has the lowest shear modulus, so the glass panels would be able to work together less, which lead to higher deflection.

For the 2D linear static model, the highest stress appears at the centre of the bottom layer, and the amount of stress decreases as you move outwards from the centre. The stress at the centre of the bottom layer for the point load condition is higher and more concentrated than that of the distributed load condition. The lowest stress appear at the centre of the top layer, and the amount of stress increases as you move outwards. Since the load is applied on top of the panel, it is reasonable that the highest stress appear at the centre of the bottom layer. It is also reasonable that the maximum stress from the point load is higher and more concentrated than that of the distributed load.

The stress pattern at the bottom layer of the 3D model is similar to that of the 2D model. The highest stress appears at the centre of the bottom layer, and the value of the stress decreases as you move outwards. The stress at the centre of the bottom layer for the point load conditions has a higher value and is more concentrated than that of the distributed load condition. The only difference is that the 3D model has lower stress than that of the 2D model for the top layer.

Stacked shell elements with interface elements that was used in the end for the 3D model. Layered shell element was also considered, but it was concluded that it would not be a good option to model laminated glass. This is because the layered shell element assumes the same strain and displacement for all the different sections, so the resultant model would not allow for any shear deformation in the interlayer.

The percent difference in between the hand calculations, the 2D linear static analysis, the 2D geometrically nonlinear analysis, and the 3D linear static analysis are within 10% for all of the stress values in ultimate limit state and the post-breakage scenarios. This means that the ultimate limit state and the post-breakage scenarios for both the hand calculations and the DIANA simulations can be considered correct.

For the SGP 12.12.10 and the EVA 12.12.10.10 configuration, the 3D models are first created with the thinner panels at the top and the thicker panels at the bottom. This means that the 11.7mm panels are placed on the bottom and the 9.7mm panels are placed at the top. However, with this type of configuration, the amount of stress from the 3D model of EVA 12.12.10.10 doesn’t align with that from the hand calculations and the 2D models. So the configuration in the 3D model is changed to one with thicker panels at the top and thinner panels at the bottom, and the amount of stress from the 3D model do align with that from the hand calculations and the 2D models. The stress of the 3D model with thicker panels at the top and thinner at the bottom is lower than that from the reverse.

However, for the serviceability limit state of SGP 12.12.10 and EVA 12.12.10.10, the amount of deflection from the 3D model doesn’t align with that from the hand calculations and the 2D models. The percent difference for SGP 12.12.10 and EVA 12.12.10.10 are 17% and 15% respectively. For laminated glass with PVB 12.12.12.12, the percent different in between the 3D model and the hand calculation and the 2D models is very small, so perhaps the large disparities for SPG 12.12.10 and EVA 12.12.10.10 is due to the fact that the formula for the equivalent thickness of the serviceability limit state in NEN2608 doesn’t take the configuration of the laminated glass into account. So I think the displacement values from the 3D model would be a more accurate representation of the real-life scenario.

12.2. Durability

The mid-span deflection from literature of samples that are aged in heat, solar radiation, and humidity are compared for the durability performances. For specimens that have been aged under increased temprature, the mid-span deflection of laminated glass with SGP interlayer is affected the least, and laminated glass with PVB and EVA interlayers are affected by the same amount. For specimens that have been aged under a radiation source, the mid-span deflection of laminated glass with EVA interlayer is affected the least, and laminated glass with PVB and SGP interlayers are affected by the same amount. Relative humidity does not affect the mid-span deflection of laminated glass with PVB, SGP, and EVA interlayers.

The samples are aged in heat, solar radiation, and humidity in the same manner, so the results are comparable. The temperature test is performed on samples that has been aged at a temperature of 100 °C for 2 hours. The solar radiation test is performed on samples that has been aged under a radiation source that emit spectrum similar to solar radiation at 45 °C and a RH of 50% for 83 days. The relative humidity test is done on samples that has been kept at a temperature of 50 °C and a RH of 100% for 14 days.

The change in the mid-span deflection could indicate the interlayer's ability to withstand the effect of temperature, solar radiation, and humidity. However, the samples were only aged in increased temperature, solar radiation, and increase humidity for 2 hours, 83 days, and 14 days. It would be more conclusive if laminated glass with PVB, SGP, and EVA interlayer that has been used for a long duration of time were examined.

Laminated glass with SGP and EVA interlayer is less influenced by temperature, relative humidity, and UV radiation than laminated glass PVB interlayer. So perhaps laminated glass with SGP and EVA interlayer would be better for reuse. However, it would also be important to consider the temperature and relative humidity of the location of usage. In addition, if laminated glass with SGP interlayer is less influenced by temperature, relative humidity, and UV radiation, so it would also be better for reuse, and there would also be lower delamination risks.

12.3. Sustainability Performance: EPD and Shadow Costs

Stage A of the EPD is related to the production stage; within the production stage, stage A1 is related to the raw material, and stage A3 is related to the manufacturing process. The EPDs show that the shadow cost of stage A3 is 16% higher than that of stage A1, so it is more impactful to make improvements in the manufacturing process. The raw materials required for glass production from stage A1 are not scarce, so the glass production process does not depend on the availability of its raw material. 70% of the raw material required to produce glass is high quality silica sand. Other raw materials include soda ash, which are used to help with the melting process, and limestone and dolomite, which are added for durability and weather performances. Renewable energy can be used during glass production to decrease the environmental impact in stage A3. For example, at Saint Gobain, 37% of the electricity for glass production are generated through renewable energy.

The total shadow cost is divided into the float glass component, the interlayer component, and the fixed process component. For the production stages of laminated glass, the shadow cost from the float glass component and the interlayer component makeup 71~96% and 0~19% of the total shadow cost respectively. For the disposal stages of laminated glass, the shadow cost from the float glass component and the interlayer component makeup 62~93% and 7~38% of the total shadow cost depending on the impact category. The amount of shadow cost from the interlayer component is significantly lower than that from the glass component, so the type of interlayer doesn't significantly affect the overall environmental impact of laminated glass in its entire life cycle.

The lamination process for PVB and SGP interlayer requires an autoclave to apply heat and pressure. Howevwer, the lamination process for EVA interlayer can achieved through either an infrared furnace, a convection furnace, or an autoclave with lower pressure and temperature. EVA interlayers can also be combined with glass through a vaccum lamination process, which is when the glass and interlayer are placed in a silicon vacuum bag and is heated with a vacuum pump.

However, the difference in lamination process is not that significant, because very little percentage of the shadow cost comes from the process of combining interlayer with glass. The focus should be on the global warming impact, acidification impact, and eutrophication impact of the production stage. makes up the majority of the shadow cost. During the production stage, only 0.25%, 0.63%, and 0.34% of the shadow cost of global warming impact, acidification impact, and eutrophication impact respectively comes from the fixed process of laminated glass.

The total shadow cost in each of the stages is also divided into 7 impact categories. The shadow cost of the global warming impact is always the highest at around 60~70% of the shadow cost from all 7 impact categories. The shadow costs of the acidification impact and the eutrophication impact is at around 20~30% and 10% of the shadow cost from all 7 impact categories respectively. The similarity in the amount of shadow cost in the different impact categories show that the producers use similar production methods.

It is reasonable that the global warming impact is the most significant. During the production of float glass, CO2 is generated through electricity generation, natural gas combustion to heat the furnace, and the glassmaking chemical process which release CO2 from carbonate raw materials. The release of CO2 bubbles help to remove air bubble during the refining process, so the release of CO2 help with produce glass without bubbles. 1m2 of low-e double glazing lead to 25 kilogram of CO2 emission [10]. Across the EU, recycling of all building glass waste would reduce carbon emissions by 230,000 tonnes per year [2].

The global warming impact is the most significant by far in comparison with the other impact categories, so the main focus should be on reducing carbon emission.

In addition, acidification impact and eutrophication impact are also substantial. Acidification is the decrease in the ocean's pH from the uptake of CO_2 from the atmosphere, and eutrophication is the increase in the water body's concentration of plant nutrient like phosphorus and nitrogen. Acidification is most often caused by burning fossil fuel, and eutrophication is caused by industrial waste and fertilizers.

Stage C of the EPD shows the environmental impact at the end of the product's life-time through either recycling or disposal. The Environmental Product Declaration of Saint Gobain assumes 5% recycling and 95% waste disposal in while that of AGC assumes 100% waste disposal. The shadow cost of Saint Gobain with 5% recycling and 95% disposal is 18% lower than that of AGC with 100% disposal. This shows that the shadow cost can be reduced in almost all of the impact categories even with a 5% recycling rate.

It is important to consider glass recycling and glass reuse with regards to stage A1 and stage A3. Glass recycling would affect stage A1, because now energy is no longer required to process the raw material. Raw materials is now readily available in the form of cullet. Across the EU, recycling of all building glass waste would save 1.23 million tonnes of raw material per year [2]. The use of cullet will also reduce the amount of energy in stage A3, because cullet can melt at a lower energy. Around 314 kg of CO_2 can be save with every tonne of glass recycling into glass containers. Glass reuse would also affect both stage A1 and stage A3, but the amount would be higher than that of glass recycling. In addition, reusing glass would lead to a more circular building industry.

However, in comparison with reusing glass, recycling glass will require shadow cost in the waste disposal stage and the productions stage. However, by using cullet instead of raw materials to produce glass, the amount of shadow cost can be reduced. In addition, for every tonne of cullet used to produce float glass, 1.2 tonnes of raw material can be saved, which also led to a reduction in mining, quarrying, and transportation (UK Glass Manufacture, 2018). Cullet can melt at a lower temperature than raw materials, so 3% less energy can be used for every 10% cullet used in production (UK Glass Manufacture, 2018). For every tonne of cullet added to the furnace, 250 to 300 kilogram reduction in CO_2 emission (UK Glass Manufacture, 2018).

Section D of the EPD shows the amount of Benefit and Loads Beyond the System Boundaries. The amount Benefit and Loads Beyond the System Boundaries from AGC are due to the recycling of PVB, glass trimming, and packing waste like wood and cardboard. The EPD from Saint Gobain did not include its Benefit and Loads Beyond the System Boundaries, but the cullents are considered input material without any environmental burden in section A3.

It was found that there is no harmonization in Europe in the environmental product declaration of laminated glass; for example, the shadow cost from the TRACI2.1 method and the CML4.1 method are very different. The shadow cost derived from the TRACI2.1 software is almost 3 times as high as the shadow cost derived from the CML4.1 software. This significant difference is caused by the fact that the shadow cost of the photochemical oxidation impact for TRACI2.1 is extremely high, and it is at around 60% of the sum of all 7 impact categories. This extremely high shadow cost is most likely due to the fact that TRACI2.1 considered photochemical impact to be more damaging to your health and weighed this impact more heavily. In addition, the system determined by the SBK in the Netherlands contain 11 impact categories, but all of the environmental product declaration found for this thesis only contain 7 impact categories.

For the case study for the glass floor at Delft Station, the shadow cost of PVB, SGP, and EVA during the production stage is €31.6, €22.3, and €29.1 respectively. The shadow cost of PVB, SGP, and EVA during the disposal stage is €0.5, €0.3, and €0.4 respectively. This shows that the reduction in the amount of shadow cost with SGP interlayer is quite significant during the production stage.

12.4. Sustainability Performance: End-of-life Options

First, float glass recycling is analysed. The vast majority of recycled float glass are downcycled to produce bottles, insulation materials, or embankments. One company that downcycle glass is Maltha, which transform glass waste into glass cullet, and these cullet can be used to create new glass products like bottles. However, downcycling is not ideal, because it is not circular. The cost of float glass is 1.37551347 dollars/kg, and the cost glass containers and bottles is 1.13645535 dollars/kg. So the amount of downcycling is relatively low at a factor of 1.2.

It is possible to upcycle, or break down existing float glass into cullet and to create new float glass with these cullet. One company that does this is Saint Gobain. 30% of Saint Gobain's float glass comes from recycled glass: 19% and 11% are from internal factory cullet and from pre-consumer cut-offs respectively. However, this 30% is already at the maximum amount of pre-consumer glass that is recyclable. So in order to increase the amount of recycled glass in the industry from that 30%, it would be necessary to recycle glass that has been released into the market and have been used. If the glass has never the factory and this 30% cannot be increase anymore, it should be debatable whether this should be considered true recycling.

However, at the moment, recycling post-consumer glass has never been done before. The problem with recycling float glass is that glass can only be upcycled back into the float glass industry if it do not have any contamination like aluminium or nickel. Coating applied to control solar gain or thermal performances are not good for optical characteristics. Research by Telesilla analysed the possibility of transforming everyday waste glass like from beer bottles and mobile phone screens into casted glass.

In addition to float glass recycling, interlayer recycling is also considered. One company that downcycle interlayer is Shark Solutions, which turn PVB interlayers into carpet backing, paint and coatings, and sound dampening. Downcycling, however, is not the most ideal compared to upcycling and reusing. However, if the quality could not be guaranteed with upcycling, it would be better to downcycle, because having a better quality and lasting longer will also lead to lower environmental cost over its lifetime.

One company that upcycle interlayer is Kuraray. Kuraray offers a product called Butacite G, which are recycled PVB interlayer that are produced from PVB trimmings. If the interlayer has never the factory and this amount of recycling is not scalable, it should be debatable whether this should be considered true recycling.

One problem with upcycling interlayer is that it is difficult to ensure the quality of the product, because it is difficult to identify the manufacturer and the formulation after a number of years. However, experiments by researchers show that the recycled PVB has similar chemical composition, tensile properties, and weight fraction of plasticizer as that of the original PVB, and no loss of optical clarity. The manufacturers are looking into the possibilities; for example, a number of paper in this field are being published by the PVB manufacturer Eastman.

In addition to float glass recycling and interlayer recycling, laminated glass recycling is also analysed. One company that downcycle laminated glass is Covanord. The laminated glass are first aged for 3 months outside so that the sun and water can attack the interlayer. Pulverizing and separating machine to grind the glass into small pieces and to remove the laminate layer. However, the size of the cullet cannot be used by the float glass industry, so the resultant cullet has to go into the container glass industry. The PVB interlayer can be used in the carpet tile industry.

A product that can be used to downcycle laminated glass is the chemical D201 nonionic surfactant developed by Jeong Chem Ltd Incheon. The chemical D201 nonionic surfactant can be used to separate glass and PVB. Waste PVB chunks are mechanically stirred in the nonionic surfactant D201 for a certain period of time, and the glass and PVB components are separated by a stainless steel mesh-screening filter.

Another possibility of very low level downcycling is to burn-off the interlayer in the float oven and contribute to the energy consumption of the furnace. Recovery means incineration with energy recovery, or gasification and pyrolysis to produce energy. This process will also be able to reduce the amount of CO_2 pollution, because recycled glass can melt at a lower temperature. However, this is very low-level recycling, and too much interlayers would lead to an uncontrolled burning.

Delaminating Resources (Delam) is a company can upcycle laminated glass with its patented machine. Delaminating Resources (Delam) can delaminate laminated glass with heat, time, and steam. The delaminated glass and interlayer components can also be 100% recycled. The current system can be used for curved glass, tempered glass, heat strengthened glass, PVB, SGP, and EVA interlayers.

The problem with fully separating the two components to produce new laminated glass is that it is difficult to completely remove the glass shards from the interlayer. The surface of interlayer is not smooth, and this makes it difficult to identify any residual glass shards in the interlayer.

12.5. Multi-Criteria Analysis

The information mentioned in the previous sections of the conclusion are organized into a multi-criteria analysis for different interlayers as well as a multi-criteria analysis for laminated glass with different interlayers. The multi-criteria analysis for different interlayers is shown in figure 117.

The tensile tests from literature shows that PVB and SGP has higher maximum stress in comparison with that of EVA. The same tensile tests also show that SGP has the highest initial stress, and EVA has the lowest initial stress. EVA interlayer has the highest strain before breakage, and SGP has the lowest strain before breakage.

The mid-span deflection of samples aged in temperature, solar radiation, and humidity, and the results show that SGP has the best resistance against temperature and EVA has the best resistance against solar radiation. However, it should be noted that SGP will show less delamination over time, so it should have better durability against relative humidity. PVB is more than twice as expensive as EVA interlayer in euros per square meter (Martín et al., 2020).

SGP interlayer shows much better performance in 4 out of the 7 categories, and these cateories include maximum stress, stiffness, durability against temperature, and durability against relative humidity. The cost of PVB interlayer and EVA interlayer is shown in this table, but it is debatable whether it is reasonable to look at the price of the interlayer without considering the design.

	Tensile strength of Interlayer	Stiffness	Strain before Breakage	Durability against temp.	Durability against solar radiation	Durability against RH	Cost per m3 (Martín et al., 2020)
PVB	+ (High maximum stress 43 MPa)	0	0 (strain of 5)	0	0	0	- (4.02 – 4.82 €/m2)
SGP	+ (highest maximum stress 45MPa)	+	- (lowest ductility at strain of 2)	+ (deflection at mid-span is the least affected by temperature)	0	+ (less delamination over time)	N/A
EVA	- (low maximum stress at 10 MPa)	-	+ (highest ductility at strain of 7)	0	+ (deflection at mid-span is the least affected by solar radiation)	0	+ (1.74 – 1.91 €/m2)

Figure 117. Multi-Criteria Analysis of Interlayer

The multi-criteria analysis for laminated glass with different interlayers is shown in figure 118. However, it should be noted that this case study was performed for the glass floor at Delft Station, so the situation could be different for a vertical glazing unit.

Hand calculations and DIANA simulations were used to design for the glass floor at Delft Station, and the shadow cost of the configurations of laminated glass were calculated and compared. The results show that shadow cost of the laminated glass with SGP is the lowest, and the shadow cost of laminated glass with PVB is the highest. SGP is more durable, so it would be reasonable that it would be better for reuse. In terms of recycling, there are more studies done on the possibility of recycling PVB interlayer; in addition, it would be easier to delaminate PVB interlayer for recycling. In terms of the cost of the laminated glass configuration for the case study, the configuration of laminated glass with SGP interlayer is cheaper than that with PVB (Octatube, 2021).

Laminated glass with SGP interlayer shows much better performance in 3 out of the 4 categories. In the case study, laminated glass with SGP interlayer is cheaper in terms of its shadow cost and its economic cost. In addition, laminated glass with SGP interlayer could be better for reuse due to the fact that it is more durable and has better resistance against delamination.

	Shadow cost	**Reuse**	**Recycling**	**Cost (Octatube, 2021)**
PVB (12.12.12.12 HS)	-	0	+ (easier delamination)	- (450 €/m2 12.12.12.12)
SGP (12.12.10 HS)	+	+ (more durable)	0	+ (400 €/m2 12.12.10)
EVA (12.12.10.10 HS)	0	0	0	N/A

Figure 118. Multi-Criteria Analysis of Laminated Glass

13. References

Achintha, M. (2016). Sustainability of glass in construction. *Sustainability of Construction Materials*, 79-104. doi:10.1016/b978-0-08-100370-1.00005-6

Allnex. (2018). Retrieved December 16, 2020, from https://allnex.com/en/product/587e25e6-402d-4f22-9dcd-292666aefefc/uvekol-s-15

Awrejcewicz, J. (2018). *DYNAMICAL SYSTEMS IN APPLICATIONS: Lodz, poland december 11 -14, 2017*. Lodz, Poland: SPRINGER INTERNATIONAL PU.

Belis, J., Depauw, J., Callewaert, D., Delincé, D., & Impe, R. V. (2009). Failure mechanisms and residual capacity of annealed glass/SGP laminated beams at room temperature. Engineering Failure Analysis, 16(6), 1866-1875. doi:10.1016/j.engfailanal.2008.09.023

Bristogianni, T., Oikonomopoulou, F., Yu, R., Veer, F. A., & Nijsse, R. (2020). Investigating the flexural strength of recycled cast glass. *Glass Structures and Engineering*, *5*(3), 445–487. https://doi.org/10.1007/s40940-020-00138-2

British Glass & GTS, 2017. Recycling glass from building refurbishment projects-Best practice guidance.

Castori, G., & Speranzini, E. (2017). Structural analysis of failure behavior of laminated glass. Composites Part B: Engineering, 125, 89-99. doi:10.1016/j.compositesb.2017.05.062

Centelles, X., Martín, M., Solé, A., Castro, J. R., & Cabeza, L. F. (2020). Tensile test on interlayer materials for laminated glass under diverse ageing conditions and strain rates. Construction and Building Materials, 243, 118230. doi:10.1016/j.conbuildmat.2020.118230

CNC Glass. (2013, June 20). How to Process Laminated Glass with EVA Film Interlayer Successfully. Retrieved December 16, 2020, from https://www.evafilms.com/how-to-process-laminated-glass-with-eva-film-interlayer-successfully/

Debrincat, G., & Babic, E. (20209). Re-thinking the life-cycle of architectural glass. Re-thinking the Life-cycle of Architectural Glass.

Delam. (2020). Revolutionary New Technology For The Separation Of Laminated Glass. Retrieved September 10, 2020, from http://www.delam.com.au/

Dhaliwal, A., & Hay, J. (2002). The characterization of polyvinyl butyral by thermal analysis. Thermochimica Acta, 391(1-2), 245-255. doi:10.1016/s0040-6031(02)00187-9

Entwistle, D. (2019). Live CPD Webinar: Glass Forever - Sustainability Matters.

Fors, C. (2014). Mechanical Properties of Interlayers in Laminated Glass: Experimental and Numerical Evaluation (Unpublished master's thesis). Lund University.

Garside, M. (2021, April 12). *Flat glass global market value 2027*. Statista. https://www.statista.com/statistics/1132697/flat-glass-market-value-worldwide/.

Haldimann, M., Luible, A., & Overend, M. (2008). *Structural use of glass*. Zürich, Switzerland: International Association for Bridge and Structural Engineering.

Hána, T., Janda, T., Schmidt, J., Zemanová, A., Šejnoha, M., Eliášová, M., & Vokáč, M. (2019). Experimental and Numerical Study of Viscoelastic Properties of Polymeric Interlayers Used for Laminated Glass: Determination of Material Parameters. *Materials, 12*(14), 2241. doi:10.3390/ma12142241

Heesbeen, C., 2012. Glass Recycling Guide. Arup Report, Berlin February 2012.

Hestin, M., Veron, S. D., & Burgos, S. (2018, June 15). Economic study on recycling of building glass in Europe - Deloitte. Retrieved September 10, 2020, from https://glassforeurope.com/economic-study-on-recycling2/

Hoogerwaard, G. (2020). *The road to sustainable load bearing glass designs: possibilities and limitations of current glass design with focus on the connections* (Unpublished master's thesis). Technical University of Delft.

Hydrosight (2004). Acrylic vs Polycarbonate. Retrieved February 21, 2021, from https://www.hydrosight.com/acrylic-vs-polycarbonate-a-quantitative-and-qualitative-comparison/

Kuraray. (2020).*Trosifol Architectural Glazing*. https://www.trosifol.com/fileadmin/user_upload/TROSIFOL/support/downloads/product_brochures/pdf_documents/architecture/trosifol-architectural-glazing-product-portfolio.pdf.

Kuraray. (2019). *SentryGlas*. https://www.trosifol.com/fileadmin/user_upload/TROSIFOL/support/downloads/product_brochures/pdf_documents/sentryglas/SentryGlas_8_2019_engl_web.pdf

Interface: Recycled PVB (2020). Retrieved January 27, 2021, from https://www.interface.com/EU/en-GB/about/modular-system/PVB-en_GB

Liu, B., Sun, Y., Li, Y., Wang, Y., Ge, D., & Xu, J. (2012). Systematic experimental study on mechanical behavior of PVB (polyvinyl butyral) material under various loading conditions. *Polymer Engineering & Science, 52*(5), 1137-1147. doi:10.1002/pen.22175

Martín, M., Centelles, X., Solé, A., Barreneche, C., Fernández, A. I., & Cabeza, L. F. (2020). Polymeric interlayer materials for laminated glass: A review. *Construction and Building Materials*, *230*, 116897. doi:10.1016/j.conbuildmat.2019.116897

Ministerie van Algemene Zaken. (2020, February 04). Dutch goals within the EU. Retrieved September 10, 2020, from https://www.government.nl/topics/climate-change/eu-policy

Octatube. (2021). Personal interview [Personal interview].

Pilkington. (2020). The Float Process Step by step. Retrieved September 10, 2020, from https://www.pilkington.com/en/global/about/education/the-float-process/the-float-process-step-by-step

Physical properties of Glass. Physical properties of glass | Saint Gobain Building Glass UK. (2021). https://uk.saint-gobain-building-glass.com/en-gb/architects/physical-properties.

Ritchie, H., & Roser, M. (2017, May 11). CO_2 and Greenhouse Gas Emissions. Retrieved September 10, 2020, from https://ourworldindata.org/co2-and-other-greenhouse-gas-emissions

Sable, L., Kinsella, D., & Kozłowski, M. (2019). Influence of EVA, PVB and Ionoplast Interlayers on the Structural Behaviour and Fracture Pattern of Laminated Glass. *International Journal of Structural Glass and Advanced Materials Research, 3*(1), 62-78. doi:10.3844/sgamrsp.2019.62.78

Sable, L., Skukis, E., Japins, G., & Kalnins, K. (2017). Correlation between Numerical and Experimental Tests of Laminated Glass Panels with Visco-elastic Interlayer. *Procedia Engineering, 172*, 945-952. doi:10.1016/j.proeng.2017.02.107

Schittich, C., Staib, G., Balkow, D., Schuler, M., Sobek, W. (1999) Glass Construction Manual, Basel: Birkhäuser.

Serafinavicius, T., Kvedaras, A. K., & Sauciuvenas, G. (2013). Bending Behavior of Structural Glass Laminated With Different Interlayers. *Mechanics of Composite Materials, 49*(4), 437-446. doi:10.1007/s11029-013-9360-4

Serafinavičius, T., Lebet, J., Louter, C., Lenkimas, T., & Kuranovas, A. (2013). Long-term Laminated Glass Four Point Bending Test with PVB, EVA and SG Interlayers at Different Temperatures. *Procedia Engineering, 57,* 996-1004. doi:10.1016/j.proeng.2013.04.126

Serafinavicius, T., Lebet, J., Louter, C., Kuranovas, A., & Lenkimas, T. (2014). The effects of environmental impacts on durability of laminated glass plates with interlayers (SG, EVA, PVB). Challenging Glass 4 & COST Action TU0905 Final Conference, 455-462. doi:10.1201/b16499-66

Stevels, W., & D'Haene, P. (2020). Determination and Verification of PVB Interlayer Modulus Properties.

Stichting Vlakglas Recycling Nederland. (2018). Retrieved September 10, 2020, from https://www.vlakglasrecycling.nl/ uploads/jaarverslagen/Jaarverslag 2018.pdf

Swain, B., Park, J. R., Shin, D. Y., Park, K., Hong, M. H., & Lee, C. G. (2015). Recycling of waste automotive laminated glass and valorization of polyvinyl butyral through mechanochemical separation. Environmental Research, 142, 615-623. doi:10.1016/j.envres.2015.08.017

SWM. (2017). *SE-381HF General Description and Use*. https://www.swmintl.com/media/2250/se-381hf-swm-eva-interlayer-film.pdf.

Tup, M., Mnsk, D., & Kaprkov, V. (2012). PVB Sheet Recycling and Degradation. Material Recycling - Trends and Perspectives. doi:10.5772/36838

UK glass manufacture – a mass balance study (2008). (2018, April 03). Retrieved January 06, 2021, from https://www.britglass.org.uk/knowledge-base/resources-and-publications/uk-glass-manufacture-%E2%80%93-mass-balance-study-2008

WorldGBC. (2019, September 23). New report: The building and construction sector can reach net zero carbon emissions by 2050. Retrieved September 10, 2020, from https://www.worldgbc.org/news-media/WorldGBC-embodied-carbon-report-published

Young, W. C., & Budynas, R. G. (2002). *Roark's formulas for stress and strain: Warren C. Young; Richard G. Budynas*. New York: McGraw-Hill.

Yu, R. (2019). *Recycled Glass Beam* (Unpublished master's thesis). Technical University of Delft.

Zhang, X., Shi, Y., Hao, H., & Cui, J. (2015). The mechanical properties of ionoplast interlayer material at high strain rates. *Materials & Design*, *83*, 387-399. doi:10.1016/j.matdes.2015.06.076

14. Appendices

Appendix A. Distributed Load and Point Load Calculations

Interlayer	length (mm)	width (mm)	ka	ke	load duration (years)	kmod	ksp	fg;k (N/mm2)	γm;A	fmt;u;d (N/mm2)	kz	fb;k (N/mm2)	γm;v
PVB Distributed Load	2700	1000	0.91	1	50	0.29	1	45	1.8	27.52	1	70	1.2
SGP Distributed Load	2700	1000	0.91	1	50	0.29	1	45	1.8	27.52	1	70	1.2
EVA Distributed Load	2700	1000	0.91	1	50	0.29	1	45	1.8	27.52	1	70	1.2

z (mm)	B/H	kw	kσ	a	Lσ	Lw	LA^2	X	Eg N/mm2	vg	Gtl	β	ωw	ωσ	tgg;1;u (mm)	tgg,ser (mm)
1850	2.7	0.893	1.697	1000	1.618304069	0.889973899	879372.7382	26.676	70000	0.23	0.05	221.2838199	0.004005755512	0.007260155445	24.38	18.94
1850	2.7	0.893	1.697	1000	1.618304069	0.889973899	879372.7382	17.784	70000	0.23	6.42	1.148929491	0.4364963556	0.5848093535	30.76	26.28
1850	2.7	0.893	1.697	1000	1.618304069	0.889973899	879372.7382	25.156	70000	0.23	1.33	7.844926888	0.1018871216	0.171009677	32.14	23.21

Weight of laminated glass kN/m2	live load kN/m2	ULS load case kN/m2	SLS load case kN/m2	mx kNm/m	wy m3	σed (kN/m2)	σed (N/mm2)	UC ULS	σed 2D DIANA Linear (N/mm2)	% Difference	σed 2D DIANA Nonlinear (N/mm2)	σed 3D DIANA Model (N/mm2)	% Difference
1.17	5	8.904	6.17	1.00	0.0000990	10140.937	10.14	0.37	10.33	1.83	10.33	10.77	5.84
0.8275	5	8.493	5.8275	0.96	0.0001577	6073.657	6.07	0.22	6.13	0.92	6.13	6.68	9.08
1.07	5	8.784	6.07	0.99	0.0001721	5756.318	5.76	0.21	5.76	0.06	5.76	6.27	8.19

Umax (mm)	Iy mm4	Iy/Ix	Factor	SLS load case kN/m	δSLS mm	UC SLS	δ 2D DIANA Linear(mm)	% Difference	δ 2D DIANA Nonlinear (mm)	δ 3D DIANA Model (mm)	% Difference
4	1528063.25	2.7	11.54	16.659	1.80	0.45	1.75	2.63	1.75	1.97	8.77
4	4083464.15	2.7	11.54	15.73425	0.64	0.16	0.62	2.40	0.62	0.58	8.69
4	2813502.60	2.7	11.54	16.389	0.96	0.24	0.94	2.12	0.94	0.91	5.24

Post Breakage

WS	BS	ES	RS
1	10	3	30

Interlayer	length (mm)	width (mm)	ka	ke	load duration (years)	kmod	ksp	fg;k (N/mm2)	γm;A	fmt;u;d (N/mm2)	kz	fb;k (N/mm2)	γm;v
PVB Distributed Load	2700	1000	0.909174534	1	50	0.2943232613	1	45	1.8	27.52311368	1	70	1.2
SGP Distributed Load	2700	1000	0.909174534	1	50	0.2943232613	1	45	1.8	27.52311368	1	70	1.2
EVA Distributed Load	2700	1000	0.909174534	1	50	0.2943232613	1	45	1.8	27.52311368	1	70	1.2

z (mm)	B/H	kw	kσ	a	Lσ	Lw	LA^2	X	Eg N/mm2	vg	Gtl	β	ωw	ωσ	tgg;1;u (mm)
1850	2.7	0.893	1.697	1000	1.618304069	0.889973899	879372.7382	17.784	70000	0.23	0.05	147.5225466	0.005996622766	0.01085084376	20.90
1850	2.7	0.893	1.697	1000	1.618304069	0.889973899	879372.7382	8.892	70000	0.23	6.42	0.5744647453	0.6077235823	0.7380185537	22.50
1850	2.7	0.893	1.697	1000	1.618304069	0.889973899	879372.7382	17.784	70000	0.23	1.33	5.545960398	0.1382820051	0.2258855848	26.23

Weight of laminated glass kN/m2	live load kN/m2	SLS load case kN/m2	mx kNm/m	wy m3	σed (kN/m2)	σed (N/mm2)	UC ULS	σed 2D DIANA Linear (N/mm2)	% Difference	σed 2D DIANA Nonlinear (N/mm2)	σed 3D DIANA Model (N/mm2)	% Difference
0.8775	5	5.8775	0.66	0.0000728	9106.086956	9.11	0.33	9.28	1.87	9.27	9.38	2.92
0.585	5	5.585	0.63	0.0000844	7465.91125	7.47	0.27	7.61	1.89	7.61	8.08	7.60
0.8275	5	5.8275	0.66	0.0001147	5731.379639	5.73	0.21	5.84	1.86	5.84	5.83	1.69

Interlayer	length (mm)	width (mm)
PVB Distributed Load	2700	1000
SGP Distributed Load	2700	1000
EVA Distributed Load	2700	1000

PVB Point Load	14.5	0.76	3	100	100	1.137370116	1	50	0.2943232613	1	45	1.8	29.20	1	70	1.2
SGP Point Load	9.7	0.76	3	100	100	1.137370116	1	50	0.2943232613	1	45	1.8	29.20	1	70	1.2
EVA Point Load	11.7	0.76	3	100	100	1.137370116	1	50	0.2943232613	1	45	1.8	29.20	1	70	1.2

z (mm)	B/H	kw	kσ	a	Lσ	Lw	LA^2	X	Eg N/mm2	vg	Gtl	β	ωw	ωσ	tgg;1;u (mm)	tgg,ser (mm)
100	2.7	0.893	1.697	1000	0.2737010813	0.7837988336	879372.7382	26.676	70000	0.23	0.05	221.2838199	0.003529550315	0.00123534999	23.57	18.89
100	2.7	0.893	1.697	1000	0.2737010813	0.7837988336	879372.7382	16.264	70000	0.23	6.42	1.050730389	0.4272479414	0.2066555254	25.83	26.14
100	2.7	0.893	1.697	1000	0.2737010813	0.7837988336	879372.7382	23.636	70000	0.23	1.33	7.370913178	0.09611606547	0.03580312518	24.44	22.95

Point load kN	ULS load case kN	SLS load case kN	a mm	σed (N/mm2)	UC ULS	σed 2D DIANA Linear (N/mm2)	% Difference	σed 2D DIANA Nonlinear (N/mm2)	% Difference	σed 3D DIANA Model (N/mm2)	% Difference	UC ULS
7	10.5	7	100	32.69	1.12	32.64	0.16	32.87	0.70	31.05	5.02	1.06
7	10.5	7	100	27.22	0.93	27.19	0.11	27.33	0.51	25.54	6.17	0.87
7	10.5	7	100	30.40	1.04	30.36	0.14	30.55	0.62	28.71	5.57	0.98

δSLS mm	Umax (mm)	UC SLS	δ 2D DIANA Linear(mm)	% Difference	δ 2D DIANA Nonlinear (mm)	% Difference	δ 3D DIANA Model (mm)	% Difference
2.68	4	0.67	2.82	5.11	2.81	0.35	2.80	4.44
1.01	4	0.25	1.07	5.50	1.07	0.00	1.22	17.12
1.49	4	0.37	1.57	4.84	1.57	0.00	1.76	15.11

Post Breakage

WS	BS	ES	RS
1	10	3	30

Interlayer	length (mm)	width (mm)
PVB Distributed Load	2700	1000
SGP Distributed Load	2700	1000
EVA Distributed Load	2700	1000

PVB Point Load	14.5	0.76	2	100	100	1.137370116	1	50	0.2943232613	1	45	1.8	29.20219538	1	70	1.2
SGP Point Load	11.7	0.76	2	100	100	1.137370116	1	50	0.2943232613	1	45	1.8	29.20219538	1	70	1.2
EVA Point Load	11.7	0.76	2	100	100	1.137370116	1	50	0.2943232613	1	45	1.8	29.20219538	1	70	1.2

z (mm)	B/H	kw	kσ	a	Lσ	Lw	LA^2	X	Eg N/mm2	vg	Gtl	β	ωw	ωσ	tgg;1;u (mm)
100	2.7	0.893	1.697	1000	0.2737010813	0.7837988336	879372.7382	17.784	70000	0.23	0.05	147.5225466	0.005284998639	0.001851881124	20.38
100	2.7	0.893	1.697	1000	0.2737010813	0.7837988336	879372.7382	8.892	70000	0.23	6.42	0.5744647453	0.5770594499	0.3226976055	20.18
100	2.7	0.893	1.697	1000	0.2737010813	0.7837988336	879372.7382	17.784	70000	0.23	1.33	5.545960398	0.1238275904	0.04703041273	22.83

Point load kN	SLS load case kN	a mm	σed (N/mm2)	UC	σed 2D DIANA Linear (N/mm2)	% Difference	σed 2D DIANA Nonlinear (N/mm2)	% Difference	σed 3D DIANA Model (N/mm2)	% Difference	UC
7	7	100	29.17	1.00	29.09	0.26	29.33	0.82	27.62	5.30	0.95
7	7	100	29.73	1.02	29.67	0.19	29.92	0.84	29.97	0.81	1.03
7	7	100	23.24	0.80	23.19	0.22	23.32	0.56	24.68	5.83	0.85

Appendix B. Shadow Cost Calculations

Functional Unit [m2 Glass]	2.7	AGC 2018 Production Stage A1/A2/A3						
Thickness of Glass [mm]	44							
# of Interlayer	6							
Impact Category	Unit	Environmental cost [euro/kg X]	Env. Impact of the Fixed Process (from EPD) [kg X/1m2Glass]	Env. Impact per 1mm Float Glass (from EPD) [kg X/1m2Glass]	Env. Impact per Interlayer (from EPD) [kg X/1m2Glass]	Env. Impact of Laminated glass [kg X/1m2Glass]	Shadow Cost of Laminated Glass [Euro/1m2Glass]	Shadow Cost of Laminated Glass [Euro/FU]
Global warming (GWP100)	kg CO2	0.05	0.074	3.100	2.000	148.474	7.424	20.044
Ozone layer depletion (ODP)	kg CFC-11	30	0.000	0.000	0.000	0.000	0.000	0.000
Acidification	kg SO2	4	0.001	0.013	0.003	0.584	2.336	6.306
Eutrophication	kg (PO4)3-	9	0.000	0.002	0.000	0.087	0.780	2.106
Photochemical oxidation	kg Ethene	2	0.000	0.001	0.001	0.040	0.079	0.213
Abiotic depletion, non fuel	kg Antimone	0.16	0.000	0.000	0.000	0.000	0.000	0.000
Abiotic depletion, fuel	MJ	0.16	0.780	40.500	39.200	0.971	0.155	0.419
TOTAL	euro/1m2							29.089

Functional Unit [m2 Glass]	2.7	AGC 2018 Production Stage A1/A2/A3	End-of-life: C4 Disposal					
Thickness of Glass [mm]	44							
# of Interlayer	6							
Impact Category	Unit	Environmental cost [euro/kg X]	Env. Impact of the Fixed Process (from EPD) [kg X/1m2Glass]	Env. Impact per 1mm Float Glass (from EPD) [kg X/1m2Glass]	Env. Impact per Interlayer (from EPD) [kg X/1m2Glass]	Env. Impact of Laminated glass [kg X/1m2Glass]	Shadow Cost of Laminated Glass [Euro/1m2Glass]	Shadow Cost of Laminated Glass [Euro/FU]
Global warming (GWP100)	kg CO2	0.05	0.000	0.040	0.028	1.917	0.096	0.259
Ozone layer depletion (ODP)	kg CFC-11	30	0.000	0.000	0.000	0.000	0.000	0.000
Acidification	kg SO2	4	0.000	0.000	0.000	0.011	0.043	0.116
Eutrophication	kg (PO4)3-	9	0.000	0.000	0.000	0.002	0.017	0.046
Photochemical oxidation	kg Ethene	2	0.000	0.000	0.000	0.001	0.002	0.005
Abiotic depletion, non fuel	kg Antimone	0.16	0.000	0.000	0.000	0.000	0.000	0.000
Abiotic depletion, fuel	MJ	0.16	0.000	0.514	0.402	0.012	0.002	0.005
TOTAL	euro/1m2							0.430

Functional Unit [m2 Glass]	2.7	AGC 2018 Production Stage A1/A2/A3	D Benefits and loads beyond system boundaries					
Thickness of Glass [mm]	44							
# of Interlayer	6							
Impact Category	Unit	Environmental cost [euro/kg X]	Env. Impact of the Fixed Process (from EPD) [kg X/1m2Glass]	Env. Impact per 1mm Float Glass (from EPD) [kg X/1m2Glass]	Env. Impact per Interlayer (from EPD) [kg X/1m2Glass]	Env. Impact of Laminated glass [kg X/1m2Glass]	Shadow Cost of Laminated Glass [Euro/1m2Glass]	Shadow Cost of Laminated Glass [Euro/FU]
Global warming (GWP100)	kg CO2	0.05	0.000	0.153	0.000	6.732	0.337	0.909
Ozone layer depletion (ODP)	kg CFC-11	30	0.000	0.000	0.000	0.000	0.000	0.000
Acidification	kg SO2	4	0.000	0.000	0.000	0.013	0.051	0.136
Eutrophication	kg (PO4)3-	9	0.000	0.000	0.000	0.002	0.022	0.058
Photochemical oxidation	kg Ethene	2	0.000	0.000	0.000	0.001	0.002	0.005
Abiotic depletion, non fuel	kg Antimone	0.16	0.000	0.000	0.000	0.000	0.000	0.000
Abiotic depletion, fuel	MJ	0.16	0.000	1.500	0.000	0.032	0.005	0.014
TOTAL	euro/1m2							1.123

Functional Unit [m2 Glass]	2.7	AGC 2018 Production Stage A1/A2/A3						
Thickness of Glass [mm]	48							
# of Interlayer	6							
Impact Category	Unit	Environmental cost [euro/kg X]	Env. Impact of the Fixed Process (from EPD) [kg X/1m2Glass]	Env. Impact per 1mm Float Glass (from EPD) [kg X/1m2Glass]	Env. Impact per Interlayer (from EPD) [kg X/1m2Glass]	Env. Impact of Laminated glass [kg X/1m2Glass]	Shadow Cost of Laminated Glass [Euro/1m2Glass]	Shadow Cost of Laminated Glass [Euro/FU]
Global warming (GWP100)	kg CO2	0.05	0.074	3.100	2.000	160.874	8.044	21.718
Ozone layer depletion (ODP)	kg CFC-11	30	0.000	0.000	0.000	0.000	0.000	0.000
Acidification	kg SO2	4	0.001	0.013	0.003	0.635	2.542	6.863
Eutrophication	kg (PO4)3-	9	0.000	0.002	0.000	0.094	0.850	2.294
Photochemical oxidation	kg Ethene	2	0.000	0.001	0.001	0.043	0.086	0.231
Abiotic depletion, non fuel	kg Antimone	0.16	0.000	0.000	0.000	0.000	0.000	0.000
Abiotic depletion, fuel	MJ	0.16	0.780	40.500	39.200	1.049	0.168	0.453
TOTAL	euro/1m2							31.559

Functional Unit [m2 Glass]	2.7	AGC 2018 Production Stage A1/A2/A3	End-of-life: C4 Disposal					
Thickness of Glass [mm]	48							
# of Interlayer	6							
Impact Category	Unit	Environmental cost [euro/kg X]	Env. Impact of the Fixed Process (from EPD) [kg X/1m2Glass]	Env. Impact per 1mm Float Glass (from EPD) [kg X/1m2Glass]	Env. Impact per Interlayer (from EPD) [kg X/1m2Glass]	Env. Impact of Laminated glass [kg X/1m2Glass]	Shadow Cost of Laminated Glass [Euro/1m2Glass]	Shadow Cost of Laminated Glass [Euro/FU]
Global warming (GWP100)	kg CO2	0.05	0.000	0.040	0.028	2.077	0.104	0.280
Ozone layer depletion (ODP)	kg CFC-11	30	0.000	0.000	0.000	0.000	0.000	0.000
Acidification	kg SO2	4	0.000	0.000	0.000	0.012	0.047	0.126
Eutrophication	kg (PO4)3-	9	0.000	0.000	0.000	0.002	0.018	0.049
Photochemical oxidation	kg Ethene	2	0.000	0.000	0.000	0.001	0.002	0.005
Abiotic depletion, non fuel	kg Antimone	0.16	0.000	0.000	0.000	0.000	0.000	0.000
Abiotic depletion, fuel	MJ	0.16	0.000	0.514	0.402	0.013	0.002	0.006
TOTAL	euro/1m2							0.466

Functional Unit [m2 Glass]	2.7	AGC 2018 Production Stage A1/A2/A3	D Benefits and loads beyond system boundaries					
Thickness of Glass [mm]	48							
# of Interlayer	6							
Impact Category	Unit	Environmental cost [euro/kg X]	Env. Impact of the Fixed Process (from EPD) [kg X/1m2Glass]	Env. Impact per 1mm Float Glass (from EPD) [kg X/1m2Glass]	Env. Impact per Interlayer (from EPD) [kg X/1m2Glass]	Env. Impact of Laminated glass [kg X/1m2Glass]	Shadow Cost of Laminated Glass [Euro/1m2Glass]	Shadow Cost of Laminated Glass [Euro/FU]
Global warming (GWP100)	kg CO2	0.05	0.000	0.153	0.000	7.344	0.367	0.991
Ozone layer depletion (ODP)	kg CFC-11	30	0.000	0.000	0.000	0.000	0.000	0.000
Acidification	kg SO2	4	0.000	0.000	0.000	0.014	0.055	0.149
Eutrophication	kg (PO4)3-	9	0.000	0.000	0.000	0.003	0.024	0.064
Photochemical oxidation	kg Ethene	2	0.000	0.000	0.000	0.001	0.002	0.006
Abiotic depletion, non fuel	kg Antimone	0.16	0.000	0.000	0.000	0.000	0.000	0.000
Abiotic depletion, fuel	MJ	0.16	0.000	1.500	0.000	0.035	0.006	0.015
TOTAL	euro/1m2							1.225

Functional Unit [m2 Glass]	2.7	AGC 2018 Production Stage A1/A2/A3						
Thickness of Glass [mm]	34							
# of Interlayer	4							
Impact Category	Unit	Environmental cost [euro/kg X]	Env. Impact of the Fixed Process (from EPD) [kg X/1m2Glass]	Env. Impact per 1mm Float Glass (from EPD) [kg X/1m2Glass]	Env. Impact per Interlayer (from EPD) [kg X/1m2Glass]	Env. Impact of Laminated glass [kg X/1m2Glass]	Shadow Cost of Laminated Glass [Euro/1m2Glass]	Shadow Cost of Laminated Glass [Euro/FU]
Global warming (GWP100)	kg CO2	0.05	0.074	3.100	2.000	113.474	5.674	15.319
Ozone layer depletion (ODP)	kg CFC-11	30	0.000	0.000	0.000	0.000	0.000	0.000
Acidification	kg SO2	4	0.001	0.013	0.003	0.450	1.799	4.857
Eutrophication	kg (PO4)3-	9	0.000	0.002	0.000	0.067	0.601	1.623
Photochemical oxidation	kg Ethene	2	0.000	0.001	0.001	0.030	0.060	0.163
Abiotic depletion, non fuel	kg Antimone	0.16	0.000	0.000	0.000	0.000	0.000	0.000
Abiotic depletion, fuel	MJ	0.16	0.780	40.500	39.200	0.738	0.118	0.319
TOTAL	euro/1m2							22.281

Functional Unit [m2 Glass]	2.7	AGC 2018 Production Stage A1/A2/A3	End-of-life: C4 Disposal					
Thickness of Glass [mm]	34							
# of Interlayer	4							
Impact Category	Unit	Environmental cost [euro/kg X]	Env. Impact of the Fixed Process (from EPD) [kg X/1m2Glass]	Env. Impact per 1mm Float Glass (from EPD) [kg X/1m2Glass]	Env. Impact per Interlayer (from EPD) [kg X/1m2Glass]	Env. Impact of Laminated glass [kg X/1m2Glass]	Shadow Cost of Laminated Glass [Euro/1m2Glass]	Shadow Cost of Laminated Glass [Euro/FU]
Global warming (GWP100)	kg CO2	0.05	0.000	0.040	0.028	1.464	0.073	0.198
Ozone layer depletion (ODP)	kg CFC-11	30	0.000	0.000	0.000	0.000	0.000	0.000
Acidification	kg SO2	4	0.000	0.000	0.000	0.008	0.033	0.089
Eutrophication	kg (PO4)3-	9	0.000	0.000	0.000	0.001	0.013	0.034
Photochemical oxidation	kg Ethene	2	0.000	0.000	0.000	0.001	0.001	0.004
Abiotic depletion, non fuel	kg Antimone	0.16	0.000	0.000	0.000	0.000	0.000	0.000
Abiotic depletion, fuel	MJ	0.16	0.000	0.514	0.402	0.009	0.001	0.004
TOTAL	euro/1m2							0.328

Functional Unit [m2 Glass]	2.7	AGC 2018 Production Stage A1/A2/A3	D Benefits and loads beyond system boundaries					
Thickness of Glass [mm]	34							
# of Interlayer	4							
Impact Category	Unit	Environmental cost [euro/kg X]	Env. Impact of the Fixed Process (from EPD) [kg X/1m2Glass]	Env. Impact per 1mm Float Glass (from EPD) [kg X/1m2Glass]	Env. Impact per Interlayer (from EPD) [kg X/1m2Glass]	Env. Impact of Laminated glass [kg X/1m2Glass]	Shadow Cost of Laminated Glass [Euro/1m2Glass]	Shadow Cost of Laminated Glass [Euro/FU]
Global warming (GWP100)	kg CO2	0.05	0.000	0.153	0.000	5.202	0.260	0.702
Ozone layer depletion (ODP)	kg CFC-11	30	0.000	0.000	0.000	0.000	0.000	0.000
Acidification	kg SO2	4	0.000	0.000	0.000	0.010	0.039	0.105
Eutrophication	kg (PO4)3-	9	0.000	0.000	0.000	0.002	0.017	0.045
Photochemical oxidation	kg Ethene	2	0.000	0.000	0.000	0.001	0.002	0.004
Abiotic depletion, non fuel	kg Antimone	0.16	0.000	0.000	0.000	0.000	0.000	0.000
Abiotic depletion, fuel	MJ	0.16	0.000	1.500	0.000	0.025	0.004	0.011
TOTAL	euro/1m2							0.867

			Saint Gobain		2020	Saint Gobain		2020	Saint Gobain		2020
		Environ mental cost	3mm SSG			4mm SSG			5mm SSG		
Impact Category	Unit	[euro/x]	7.5	[/kg]	[euro/kg]	10	[/kg]	[euro/kg]	12.5	[/kg]	[euro/kg]
Global warming (GWP100)	kg CO2	0.05	9.650	1.287	0.064	12.700	1.270	0.064	15.800	1.264	0.063
Ozone layer depletion (ODP)	kg CFC-11	30	0.000	0.000	0.000	0.000	0.000	0.000	0.000	0.000	0.000
Acidification	kg SO2	4	0.062	0.008	0.033	0.082	0.008	0.033	0.102	0.008	0.033
Eutrophication	kg (PO4)3-	9	0.023	0.003	0.027	0.030	0.003	0.027	0.038	0.003	0.027
Photochemical oxidation	kg Ethene	2	0.004	0.001	0.001	0.005	0.001	0.001	0.006	0.001	0.001
Abiotic depletion, non fuel	kg Antimone	0.16	0.000	0.000	0.000	0.000	0.000	0.000	0.000	0.000	0.000
Abiotic depletion, fuel	MJ	0.16	143.000	0.009	0.001	189.000	0.009	0.001	235.000	0.009	0.001
TOTAL	euro/kg/1m2				**0.127**			**0.126**			**0.125**

			Saint Gobain		2020	Saint Gobain		2020	Saint Gobain		2020
		Environ mental cost	6mm SSG			8mm SSG			10mm SSG		
Impact Category	Unit	[euro/x]	15	[/kg]	[euro/kg]	20	[/kg]	[euro/kg]	25	[/kg]	[euro/kg]
Global warming (GWP100)	kg CO2	0.05	18.900	1.260	0.063	25.000	1.250	0.063	31.200	1.248	0.062
Ozone layer depletion (ODP)	kg CFC-11	30	0.000	0.000	0.000	0.000	0.000	0.000	0.000	0.000	0.000
Acidification	kg SO2	4	0.123	0.008	0.033	0.163	0.008	0.033	0.204	0.008	0.033
Eutrophication	kg (PO4)3-	9	0.045	0.003	0.027	0.060	0.003	0.027	0.075	0.003	0.027
Photochemical oxidation	kg Ethene	2	0.008	0.001	0.001	0.010	0.001	0.001	0.013	0.001	0.001
Abiotic depletion, non fuel	kg Antimone	0.16	0.000	0.000	0.000	0.000	0.000	0.000	0.000	0.000	0.000
Abiotic depletion, fuel	MJ	0.16	281.000	0.009	0.001	373.000	0.009	0.001	464.000	0.009	0.001
TOTAL	euro/kg/1m2				**0.125**			**0.125**			**0.125**

			Saint Gobain		2020
		Environ mental cost	12mm SSG		
Impact Category	Unit	[euro/x]	30	[/kg]	[euro/kg]
Global warming (GWP100)	kg CO2	0.05	37.400	1.247	0.062
Ozone layer depletion (ODP)	kg CFC-11	30	0.000	0.000	0.000
Acidification	kg SO2	4	0.244	0.008	0.033
Eutrophication	kg (PO4)3-	9	0.090	0.003	0.027
Photochemical oxidation	kg Ethene	2	0.015	0.001	0.001
Abiotic depletion, non fuel	kg Antimone	0.16	0.000	0.000	0.000
Abiotic depletion, fuel	MJ	0.16	556.000	0.009	0.001
TOTAL	euro/kg/1m2				**0.124**

			Saint Gobain		2019	Saint Gobain		2019	Saint Gobain		2019
		Environ mental	**44.2 SGG STADIP**	**Production Stage**		**44.2 SGG STADIP**	**End-of-life: C2 transport**		**44.2 SGG STADIP**	**End-of-life: C3 waste**	
Impact Category	Unit	[euro/x]	20.76	[/kg]	[euro/kg]	20.76	[/kg]	[euro/kg]	20.76	[/kg]	[euro/kg]
Global warming (GWP100)	kg CO2	0.05	32.100	1.546	0.077	0.052	0.002	0.000	0.002	0.000	0.000
Ozone layer depletion (ODP)	kg CFC-11	30	0.000	0.000	0.000	0.000	0.000	0.000	0.000	0.000	0.000
Acidification	kg SO2	4	0.131	0.006	0.025	0.000	0.000	0.000	0.000	0.000	0.000
Eutrophication	kg (PO4)3-	9	0.039	0.002	0.017	0.000	0.000	0.000	0.000	0.000	0.000
Photochemical oxidation	kg Ethene	2	0.008	0.000	0.001	0.000	0.000	0.000	0.000	0.000	0.000
Abiotic depletion, non fuel	kg Antimone	0.16	0.000	0.000	0.000	0.000	0.000	0.000	0.000	0.000	0.000
Abiotic depletion, fuel	MJ	0.16	416.000	0.010	0.002	0.711	0.000	0.000	0.023	0.000	0.000
TOTAL	euro/kg/1m2				**0.122**			**0.000**			**0.000**

			Saint Gobain		2019
		Environ mental	**44.2 SGG STADIP**	**End-of-life: C4 Disposal**	
Impact Category	Unit	[euro/x]	20.76	[/kg]	[euro/kg]
Global warming (GWP100)	kg CO2	0.05	0.315	0.015	0.001
Ozone layer depletion (ODP)	kg CFC-11	30	0.000	0.000	0.000
Acidification	kg SO2	4	0.002	0.000	0.000
Eutrophication	kg (PO4)3-	9	0.000	0.000	0.000
Photochemical oxidation	kg Ethene	2	0.000	0.000	0.000
Abiotic depletion, non fuel	kg Antimone	0.16	0.000	0.000	0.000
Abiotic depletion, fuel	MJ	0.16	4.070	0.000	0.000
TOTAL	euro/kg/1m2				**0.001**

			AGC		2018	AGC		2018	AGC		2018
		Environ mental	44.2	Production Stage		44.2	End-of-life: C2 transport		44.2	End-of-life: C3 waste	
Impact Category	Unit	[euro/x]	20.76	[/kg]	[euro/kg]	20.76	[/kg]	[euro/kg]	20.76	[/kg]	[euro/kg]
Global warming (GWP100)	kg CO2	0.05	28.800	1.387	0.069	0.105	0.005	0.000	0.000	0.000	0.000
Ozone layer depletion (ODP)	kg CFC-11	30	0.000	0.000	0.000	0.000	0.000	0.000	0.000	0.000	0.000
Acidification	kg SO2	4	0.109	0.005	0.021	0.001	0.000	0.000	0.000	0.000	0.000
Eutrophication	kg (PO4)3-	9	0.016	0.001	0.007	0.000	0.000	0.000	0.000	0.000	0.000
Photochemical oxidation	kg Ethene	2	0.008	0.000	0.001	0.000	0.000	0.000	0.000	0.000	0.000
Abiotic depletion, non fuel	kg Antimone	0.16	0.000	0.000	0.000	0.000	0.000	0.000	0.000	0.000	0.000
Abiotic depletion, fuel	MJ	0.16	403.000	0.009	0.001	1.450	0.000	0.000	0.000	0.000	0.000
TOTAL	euro/kg/1m2				**0.100**			**0.000**			**0.000**

			AGC		2018	AGC		2018
		Environ mental	44.2	End-of-life: C4 Disposal		44.2	D Benefits and loads	
Impact Category	Unit	[euro/x]	20.76	[/kg]	[euro/kg]	20.76	[/kg]	[euro/kg]
Global warming (GWP100)	kg CO2	0.05	0.374	0.018	0.001	1.220	0.059	0.003
Ozone layer depletion (ODP)	kg CFC-11	30	0.000	0.000	0.000	0.000	0.000	0.000
Acidification	kg SO2	4	0.002	0.000	0.000	0.002	0.000	0.000
Eutrophication	kg (PO4)3-	9	0.000	0.000	0.000	0.000	0.000	0.000
Photochemical oxidation	kg Ethene	2	0.000	0.000	0.000	0.000	0.000	0.000
Abiotic depletion, non fuel	kg Antimone	0.16	0.000	0.000	0.000	0.000	0.000	0.000
Abiotic depletion, fuel	MJ	0.16	4.920	0.000	0.000	12.000	0.000	0.000
TOTAL	euro/kg/1m2				**0.002**			**0.004**

			Saint Gobain		2016	Saint Gobain		2016	Saint Gobain		2016
		Environmental cost	**33.1 SGG Planiclear**	**Production Stage A1/A2/A3**		**44.1 SGG Planiclear**	**Production Stage A1/A2/A3**		**33.2 SGG Planiclear**	**Production Stage A1/A2/A3**	
Impact Category	Unit	[euro/x]	15.38	[/kg]	[euro/kg]	20.38	[/kg]	[euro/kg]	15.76	[/kg]	[euro/kg]
Global warming	kg CO2	0.05	23.200	1.508	0.075	29.100	1.428	0.071	26.100	1.656	0.083
Ozone layer depletion (ODP)	kg CFC-11	30	0.000	0.000	0.000	0.000	0.000	0.000	0.000	0.000	0.000
Acidification	kg SO2	4	0.100	0.006	0.026	0.130	0.006	0.026	0.103	0.007	0.026
Eutrophication	kg (PO4)3-	9	0.029	0.002	0.017	0.038	0.002	0.017	0.029	0.002	0.017
Photochemical oxidation	kg Ethene	2	0.007	0.000	0.001	0.009	0.000	0.001	0.008	0.000	0.001
Abiotic depletion, non fuel	kg Antimone	0.16	0.000	0.000	0.000	0.000	0.000	0.000	0.000	0.000	0.000
Abiotic depletion, fuel	MJ	0.16	292.000	0.009	0.001	363.000	0.009	0.001	342.000	0.010	0.002
TOTAL	euro/kg/1m2				**0.121**			**0.116**			**0.128**

			Saint Gobain		2016	Saint Gobain		2016	Saint Gobain		2016
		Environmental cost	**44.2 SGG Planiclear**	**Production Stage A1/A2/A3**		**55.2 SGG Diamant**	**Production Stage A1/A2/A3**		**66.2 SGG Planiclear**	**Production Stage A1/A2/A3**	
Impact Category	Unit	[euro/x]	20.76	[/kg]	[euro/kg]	25.76	[/kg]	[euro/kg]	30.76	[/kg]	[euro/kg]
Global warming	kg CO2	0.05	32.000	1.541	0.077	40.800	1.584	0.079	43.800	1.424	0.071
Ozone layer depletion (ODP)	kg CFC-11	30	0.000	0.000	0.000	0.000	0.000	0.000	0.000	0.000	0.000
Acidification	kg SO2	4	0.133	0.006	0.026	0.174	0.007	0.027	0.193	0.006	0.025
Eutrophication	kg (PO4)3-	9	0.038	0.002	0.017	0.043	0.002	0.015	0.057	0.002	0.017
Photochemical oxidation	kg Ethene	2	0.010	0.000	0.001	0.011	0.000	0.001	0.014	0.000	0.001
Abiotic depletion, non fuel	kg Antimone	0.16	0.000	0.000	0.000	0.000	0.000	0.000	0.000	0.000	0.000
Abiotic depletion, fuel	MJ	0.16	412.000	0.010	0.002	516.000	0.010	0.002	554.000	0.009	0.001
TOTAL	euro/kg/1m2				**0.122**			**0.123**			**0.115**

						AGC		2018			
		Environmental cost	Fix impact	Impact per 1mm float thickness	impact per PVB interlayer	33.1	Production Stage A1/A2/A3				
Impact Category	Unit	[euro/x]		6	1	15.38	[/kg]	fixed	Float	pvb	[euro/kg]
Global warming (GWP100)	kg CO2	0.05	0.074	3.100	2.000	20.674	1.344	0.000	0.060	0.007	0.067
Ozone layer depletion	kg CFC-11	30	0.000	0.000	0.000	0.000	0.000	0.000	0.000	0.000	0.000
Acidification	kg SO2	4	0.001	0.013	0.003	0.081	0.005	0.000	0.020	0.001	0.021
Eutrophication	kg (PO4)3-	9	0.000	0.002	0.000	0.012	0.001	0.000	0.007	0.000	0.007
Photochemical	kg Ethene	2	0.000	0.001	0.001	0.006	0.000	0.000	0.001	0.000	0.001
Abiotic depletion, non fuel	kg Antimone	0.16	0.000	0.000	0.000	0.000	0.000	0.000	0.000	0.000	0.000
Abiotic depletion, fuel	MJ	0.16	0.780	40.500	39.200	282.980	0.009	0.000	0.001	0.000	0.001
TOTAL	euro/kg/1m2										0.097

						AGC		2018			
		Environmental cost	Fix impact	Impact per 1mm float thickness	impact per PVB interlayer	44.1	Production Stage A1/A2/A3				
Impact Category	Unit	[euro/x]		8	1	20.38	[/kg]	fixed	Float	pvb	[euro/kg]
Global warming (GWP100)	kg CO2	0.05	0.074	3.100	2.000	26.874	1.319	0.000	0.061	0.005	0.066
Ozone layer depletion	kg CFC-11	30	0.000	0.000	0.000	0.000	0.000	0.000	0.000	0.000	0.000
Acidification	kg SO2	4	0.001	0.013	0.003	0.106	0.005	0.000	0.020	0.001	0.021
Eutrophication	kg (PO4)3-	9	0.000	0.002	0.000	0.016	0.001	0.000	0.007	0.000	0.007
Photochemical	kg Ethene	2	0.000	0.001	0.001	0.007	0.000	0.000	0.001	0.000	0.001
Abiotic depletion, non fuel	kg Antimone	0.16	0.000	0.000	0.000	0.000	0.000	0.000	0.000	0.000	0.000
Abiotic depletion, fuel	MJ	0.16	0.780	40.500	39.200	363.980	0.009	0.000	0.001	0.000	0.001
TOTAL	euro/kg/1m2										0.096

						AGC		2018			
		Environmental cost	Fix impact	Impact per 1mm float thickness	impact per PVB interlayer	33.2	Production Stage A1/A2/A3				
Impact Category	Unit	[euro/x]		6	2	15.76	[/kg]	fixed	Float	pvb	[euro/kg]
Global warming (GWP100)	kg CO2	0.05	0.074	3.100	2.000	22.674	1.439	0.000	0.059	0.013	0.072
Ozone layer depletion	kg CFC-11	30	0.000	0.000	0.000	0.000	0.000	0.000	0.000	0.000	0.000
Acidification	kg SO2	4	0.001	0.013	0.003	0.083	0.005	0.000	0.020	0.001	0.021
Eutrophication	kg (PO4)3-	9	0.000	0.002	0.000	0.012	0.001	0.000	0.007	0.000	0.007
Photochemical	kg Ethene	2	0.000	0.001	0.001	0.006	0.000	0.000	0.001	0.000	0.001
Abiotic depletion, non fuel	kg Antimone	0.16	0.000	0.000	0.000	0.000	0.000	0.000	0.000	0.000	0.000
Abiotic depletion, fuel	MJ	0.16	0.780	40.500	39.200	322.180	0.010	0.000	0.001	0.000	0.002
TOTAL	euro/kg/1m2										0.102

						AGC		2018			
		Environmental cost	Fix impact	Impact per 1mm float thickness	impact per PVB interlayer	44.2	Production Stage A1/A2/A3				
Impact Category	Unit	[euro/x]		8	2	20.76	[/kg]	fixed	Float	pvb	[euro/kg]
Global warming	kg CO2	0.05	0.074	3.100	2.000	28.874	1.391	0.000	0.060	0.010	0.070
Ozone layer depletion (ODP)	kg CFC-11	30	0.000	0.000	0.000	0.000	0.000	0.000	0.000	0.000	0.000
Acidification	kg SO2	4	0.001	0.013	0.003	0.109	0.005	0.000	0.020	0.001	0.021
Eutrophication	kg (PO4)3-	9	0.000	0.002	0.000	0.016	0.001	0.000	0.007	0.000	0.007
Photochemical oxidation	kg Ethene	2	0.000	0.001	0.001	0.008	0.000	0.000	0.001	0.000	0.001
Abiotic depletion, non	kg Antimone	0.16	0.000	0.000	0.000	0.000	0.000	0.000	0.000	0.000	0.000
Abiotic depletion, fuel	MJ	0.16	0.780	40.500	39.200	403.180	0.009	0.000	0.001	0.000	0.001
TOTAL	euro/kg/1m2										0.100

						AGC		2018			
		Environmental cost	Fix impact	Impact per 1mm float thickness	impact per PVB interlayer	55.2	Production Stage A1/A2/A3				
Impact Category	Unit	[euro/x]		10	2	25.76	[/kg]	fixed	Float	pvb	[euro/kg]
Global warming	kg CO2	0.05	0.074	3.100	2.000	35.074	1.362	0.000	0.060	0.008	0.068
Ozone layer depletion (ODP)	kg CFC-11	30	0.000	0.000	0.000	0.000	0.000	0.000	0.000	0.000	0.000
Acidification	kg SO2	4	0.001	0.013	0.003	0.135	0.005	0.000	0.020	0.001	0.021
Eutrophication	kg (PO4)3-	9	0.000	0.002	0.000	0.020	0.001	0.000	0.007	0.000	0.007
Photochemical oxidation	kg Ethene	2	0.000	0.001	0.001	0.009	0.000	0.000	0.001	0.000	0.001
Abiotic depletion, non	kg Antimone	0.16	0.000	0.000	0.000	0.000	0.000	0.000	0.000	0.000	0.000
Abiotic depletion, fuel	MJ	0.16	0.780	40.500	39.200	484.180	0.009	0.000	0.001	0.000	0.001
TOTAL	euro/kg/1m2										0.098

						AGC		2018			
		Environmental cost	Fix impact	Impact per 1mm float thickness	impact per PVB interlayer	66.2	Production Stage A1/A2/A3				
Impact Category	Unit	[euro/x]		12	2	30.76	[/kg]	fixed	Float	pvb	[euro/kg]
Global warming	kg CO2	0.05	0.074	3.100	2.000	41.274	1.342	0.000	0.060	0.007	0.067
Ozone layer depletion (ODP)	kg CFC-11	30	0.000	0.000	0.000	0.000	0.000	0.000	0.000	0.000	0.000
Acidification	kg SO2	4	0.001	0.013	0.003	0.161	0.005	0.000	0.020	0.001	0.021
Eutrophication	kg (PO4)3-	9	0.000	0.002	0.000	0.024	0.001	0.000	0.007	0.000	0.007
Photochemical oxidation	kg Ethene	2	0.000	0.001	0.001	0.011	0.000	0.000	0.001	0.000	0.001
Abiotic depletion, non	kg Antimone	0.16	0.000	0.000	0.000	0.000	0.000	0.000	0.000	0.000	0.000
Abiotic depletion, fuel	MJ	0.16	0.780	40.500	39.200	565.180	0.009	0.000	0.001	0.000	0.001
TOTAL	euro/kg/1m2										0.097

				Impact per 1mm float thickness	impact per PVB interlayer	AGC		2018			
		Environ mental	Fix impact			44.2	Production Stage A1/A2/A3				
Impact Category	Unit	[euro/x]		8	2	20.76	[/kg]	fixed	Float	pvb	[euro/kg]
Global warming (GWP100)	kg CO2	0.05	0.074	3.100	2.000	28.874	1.391	0.000	0.060	0.010	0.070
Ozone layer depletion (ODP)	kg CFC-11	30	0.000	0.000	0.000	0.000	0.000	0.000	0.000	0.000	0.000
Acidification	kg SO2	4	0.001	0.013	0.003	0.109	0.005	0.000	0.020	0.001	0.021
Eutrophication	kg (PO4)3-	9	0.000	0.002	0.000	0.016	0.001	0.000	0.007	0.000	0.007
Photochemical oxidation	kg Ethene	2	0.000	0.001	0.001	0.008	0.000	0.000	0.001	0.000	0.001
Abiotic depletion, non fuel	kg Antimone	0.16	0.000	0.000	0.000	0.000	0.000	0.000	0.000	0.000	0.000
Abiotic depletion, fuel	MJ	0.16	0.780	40.500	39.200	403.180	0.009	0.000	0.001	0.000	0.001
TOTAL	euro/kg/1m2										0.100

				Impact per 1mm float thickness		AGC		2018			
		Environmental cost	Fix impact		impact per PVB interlayer	44.2	End-of-life: C3 waste processing				
Impact Category	Unit	[euro/x]		8	2	20.76	[/kg]	fixed	Float	pvb	[euro/kg]
Global warming (GWP100)	kg CO2	0.05	0.000	0.000	0.000	0.000	0.000	0.000	0.000	0.000	0.000
Ozone layer depletion (ODP)	kg CFC-11	30	0.000	0.000	0.000	0.000	0.000	0.000	0.000	0.000	0.000
Acidification	kg SO2	4	0.000	0.000	0.000	0.000	0.000	0.000	0.000	0.000	0.000
Eutrophication	kg (PO4)3-	9	0.000	0.000	0.000	0.000	0.000	0.000	0.000	0.000	0.000
Photochemical oxidation	kg Ethene	2	0.000	0.000	0.000	0.000	0.000	0.000	0.000	0.000	0.000
Abiotic depletion, non fuel	kg Antimone	0.16	0.000	0.000	0.000	0.000	0.000	0.000	0.000	0.000	0.000
Abiotic depletion, fuel	MJ	0.16	0.000	0.000	0.000	0.000	0.000	0.000	0.000	0.000	0.000
TOTAL	euro/kg/1m2										0.000

				Impact per 1mm float thickness	impact per PVB interlayer	AGC		2018			
		Environmental cost	Fix impact			44.2	End-of-life: C4 Disposal				
Impact Category	Unit	[euro/x]		8	2	20.76	[/kg]	fixed	Float	pvb	[euro/kg]
Global warming (GWP100)	kg CO2	0.05	0.000	0.040	0.028	0.374	0.018	0.000	0.001	0.000	0.001
Ozone layer depletion (ODP)	kg CFC-11	30	0.000	0.000	0.000	0.000	0.000	0.000	0.000	0.000	0.000
Acidification	kg SO2	4	0.000	0.000	0.000	0.002	0.000	0.000	0.000	0.000	0.000
Eutrophication	kg (PO4)3-	9	0.000	0.000	0.000	0.000	0.000	0.000	0.000	0.000	0.000
Photochemical oxidation	kg Ethene	2	0.000	0.000	0.000	0.000	0.000	0.000	0.000	0.000	0.000
Abiotic depletion, non fuel	kg Antimone	0.16	0.000	0.000	0.000	0.000	0.000	0.000	0.000	0.000	0.000
Abiotic depletion, fuel	MJ	0.16	0.000	0.514	0.402	4.916	0.000	0.000	0.000	0.000	0.000
TOTAL	euro/kg/1m2										0.002

				Impact per 1mm float thickness	impact per PVB interlayer	AGC		2018			
		Environmental cost	Fix impact			44.2	D Benefits and loads beyond system boundaries				
Impact Category	Unit	[euro/x]		8	2	20.76	[/kg]	fixed	Float	pvb	[euro/kg]
Global warming (GWP100)	kg CO2	0.05	0.000	0.153	0.000	1.224	0.059	0.000	0.003	0.000	0.003
Ozone layer depletion (ODP)	kg CFC-11	30	0.000	0.000	0.000	0.000	0.000	0.000	0.000	0.000	0.000
Acidification	kg SO2	4	0.000	0.000	0.000	0.002	0.000	0.000	0.000	0.000	0.000
Eutrophication	kg (PO4)3-	9	0.000	0.000	0.000	0.000	0.000	0.000	0.000	0.000	0.000
Photochemical oxidation	kg Ethene	2	0.000	0.000	0.000	0.000	0.000	0.000	0.000	0.000	0.000
Abiotic depletion, non fuel	kg Antimone	0.16	0.000	0.000	0.000	0.000	0.000	0.000	0.000	0.000	0.000
Abiotic depletion, fuel	MJ	0.16	0.000	1.500	0.000	12.000	0.000	0.000	0.000	0.000	0.000
TOTAL	euro/kg/1m2										0.004

			Trakya Cam Sanayii A.Ş. Laminated Glass		2017	Trakya Cam Sanayii A.Ş. Laminated Glass		2017	Trakya Cam Sanayii A.Ş. Laminated Glass		2017
		Environ mental	23.1kg per 1m2: 9.24mm	Production Stage A1		23.1kg per 1m2: 9.24mm	Production Stage A2		23.1kg per 1m2: 9.24mm	Production Stage A3	
Impact Category	Unit	[euro/x]	23.1	[/kg]	[euro/kg]	23.1	[/kg]	[euro/kg]	23.1	[/kg]	[euro/kg]
Global warming (GWP100)	kg CO2	0.05	7.940	0.344	0.017	1.090	0.047	0.002	17.400	0.753	0.038
Ozone layer depletion (ODP)	kg CFC-11	30	0.000	0.000	0.000	0.000	0.000	0.000	0.000	0.000	0.000
Acidification	kg SO2	4	0.042	0.002	0.007	0.006	0.000	0.001	0.042	0.002	0.007
Eutrophication	kg (PO4)3-	9	0.011	0.000	0.004	0.001	0.000	0.000	0.002	0.000	0.001
Photochemical oxidation	kg Ethene	2	0.002	0.000	0.000	0.000	0.000	0.000	0.002	0.000	0.000
Abiotic depletion, non fuel	kg Antimone	0.16	0.000	0.000	0.000	0.000	0.000	0.000	0.000	0.000	0.000
Abiotic depletion, fuel	MJ	0.16	105.000	0.002	0.000	16.300	0.000	0.000	172.000	0.004	0.001
TOTAL	euro/kg/1m2				**0.029**			**0.004**			**0.047**

			Trakya Cam Sanayii A.Ş. Float Glass		2017	Trakya Cam Sanayii A.Ş. (Şişecam Flat Glass)		2017	Trakya Cam Sanayii A.Ş. (Şişecam Flat Glass)		2017
		Environ mental cost	23.1kg per 1m2; 9.24mm thick	Production Stage A1		23.1kg per 1m2; 9.24mm thick	Production Stage A2		23.1kg per 1m2; 9.24mm thick	Production Stage A3	
Impact Category	Unit	[euro/x]	23.1	[/kg]	[euro/kg]	23.1	[/kg]	[euro/kg]	23.1	[/kg]	[euro/kg]
Global warming (GWP100)	kg CO2	0.05	3.290	0.142	0.007	0.396	0.017	0.001	9.060	0.392	0.020
Ozone layer depletion (ODP)	kg CFC-11	30	0.000	0.000	0.000	0.000	0.000	0.000	0.000	0.000	0.000
Acidification	kg SO2	4	0.018	0.001	0.003	0.002	0.000	0.000	0.010	0.000	0.002
Eutrophication	kg (PO4)3-	9	0.005	0.000	0.002	0.000	0.000	0.000	0.001	0.000	0.000
Photochemical oxidation	kg Ethene	2	0.001	0.000	0.000	0.000	0.000	0.000	0.001	0.000	0.000
Abiotic depletion, non fuel	kg Antimone	0.16	0.000	0.000	0.000	0.000	0.000	0.000	0.000	0.000	0.000
Abiotic depletion, fuel	MJ	0.16	40.100	0.001	0.000	5.850	0.000	0.000	103.000	0.002	0.000
TOTAL	euro/kg/1m2				**0.012**			**0.001**			**0.022**

						AGC		2018		
		Environ mental	Fix impact	Impact per 1mm float thickness	impact per PVB interlayer	12.12.12.12	Production Stage A1/A2/A3			
Impact Category	Unit	[euro/x]		36	3	92.28	fixed [/kg]	Float [/kg]	pvb [/kg]	[euro/kg]
Global warming (GWP100)	kg CO2	0.05	0.074	3.100	2.000	117.674	0.000	0.060	0.003	0.064
Ozone layer depletion (ODP)	kg CFC-11	30	0.000	0.000	0.000	0.000	0.000	0.000	0.000	0.000
Acidification	kg SO2	4	0.001	0.013	0.003	0.473	0.000	0.020	0.000	0.020
Eutrophication	kg (PO4)3-	9	0.000	0.002	0.000	0.070	0.000	0.007	0.000	0.007
Photochemical oxidation	kg Ethene	2	0.000	0.001	0.001	0.031	0.000	0.001	0.000	0.001
Abiotic depletion, non fuel	kg Antimone	0.16	0.000	0.000	0.000	0.000	0.000	0.000	0.000	0.000
Abiotic depletion, fuel	MJ	0.16	0.780	40.500	39.200	1576.380	0.000	0.001	0.000	0.001
TOTAL	euro/kg/1m2									**0.093**

						AGC		2018		
		Environmental cost	Fix impact	Impact per 1mm float thickness	impact per PVB interlayer	12.12.12.12	End-of-life: C4 Disposal			
Impact Category	Unit	[euro/x]		36	3	122.28	fixed [/kg]	Float [/kg]	pvb [/kg]	[euro/kg]
Global warming (GWP100)	kg CO2	0.05	0.000	0.040	0.028	1.516	0.000	0.001	0.000	0.001
Ozone layer depletion (ODP)	kg CFC-11	30	0.000	0.000	0.000	0.000	0.000	0.000	0.000	0.000
Acidification	kg SO2	4	0.000	0.000	0.000	0.009	0.000	0.000	0.000	0.000
Eutrophication	kg (PO4)3-	9	0.000	0.000	0.000	0.001	0.000	0.000	0.000	0.000
Photochemical oxidation	kg Ethene	2	0.000	0.000	0.000	0.001	0.000	0.000	0.000	0.000
Abiotic depletion, non fuel	kg Antimone	0.16	0.000	0.000	0.000	0.000	0.000	0.000	0.000	0.000
Abiotic depletion, fuel	MJ	0.16	0.000	0.514	0.402	19.710	0.000	0.000	0.000	0.000
TOTAL	euro/kg/1m2									**0.001**

						AGC		2018		
		Environmental cost	Fix impact	Impact per 1mm float thickness	impact per PVB interlayer	12.12.12.12	D Benefits and loads beyond system			
Impact Category	Unit	[euro/x]		36	3	122.28	fixed [/kg]	Float [/kg]	pvb [/kg]	[euro/kg]
Global warming (GWP100)	kg CO2	0.05	0.000	0.153	0.000	5.508	0.000	0.002	0.000	0.002
Ozone layer depletion (ODP)	kg CFC-11	30	0.000	0.000	0.000	0.000	0.000	0.000	0.000	0.000
Acidification	kg SO2	4	0.000	0.000	0.000	0.010	0.000	0.000	0.000	0.000
Eutrophication	kg (PO4)3-	9	0.000	0.000	0.000	0.002	0.000	0.000	0.000	0.000
Photochemical oxidation	kg Ethene	2	0.000	0.000	0.000	0.001	0.000	0.000	0.000	0.000
Abiotic depletion, non fuel	kg Antimone	0.16	0.000	0.000	0.000	0.000	0.000	0.000	0.000	0.000
Abiotic depletion, fuel	MJ	0.16	0.000	1.500	0.000	54.000	0.000	0.000	0.000	0.000
TOTAL	euro/kg/1m2									**0.003**

			Okalux GmbH float glass		2017	Okalux GmbH float glass		2017
		Environ mental cost	1m2 area and 1 mm thick	Production Stage A1/A2/A3		1m2 area and 1 mm thick	End-of-life: C3 waste processing	
Impact Category	Unit	[euro/x]	2.5	[/kg]	[euro/kg]	2.5	[/kg]	[euro/kg]
Global warming (GWP100)	kg CO2	0.05	2.430	0.972	0.049	0.043	0.017	0.001
Ozone layer depletion (ODP)	kg CFC-11	30	0.000	0.000	0.000	0.000	0.000	0.000
Acidification	kg SO2	4	0.014	0.006	0.023	0.000	0.000	0.000
Eutrophication	kg (PO4)3-	9	0.001	0.001	0.005	0.000	0.000	0.000
Photochemical oxidation	kg Ethene	2	0.001	0.000	0.001	0.000	0.000	0.000
Abiotic depletion, non fuel	kg Antimone	0.16	0.000	0.000	0.000	0.000	0.000	0.000
Abiotic depletion, fuel	MJ	0.16	44.370	0.009	0.001	0.460	0.000	0.000
TOTAL	euro/kg/1m2				**0.079**			**0.001**

			Okalux GmbH float glass		2017	Okalux GmbH float glass		2017
		Environ mental cost	1m2 area and 1 mm thick	End-of-life: C4 Disposal		1m2 area and 1 mm thick	D Benefits and loads beyond system boundaries	
Impact Category	Unit	[euro/x]	2.5	[/kg]	[euro/kg]	2.5	[/kg]	[euro/kg]
Global warming (GWP100)	kg CO2	0.05	0.028	0.011	0.001	-0.390	-0.156	-0.008
Ozone layer depletion (ODP)	kg CFC-11	30	0.000	0.000	0.000	0.000	0.000	0.000
Acidification	kg SO2	4	0.000	0.000	0.000	-0.002	-0.001	-0.003
Eutrophication	kg (PO4)3-	9	0.000	0.000	0.000	0.000	0.000	-0.001
Photochemical oxidation	kg Ethene	2	0.000	0.000	0.000	0.000	0.000	0.000
Abiotic depletion, non fuel	kg Antimone	0.16	0.000	0.000	0.000	0.000	0.000	0.000
Abiotic depletion, fuel	MJ	0.16	0.360	0.000	0.000	-5.290	-0.001	0.000
TOTAL	euro/kg/1m2				**0.001**			**-0.012**

			Okalux GmbH Laminated glass		**2017**	**Okalux GmbH Laminated glass**		**2017**	**C**
		Environ mental cost	**1m2 area and 1 mm thick**	**Production Stage A1/A2/A3**		**1m2 area and 1 mm thick**	**End-of-life: C3 waste processing**		**1 n**
Impact Category	Unit	[euro/x]	5.38	[/kg]	[euro/kg]	5.38	[/kg]	[euro/kg]	5
Global warming (GWP100)	kg CO2	0.05	7.930	1.474	0.074	0.043	0.008	0.000	
Ozone layer depletion (ODP)	kg CFC-11	30	0.000	0.000	0.000	0.000	0.000	0.000	
Acidification	kg SO2	4	0.049	0.009	0.037	0.000	0.000	0.000	
Eutrophication	kg (PO4)3-	9	0.004	0.001	0.007	0.000	0.000	0.000	
Photochemical oxidation	kg Ethene	2	0.003	0.001	0.001	0.000	0.000	0.000	
Abiotic depletion, non fuel	kg Antimone	0.16	0.000	0.000	0.000	0.000	0.000	0.000	
Abiotic depletion, fuel	MJ	0.16	106.950	0.010	0.002	0.460	0.000	0.000	
TOTAL	euro/kg/1m2				**0.120**			**0.001**	

			Okalux GmbH Laminated glass		**2017**	**Okalux GmbH Laminated glass**		**2017**
		Environ mental cost	**1m2 area and 1 mm thick**	**End-of-life: C4 Disposal**		**1m2 area and 1 mm thick**	**D Benefits and loads beyond system boundaries**	
Impact Category	Unit	[euro/x]	5.38	[/kg]	[euro/kg]	5.38	[/kg]	[euro/kg]
Global warming (GWP100)	kg CO2	0.05	0.029	0.005	0.000	-0.390	-0.072	-0.004
Ozone layer depletion (ODP)	kg CFC-11	30	0.000	0.000	0.000	0.000	0.000	0.000
Acidification	kg SO2	4	0.000	0.000	0.000	-0.002	0.000	-0.002
Eutrophication	kg (PO4)3-	9	0.000	0.000	0.000	0.000	0.000	0.000
Photochemical oxidation	kg Ethene	2	0.000	0.000	0.000	0.000	0.000	0.000
Abiotic depletion, non fuel	kg Antimone	0.16	0.000	0.000	0.000	0.000	0.000	0.000
Abiotic depletion, fuel	MJ	0.16	0.370	0.000	0.000	-5.240	0.000	0.000
TOTAL	euro/kg/1m2				**0.000**			**-0.006**

			Asahi India Glass Ltd		**2019**
		Environ mental cost	**6mm thick laminated glass**	**Production Stage A1/A2/A3**	
Impact Category	Unit	[euro/x]	15.380	[/kg]	[euro/kg]
Global warming (GWP100)	kg CO2	0.05	93.600	6.086	0.304
Ozone layer depletion (ODP)	kg CFC-11	30	0.000	0.000	0.000
Acidification	kg SO2	4	0.858	0.056	0.223
Eutrophication	kg (PO4)3-	9	0.046	0.003	0.027
Photochemical oxidation	kg Ethene	2	0.043	0.003	0.006
Abiotic depletion, non fuel	kg Antimone	0.16	0.000	0.000	0.000
Abiotic depletion, fuel	MJ	0.16	1124.500	0.035	0.006
TOTAL	euro/kg/1m2				**0.566**

			Tecnoglass Laminated Glass		2020	Tecnoglass Laminated Glass		2020
		Environmental cost	3/16'' low-E coated laminated IGU TRACI2.1	Production Stage A1		3/16'' thick low-E coated laminated IGU CML4.1	Production Stage A1	
Impact Category	Unit	[euro/x]	24.193	[/kg]	[euro/kg]	24.193	[/kg]	[euro/kg]
Global warming (GWP100)	kg CO2	0.05	20.400	0.843	0.042	20.600	0.852	0.043
Ozone layer depletion (ODP)	kg CFC-11	30	0.000	0.000	0.000	0.000	0.000	0.000
Acidification	kg SO2	4	0.175	0.007	0.029	0.176	0.007	0.029
Eutrophication	kg (PO4)3-	9	0.035	0.001	0.013	0.025	0.001	0.009
Photochemical oxidation	kg Ethene	2	2.050	0.085	0.169	0.006	0.000	0.001
Abiotic depletion, non fuel	kg Antimone	0.16	2.320	0.096	0.015	2.320	0.096	0.015
Abiotic depletion, fuel	MJ	0.16	27.900	0.001	0.000	222.000	0.004	0.001
TOTAL	euro/kg/1m2				**0.269**			**0.097**

			Tecnoglass Laminated Glass		2020	Tecnoglass Laminated Glass		2020
		Environmental cost	3/16'' low-E coated laminated IGU TRACI2.1	Production Stage A2		3/16'' thick low-E coated laminated IGU CML4.1	Production Stage A1	
Impact Category	Unit	[euro/x]	24.193	[/kg]	[euro/kg]	24.193	[/kg]	[euro/kg]
Global warming (GWP100)	kg CO2	0.05	6.540	0.270	0.014	6.550	0.271	0.014
Ozone layer depletion (ODP)	kg CFC-11	30	0.000	0.000	0.000	0.000	0.000	0.000
Acidification	kg SO2	4	0.033	0.001	0.005	0.033	0.001	0.005
Eutrophication	kg (PO4)3-	9	0.008	0.000	0.003	0.005	0.000	0.002
Photochemical oxidation	kg Ethene	2	0.488	0.020	0.040	0.001	0.000	0.000
Abiotic depletion, non fuel	kg Antimone	0.16	0.223	0.009	0.001	0.223	0.009	0.001
Abiotic depletion, fuel	MJ	0.16	13.600	0.000	0.000	100.000	0.002	0.000
TOTAL	euro/kg/1m2				**0.064**			**0.023**

			Tecnoglass Laminated Glass		2020	Tecnoglass Laminated Glass		2020
		Environmental cost	3/16'' low-E coated laminated IGU TRACI2.1	Production Stage A3		3/16'' thick low-E coated laminated IGU CML4.1	Production Stage A3	
Impact Category	Unit	[euro/x]	24.193	[/kg]	[euro/kg]	24.193	[/kg]	[euro/kg]
Global warming (GWP100)	kg CO2	0.05	35.000	1.447	0.072	35.500	1.467	0.073
Ozone layer depletion (ODP)	kg CFC-11	30	0.000	0.000	0.000	0.000	0.000	0.000
Acidification	kg SO2	4	0.124	0.005	0.021	0.112	0.005	0.019
Eutrophication	kg (PO4)3-	9	0.068	0.003	0.025	0.040	0.002	0.015
Photochemical oxidation	kg Ethene	2	2.300	0.095	0.190	0.005	0.000	0.000
Abiotic depletion, non fuel	kg Antimone	0.16	0.361	0.015	0.002	0.361	0.015	0.002
Abiotic depletion, fuel	MJ	0.16	64.800	0.001	0.000	533.000	0.011	0.002
TOTAL	euro/kg/1m2				**0.311**			**0.111**

			Laurier Architectural		2018	Laurier Architectural		2018	L
		Environmental cost	10.24mm thick laminated glass TRACI2.1	Production Stage A1/A2/A3		10.24mm thick laminated glass CML4.4	Production Stage A1/A2/A3		6 f T
Impact Category	Unit	[euro/x]	25.980	[/kg]	[euro/kg]	25.980	[/kg]	[euro/kg]	
Global warming (GWP100)	kg CO2	0.05	47.300	1.821	0.091	47.400	1.824	0.091	
Ozone layer depletion (ODP)	kg CFC-11	30	0.000	0.000	0.000	0.000	0.000	0.000	
Acidification	kg SO2	4	0.428	0.016	0.066	0.372	0.014	0.057	
Eutrophication	kg (PO4)3-	9	0.057	0.002	0.020	0.076	0.003	0.026	
Photochemical oxidation	kg Ethene	2	11.300	0.435	0.870	0.021	0.001	0.002	
Abiotic depletion, non fuel	kg Antimone	0.16	94.000	0.002	0.000	1760.000	0.033	0.005	
Abiotic depletion, fuel	MJ	0.16	0.866	0.000	0.000	0.000	0.000	0.000	
TOTAL	euro/kg/1m2				**1.047**			**0.182**	

			Laurier Architectural		2018	Laurier Architectural		2018
		Environmental cost	6.36mm thick flat glass TRACI2.1	Production Stage A1/A2/A3		6.36mm thick flat glass CML4.4	Production Stage A1/A2/A3	
Impact Category	Unit	[euro/x]	15.900	[/kg]	[euro/kg]	15.900	[/kg]	[euro/kg]
Global warming (GWP100)	kg CO2	0.05	26.700	1.679	0.084	26.700	1.679	0.084
Ozone layer depletion (ODP)	kg CFC-11	30	0.000	0.000	0.000	0.000	0.000	0.000
Acidification	kg SO2	4	0.251	0.016	0.063	0.217	0.014	0.055
Eutrophication	kg (PO4)3-	9	0.031	0.002	0.017	0.044	0.003	0.025
Photochemical oxidation	kg Ethene	2	6.760	0.425	0.850	0.012	0.001	0.002
Abiotic depletion, non fuel	kg Antimone	0.16	48.800	0.001	0.000	1010.000	0.031	0.005
Abiotic depletion, fuel	MJ	0.16	0.510	0.000	0.000	0.000	0.000	0.000
TOTAL	euro/kg/1m2				**1.015**			**0.170**